Journal of Superconductivity, Vol. 3, No. 4, 1990

Review

Thermal Conductivity of High-T_c Superconductors

Ctirad Uher[1]

Received 15 July, 1990

This paper reviews existing data on the thermal conductivity of high-T_c superconductors. Included are discussions of pristine polycrystalline high-T_c ceramics, single crystal specimens, and high-T_c materials structurally modified by substitution or by radiation damage. The thermal conductivity of high-T_c superconductors is compared with that of conventional superconductors, and dramatic differences are found between the two families. Mechanisms of thermal conductivity applicable to high-T_c perovskites are discussed and implications for theories of high-T_c superconductivity are noted.

KEY WORDS: High-Transition-temperature superconductors; thermal conductivity; single crystal; Mechanisms.

1. INTRODUCTION

The discovery of superconductivity in the 30 K range by Bednorz and Müller [1] and the subsequent establishment by Chu's group [2] of $YBa_2Cu_3O_{7-\delta}$ as a 90 K superconductor represented a momentous event in the development of science with a potential payoff in many areas. For the first time, mankind had available a material with a transition temperature high enough to superconduct above the boiling point of liquid nitrogen. Suddenly, many futuristic projects that had seemed a distant dream became a potential reality. Concerns about budgetary limitations replaced questions about scientific feasibility. In a short span of three years (this review is written in the spring of 1990) tremendous progress has been achieved worldwide on many facets of high-T_c research, including the discovery [3,4] of new superconducting perovskite structures with transition temperatures well in excess of 100 K.

One important property of high-T_c materials is their ability to conduct heat. There is not only an obvious technological interest in how efficiently and by what means the heat flows in these solids but also a deep theoretical desire to understand the electronic and vibrational properties of these materials. The magnitude and temperature dependence of the thermal conductivity are parameters which have an impact on a broad spectrum of devices. As an example, the responsivity of radiation detectors such as bolometers depends sensitively on the thermal conductivity of their thin superconducting element, and recent data show [5] the noise power of a high-T_c superconducting bolometer to be two orders of magnitude smaller than for a room temperature-operated pyroelectric detector. Thermal conductivity also governs how rapidly a local hot spot in a superconducting magnet spreads or is healed, an important factor in its stability. Likewise, thermal stability is vitally important to the reliable operation of superconducting thin film microbridge structures [6]. Finally, it has been shown recently [7,8] that the spatial resolution limit of novel thin film characterization techniques such as low-temperature scanning electron microscopy is influenced by the thermal conductivity of the film under study; undoubtedly, this will also apply to the new high-T_c films.

From a theoretical point of view, the thermal conductivity of superconductors offers important clues about the nature of their charge carriers and phonons and scattering processes between them. In

[1]Department of Physics, University of Michigan, Ann Arbor, Michigan 48109

0896-1107/90/1200-0337$06.00/0

high-T_c superconductors, such information is even more valuable due to the fact that traditional galvanomagnetic probes such as resistivity, Hall effect, and thermopower are inoperative in the (now) wide temperature range up to T_c. The potential of normal state transport measurements to provide insight into the nature of superconductivity is thus drastically curtailed. No such limitation exists for the thermal conductivity and one has available the entire temperature range for gathering important transport data.

In this review I hope to illustrate the main features of heat transport as they apply to the spectrum of high-T_c superconductors. I shall point out how the free carriers and lattice vibrations contribute to the transport of heat, note similarities in the behavior of ceramic samples, and highlight important characteristics of heat transport in single crystal specimens. An overview of the thermal conductivity, as part of a broader picture of the thermal behavior of high-T_c superconductors, has been the subject of two prior works [9,10]. A snapshot of the status of the thermal conductivity of high-T_c superconductors is also given in a conference paper that I presented [11] in the summer of 1989. Progress is being made steadily, including studies on single crystals and on a wider range of high-T_c materials. It is thus appropriate to provide an in-depth review of the development as it stands today.

The review is organized as follows: Section 2 covers experimental considerations pertaining to the measurement of the thermal conductivity of high-T_c superconductors. Fundamental theoretical aspects of thermal transport related to traditional superconducting materials, as well as some specific issues which have a bearing on high-T_c perovskites, are discussed in Section 3. In Section 4 are presented and reviewed the existing data on the thermal conductivity of high-T_c superconductors, and conclusions and future trends in thermal transport studies on high-T_c materials are the subject of Section 5.

2. EXPERIMENTAL CONSIDERATIONS

I have noted that thermal conductivity measurements do not involve detection of electrical potentials; hence, investigations of the heat transport can be carried out both above and below the superconducting transition temperature. The material characteristics of high-T_c superconductors do, however, impose certain limitations that should be understood and taken into consideration in thermal conductivity investigations. First of all, there are three basic structural forms of high-T_c superconductors: bulk ceramics, single crystals, and oriented thin films. So far, the vast majority of investigations have been done on ceramic samples. Although, from a technological viewpoint, this is a very relevant form of high-T_c material, the "average" structure of this polycrystalline medium precludes investigations of anisotropy of the thermal transport, a parameter of paramount importance for a thorough theoretical understanding of these materials. Single crystal specimens, in this respect, are the obvious materials of choice. Limited availability of suitable single crystals of high-T_c superconductors has been a serious impediment to thermal conductivity studies. In particular, the c-axis thermal conductivity data on $YBa_2Cu_3O_7$ would be highly desirable, but the tiny thickness of available crystals along this direction has hindered serious investigations and only one set of measurements is available in the literature at this time. However, steady progress has been made in the preparation of relatively large single crystals of the La-based and Bi-based high-T_c superconductors, and thermal transport data are now becoming available. Thin films, the third structural form of high-T_c perovskites, have undergone spectacular development over the past couple of years and in many regards have emerged as the structurally superior form of high-T_c material. Specifically, critical current densities in excess of 10^6 A/cm^2 achieved in epitaxially oriented films [12] at 77 K are opening possibilities for practical applications. Obviously, heat flow mechanisms in thin films are of interest to both design engineers as well as theoretical physicists but, so far, no experimental data are available. The difficulty with thin films is that one cannot use well established steady-state heating techniques since the film's substrate provides a very efficient thermal short. In the absence of free-standing films, one has to turn to some kind of flash heating or reflectivity technique and it is only now that such methods are being developed [13] and applied to high-T_c materials.

Let us turn our attention to bulk forms of high-T_c superconductors, i.e., ceramic samples and single crystal specimens. The technique most frequently used to determine the thermal conductivity in this case is the longitudinal steady-state method, analogous to a potentiometric measurement of the electrical resistivity. Using this technique, thermal conductivity data have been generated from as low as 50 mK to as high as room temperature. The principle of the technique is illustrated schematically in Fig. 1. One end of a sample that has a uniform

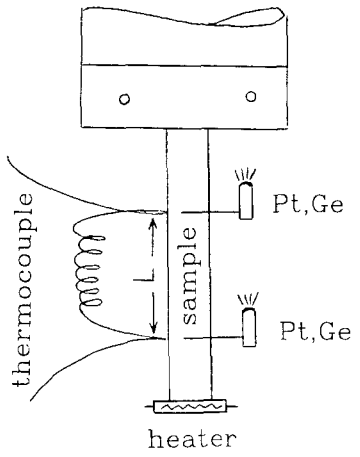

Fig. 1. Sample arrangement for measurements of the thermal conductivity by the steady-state technique.

cross-sectional area A makes a good thermal contact (e.g., by clamping or gluing using Apiezon grease or silver-loaded epoxy) with a cold tip of the cryostat while a small heater (a metal-film resistor is preferable for its small temperature coefficient of resistance) is attached to the free end of the sample. Electrical power Q dissipated in the heater provides a heat flow, and a pair of thermometers (or a differential thermocouple) separated by a distance L measures the temperature difference ΔT along the specimen. The thermal conductivity, κ, is then calculated from

$$\kappa = \frac{QL}{A\Delta T} \tag{1}$$

Provided ΔT is not too large, the value of the thermal conductivity obtained from Eq. (1) will be that corresponding to the mean temperature between the thermometers even if the thermal conductivity varies rapidly with temperature. For instance, taking a rather large relative temperature difference $\Delta T/T = 0.1$ and assuming $\kappa \propto T^3$ (such as for the typical boundary scattering regime of conduction) it can easily be shown that the difference between the true thermal conductivity and that derived from Eq. (1) is less than 0.25%. In situations where the sample is very short (such as single crystals of high-T_c superconductors) it is sometimes more advantageous to use the so-called two-heater/one thermometer technique wherein a thermometer is attached to the free end of the sample and power is alternately switched between two heaters spaced along the length of the sample. Since heaters can usually be made much smaller (e.g., by evaporating strips of a resistive film) than thermometers, they can be easily accommodated on a sample of small dimensions.

To use the longitudinal steady-state method effectively, one must make sure that virtually all heat generated by the heater flows through the specimen to the cold sink. As the thermal conductivity of the high-T_c materials is, in general, rather low, care must be exercised in the choice and size of the wires connecting the heater and thermometers so that heat loss is kept to a minimum. Of course, good vacuum must be maintained to eliminate heat exchange with the surrounding medium. Even in carefully designed experiments, heat losses by radiation effectively limit the temperature up to which this method is applicable. In high-T_c ceramics, the combination of low thermal conductivity with a rather dark and matte surface finish (high-emissivity) makes radiation losses a serious problem at temperatures as low as 200 K.

In the case of ceramic structures, special consideration has to be given to the sample porosity and grain size as these factors ultimately affect the magnitude and potentially the temperature dependence of the thermal conductivity. Samples with less than theoretical density (all sintered ceramics would fall in this category) contain voids and pores that influence the thermal conductivity in two ways: they serve as scattering centers for phonons, and they take up a fraction of the otherwise heat-conducting volume of the material. In the initial flurry of research, some investigations did not pay enough attention to this fact, and the conductivity was measured on samples not sufficiently well characterized. While the general features of the thermal conductivity seem to be present in all of the published data, the magnitude of the conductivity varies widely, undoubtedly due to variations in the filling factor of these sintered materials. Other structural features that might affect the thermal conductivity of ceramics and that should be carefully monitored are the exact oxygen stoichiometry, and the possible presence of multiple phases. The former is of special interest for the 1-2-3 compounds and, to a lesser extent, for $La_{2-x}Sr_xCuO_4$ superconductors since both are known to be sensitive to oxygen. A dependence of the thermal conductivity on oxygen content is observable at all temperatures, but it may be particularly important at very low temperatures where it has been speculated that oxygen vacancies play a role as two-level tunneling entities. On the other hand, the multi-phase nature of ceramics is more relevant to the quinary compounds of $Bi_2Sr_2Ca_{n-1}Cu_nO_{2n+4}$ and $Tl_2Ba_2Ca_{n-1}Cu_nO_{2n+4}$ where high volatility of the constituents makes it difficult to prepare these materials as single phases.

Although many of the undesirable structural features that complicate the transport behavior of sintered samples can be effectively eliminated by working with single crystals, this medium is also not entirely without problems. In addition to difficulties in their growth, crystals of high-T_c superconductors, whatever their shape, contain a high density of twins. Since twinning arises as a consequence of a high-temperature phase transformation from a tetragonal to an orthorhombic phase, twins are an unavoidable feature of the 1-2-3 compounds. Their role is to accommodate strain developed during the phase transformation and, as structural defects, they may seriously affect transport properties. Symmetry restrictions related to the tetragonal structure result in twin formation along (110). The spacing of the twins is on the order of 500–1000 Å [14]; however, it may range [15] from as low as 100 Å to several thousand Å. In single crystals, the spacing is typically [16] 750 Å. The reader may recall early attempts to link the existence of twins to the mechanism of superconductivity. While this particular intellectual exercise did not pan out [17], the twin structure is an important phenomenon and affects a variety of physical properties of high-T_c superconductors. Single crystals are the key to understanding the behavior of high-T_c superconductors and they are, indeed, indispensable for extracting the intrinsic features in thermal transport processes. Undoubtedly, as the existing crystal growth techniques are optimized and new ways to grow larger and better quality crystals are developed, single crystals will serve not only as the primary experimental medium, but will also be in demand for device applications.

I think it is clear that any meaningful investigation of the physical properties of high-T_c superconductors of whatever morphological shape or form must be accompanied by a thorough compositional and structural analysis of the samples. Only then can one hope to correlate the structure with the physical properties and move forward in the scientific inquiry into these fascinating materials.

3. THEORETICAL ASPECTS OF THERMAL CONDUCTIVITY

Thermal conductivity is an important topic in that the magnitude and temperature dependence of the thermal conductivity yield valuable information about the material under study. Specifically, such measurements shed light on the electronic and vibrational state of the material, interactions between the various heat conducting entities in the system, and on the structural integrity of the medium through which the thermal energy propagates. A phase transition, represented by the onset of charge carrier condensation as the temperature is swept through the superconducting transition point, is responsible for a sharp change in the electromagnetic and kinetic properties of superconductors and, among other things, leads to a drastic modification of the heat flow pattern in these substances. Thus, while the thermal conductivity of a superconductor is, in general, more complex than that of a normal metal, the temperature dependence of the thermal conductivity, particularly at and below T_c, provides insight into the state of the superconducting condensate and into the phonon spectrum of these materials.

3.1. Heat Conduction in Superconductors

In order to appreciate the rather unique behavior of the thermal conductivity of high-T_c superconductors, I briefly outline the main features of thermal transport in traditional superconductors. I limit the presentation to only the most basic facts that illustrate the fundamental nature of the heat conducting process in superconductors. For a detailed theoretical description of scattering mechanisms governing thermal transport processes in solids I refer the reader to specialized monographs [18,19]. The thermal conductivity of superconductors based on the microscopic theory of Bardeen, Cooper, and Schrieffer (BCS) is treated in the original papers [20,21]. An exhaustive description of the kinetic properties (thermal conductivity and sound absorption in particular) of superconductors is given in a book by Geilikman and Kresin [22].

Our starting point is a realization that the heat flux in solids consists in principle of two independent contributions: energy transport associated with the flow of the charge carriers that we generically refer to as the electronic thermal conductivity, κ_e, and the thermal energy carried by lattice vibrations that is known as the lattice or phonon thermal conductivity, κ_p. The total thermal conductivity is then

$$\kappa = \kappa_e + \kappa_p \tag{2}$$

The relative magnitude of the two contributions in Eq. (2) can be used to classify various types of solids in a way analogous to the magnitude of the electrical resistivity. Thus, in insulators, there are no free charge

carriers ($\kappa_e = 0$) and, consequently, $\kappa = \kappa_p$. While lattice vibrations also contribute to the thermal conductivity of metals, strong scattering of phonons on free carriers drastically suppresses the lattice contribution in this case and the total thermal conductivity is essentially entirely due to charge carriers. The purer the metal, the smaller the relative contribution of phonons in Eq. (2).

A remarkable feature of superconductors is the fact that, while in their normal state ($T > T_c$), the carrier contribution typically greatly exceeds the lattice term κ_p, at temperatures well below T_c, their thermal transport resembles that of a dielectric solid. It is in the intermediate temperature range, from $0.3\,T_c$ to T_c, that the condensation of electrons into a Cooper pair sea plays a decisive role in the interplay between the electron and phonon heat conducting channels. This is the temperature region on which most of the experimental work has centered and turns out to be the domain where high-T_c superconductors show a spectacular variation in their thermal conductivity. It is worth noting that flux quantization measurements on high-T_c superconductors indicate a charge $2e$. Hence, the fundamental concept of carrier condensation into a Cooper sea appears eminently reasonable for this class of superconductors as well.

It is important to realize that even if one of the two conducting channels, i.e., κ_e or κ_p, does not dominate the heat transport, the phonons do affect the magnitude and temperature dependence of the electronic contributions. Likewise, the presence of free carriers, even of relatively low density so that κ_e is small, strongly modifies the flow of phonons. The reasons for this behavior are relaxation mechanisms that ensure the stationary nature of the heat conducting process. For instance, the charge carriers (for simplicity we shall assume electrons) are scattered by phonons, yielding the electronic thermal resistivity $W_{e,p}$, by static imperfections such as impurities, stacking faults, grain boundaries, voids, etc., that lead to a term $W_{e,d}$, and by other electrons, $W_{e,e}$. According to Matthiessen's rule, the scattering processes for each homogeneous group of electrons are additive, so the electronic thermal conductivity is given by

$$1/\kappa_e \equiv W_e = W_{e,p} + W_{e,d} + W_{e,e} \tag{3}$$

In the case of multiple bands, which can be regarded as separate heat conducting channels, we would need to add a band index i to each of the terms in Eq. (3) and sum the thermal conductivity κ_{e_i} for each band to obtain the total electronic thermal conductivity κ_e.

Similarly, phonons of a given sample are scattered by different mechanisms, some of which are listed below with their associated scattering rates:

(i) scattering at the specimen boundaries, $\tau_{p,b}^{-1}$,
(ii) scattering by two-level tunneling states, $\tau_{p,t}^{-1}$,
(iii) scattering by dislocations, $\tau_{p,r}^{-1}$,
(iv) scattering by point defects, $\tau_{p,d}^{-1}$,
(v) scattering by free electrons, $\tau_{p,e}^{-1}$,
(vi) scattering by other phonons, $\tau_{p,p}^{-1}$.

As in the electronic case, the total scattering rate τ_p^{-1} for the phonons is found by summing over all the phonon scattering processes listed above. It is often necessary to consider the frequency (ω) and polarization (i) dependence of the phonon scattering rate $\tau_{p^i}^{-1}(\omega)$, in which case one usually regards phonons of different frequency as different heat conducting channels and sums their contributions to get the total phonon thermal conductivity. Using the elementary kinetic formulation, we obtain

$$\kappa_p = 1/3 \sum_i \int_0^\infty C_i(\omega) v_i^2(\omega) \tau_{p_i}(\omega)\, \mathrm{d}\omega \tag{4}$$

where $C_i(\omega)$ is the lattice heat capacity per unit volume for phonons of angular frequency ω, and $v_i(\omega)$ is the speed of the ith mode.

Within the Debye framework of lattice dynamics, neglecting polarization dependence, this becomes

$$\kappa_p = (k_B/2\pi^2 v)(k_B/\hbar)^3 T^3 \int_0^{\Theta_D/T} \tau(x) \left[x^4 e^x/(e^x-1)^2\right] dx \tag{5}$$

where $x = \hbar\omega/k_B T$ is the reduced phonon energy, Θ_D the Debye temperature, and v the (constant) speed of sound. For each scattering process of electrons and of phonons, one can calculate (using standard procedures of the quantum theory of solids) both its magnitude and temperature dependence and, in principle, solve the thermal conductivity problem. In practical situations, not all scattering processes act at the same time. One then attempts to select one or two major dissipative mechanisms and determine their scattering strength empirically by fitting to the experimental data. For instance, a normal metal can be modelled by the expression

$$1/\kappa_e \equiv W_e = aT^2 + b/T \tag{6}$$

where the first term on the right-hand side of Eq. (6) stands for the electron scattering by phonons and the second term represents the interaction of electrons with static defects in the metal lattice. By plotting

T/κ_e versus T^3 one can readily determine the coefficients a and b. The functional form of Eq. (6) is, indeed, a rather good representation of the thermal conductivity of pure metals. The lattice thermal conductivity in this case rarely exceeds 1–2% of the total conductivity because phonons are very effectively scattered by free electrons. In semimetals, such as Bi or Sb, where the intrinsic carrier density is several orders of magnitude lower than in, say, Cu or Ag, and in metal alloys where the electronic contribution is reduced due to a shorter mean-free path of electrons, the lattice contribution may become significant.

The lattice thermal resistivity of metals and alloys is determined primarily by the combined effect of the phonon–phonon U-processes that lead to a T-linear lattice resistivity contribution near and above the Debye temperature Θ_D, and the phonon–electron interaction that at low temperatures is well approximated by a T^{-2} resistivity term. It then follows that at sufficiently high and also at rather low temperatures the lattice thermal conductivity of metals and alloys is quite small. It is in the intermediate temperature range where the phonon contribution may rival the electronic thermal conductivity.

The question arises of how the formation of the Cooper condensate modifies the heat flow pattern, i.e., what is the thermal conductivity of a traditional superconductor? Although this is a complex problem that depends rather sensitively on the particular material parameters, specifically the superconducting transition temperature and the fraction of heat that is carried by electrons and phonons at T_c, we can make general comments that will be helpful in understanding the features of the thermal transport of superconductors.

There are two fundamental properties of the superconducting condensate that have an overriding effect on the thermal conductivity of a superconductor:

1. Cooper pairs carry no entropy,
2. Cooper pairs do not scatter phonons.

The first condition means that the electronic thermal conductivity vanishes rapidly below T_c. This is immediately obvious if one invokes a kinetic theory formulation of the electronic thermal conductivity

$$\kappa_e = 1/3 cvl_e \tag{7}$$

Here c is the specific heat of the carriers, v is their Fermi velocity, and l_e their mean-free path. While v is essentially constant and l_e varies as a power law of temperature, the dominant contribution comes from the specific heat that at $T < T_c$ decreases approximately exponentially. The second condition has a more subtle effect on the thermal conductivity of superconductors. Provided that the mean-free path of phonons at $T > T_c$ is limited by scattering on charge carriers, on passing into the superconducting state the phonon thermal conductivity will rise because the number of quasiparticle excitations rapidly decreases leading to an enhancement in the mean-free path of phonons, l_p. A competition between the rapidly diminishing κ_e on the one hand and increasing κ_p on the other will determine the overall dependence of the total thermal conductivity of a given superconductor. In the vast majority of cases (all pure conventional superconductors and most alloys) κ falls rapidly as the material goes superconducting. This general trend encompasses both weakly and strongly coupled superconductors. In the latter case, the decrease in the thermal conductivity is more rapid as a result of a larger prefactor α in the temperature dependence of the energy gap,

$$\left(\frac{\Delta}{k_B T}\right)_{T \to T_c} = \alpha(1 - T/T_c) \tag{8}$$

According to the BCS theory, $\alpha = 3.06$, while for a strong coupling material like lead the prefactor is $\alpha \approx 4$. In some alloys, sufficiently disordered so that κ_e is small and κ_p accounts for a large fraction of the normal-state thermal conductivity, one may observe a rise in the total conductivity as the sample enters into its superconducting domain. A classic example of this trend is lead–10% bismuth alloy [23]; see Fig. 2. Eventually, of course, the thermal conductivity must turn over and start decreasing as a function of temperature. This follows because the phonon population decreases as T falls, and phonon-defect scattering starts to dominate the transport at low temperatures.

As I have noted, the singularity represented by the phase transition at $T = T_c$ affects both the electronic and lattice thermal conductivities. Since the phonon contribution in high-T_c superconductors overwhelmingly dominates the total thermal conductivity even in the normal state, it is the decrease in phonon–electron (hole) scattering rate which is responsible for the change in the thermal conductivity as the sample is cooled past its transition temperature. The theoretical description of the behavior of the lattice thermal conductivity limited by carrier scattering was developed originally for the BCS model by Bardeen, Rickayzen, and Tewordt, the so-called BRT

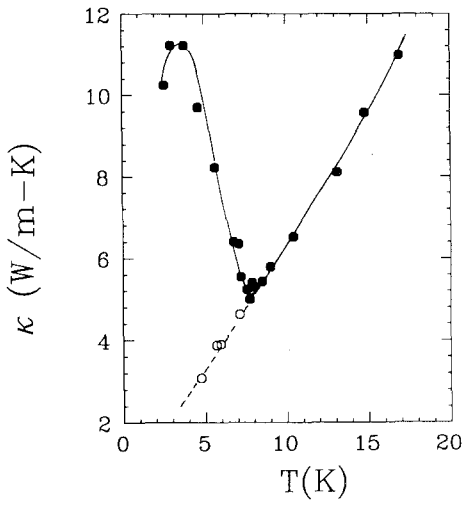

Fig. 2. Thermal conductivity of Pb–10% Bi alloy. Open symbols indicate normal-state data below the transition temperature. (Adapted from [23].)

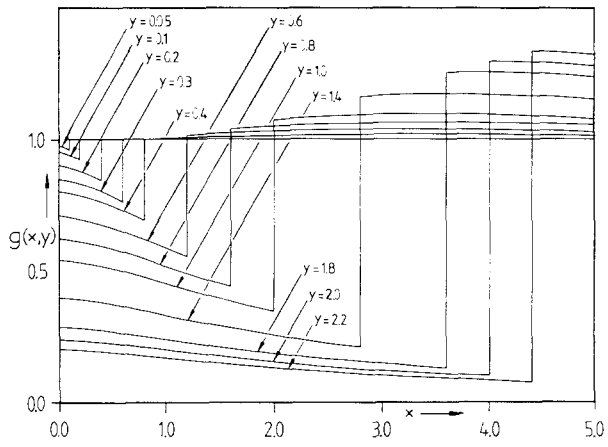

Fig. 3. The ratio of phonon relaxation times due to electron scattering in the normal and superconducting states, $\tau^n_{p-e}/\tau^s_{p-e} = g(x, y)$, from BRT theory. Here, $x = \hbar\omega/k_BT$ is the reduced phonon energy, and $y = \Delta(T)/k_BT$ is the reduced gap. (Taken from [24].)

theory, in [20]. Tewordt and Wölkhausen [24] have recently supplemented this theory by taking into account additional phonon scattering processes that might be appropriate when describing phonon transport in high-T_c superconductors. Writing the scattering terms individually and introducing the reduced temperature $t = T/T_c$, Eq. (5) becomes

$$\kappa_p(t) = At^3 \int_0^\infty dx \frac{x^4 e^x}{(e^x - 1)^2} \mathcal{F}(t, x) \qquad (9)$$

where

$$\mathcal{F}(t, x) = [1 + \alpha t^4 x^4 + \beta t^2 x^2 + \delta t x + \gamma t x g(x, y)]^{-1} \qquad (10)$$

The coefficient A refers to boundary scattering, and the Greek letters in Eq. (10) introduce terms representing point-defect scattering, sheetlike faults, dislocation scattering, and phonon–electron interaction, respectively. These coefficients are readily available in the literature. The term of greatest interest is the last term in Eq. (10), where the function $g(x, y)$ stands for the ratio of phonon–electron scattering times in the normal and superconducting states, i.e., $g(x, y) = \tau^n_{p-e}/\tau^s_{p-e}$. The exact form of $g(x, y)$ is given in [20] and it depends on the energy gap through the parameter $y = \Delta(T)/k_BT$. Figure 3 shows the dependence of $g(x, y)$ on x for several parameter values of y. With the parameter values used in [24], namely $A = 5\ \mathrm{Wcm^{-1}K^{-1}}$, $\alpha = 60$, $\beta = 35$, and $\delta = 0$, the phonon thermal conductivity for four different values of the parameter γ (proportional to the phonon–electron coupling strength) is reproduced in Fig. 4. In this plot, the function $y(t)$ is taken as a scaled BCS gap, $\Delta(T) = \chi\Delta_{BCS}(T)$, where $\chi = \Delta(0)/\Delta_{BCS}(0)$. It is clear from Fig. 4 that $\kappa_p(t)$ increases sharply at $t = 1$ and reaches a broad peak near $t = 0.5$. By increasing the parameter γ, the maximum value of κ_p shifts to lower temperatures. For a fixed value of γ (the solid curve in Fig. 4) the maximum increases and shifts to higher temperatures as the scaling parameter χ is increased from weak to strong coupling values. In spite of the fact that the above computations are limited to longitudinal acoustic phonons only, the shape of the curves in Fig. 4 is, as we shall see later, in remarkably good

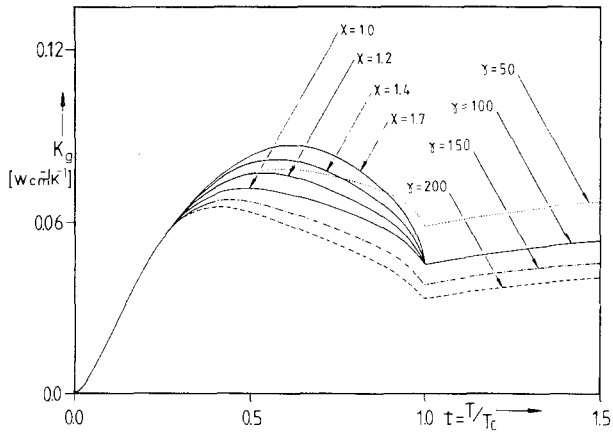

Fig. 4. Lattice thermal conductivity versus reduced temperature calculated from BRT theory for different values of the parameters γ (proportional to the strength of phonon–electron coupling), and $\chi = \Delta(0)/\Delta_{BCS}(0)$. The other parameters are $A = 5\ \mathrm{Wcm^{-1}\,K^{-1}}$, $\alpha = 60$, $\beta = 35$, and $\delta = 0$. (Taken from [24].)

agreement with the actual temperature dependence of the thermal conductivity of $YBa_2Cu_3O_{7-\delta}$. Tewordt and Wölkhausen have used this model to estimate the strength of the phonon-electron (hole) interaction. In principle, this theory should be very valuable for estimating anisotropy in phonon-electron coupling once reliable data on the thermal conductivity of single crystals in the c-direction become available.

Most recently, Tewordt and Wölkhausen [25] have extended their theory of the phonon thermal conductivity in high-T_c superconductors to the strong-coupling limit for both s- and d-wave pairing mechanisms. The authors calculate the in-plane, κ_{ab}, as well as out-of-plane, κ_c, components of the thermal conductivity by taking into account the anisotropy of the phonon-electron interaction and momentum conservation in the ab plane (the basic assumption being that the charge carriers in the ab plane can absorb or emit only the component parallel, $q_\parallel$, to the ab plane of the total phonon momentum). Calculations confirm the existence of a characteristic rise and maximum in κ_{ab} below T_c and, even though drastically reduced, a similar feature is also predicted for the out-of-plane thermal conductivity, κ_c. Experimentally, none of the existing investigations of κ_c shows any such behavior at or below T_c. It is possible that either the phonon-carrier relaxation rate is much more anisotropic than that assumed in [25] (proportional to $(q_\parallel/q)^3$) or that the phonon-defect (e.g., stacking faults) scattering is, by far, the dominant relaxation process. From Fig. 5 we note that the thermal conductivity calculated under the assumption of a strong-coupling s-wave pairing exhibits a very steep upturn at T_c, much steeper than a prediction based on the BCS model and in discord with the experimental data that suggest a more gradual upturn. On the other hand, the rounding off just below T_c predicted by a strong-coupling d-wave pairing (see Fig. 6) appears more in line with experiments, and Tewordt and Wölkhausen conclude that d-wave pairing gives a better fit to the data than does s-wave pairing. They point out, however, that an extended s-wave gap having nodes on the Fermi line yields the same results as a d-wave gap.

3.2. Effect of Circulatory Currents on Thermal Conductivity

In the previous section, I have indicated that the superconducting condensate affects the thermal conductivity of a superconductor primarily because Cooper pairs carry no entropy and do not scatter phonons. Theoretically, the onset of superconductivity alters the boundary conditions applicable to measurements of the thermal conductivity and this gives rise to an additional effect, the so-called circulatory thermal conductivity contribution. In traditional superconductors this contribution is negligible. Because it potentially plays a greater role in high-T_c superconductors, I include here a brief discussion of this effect.

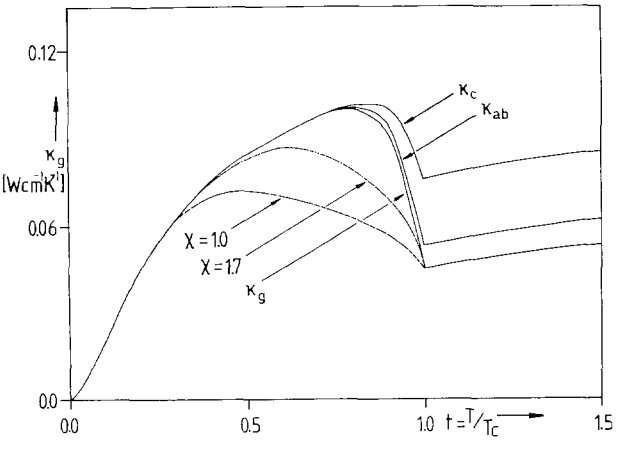

Fig. 5. Phonon thermal conductivity: κ_g (isotropic), κ_{ab} (in-plane), and κ_c (out-of-plane) plotted against $t = T/T_c$. Solid lines: strong-coupling s-wave. Dashed line: BCS. Dotted line: scaled gap ($\chi = 1.7$). Parameter values for the scattering terms are the same as used in Fig. 4. (Taken from [25].)

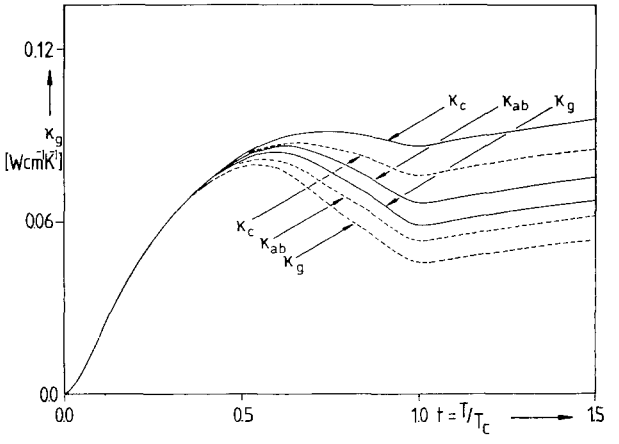

Fig. 6. Phonon thermal conductivity for d-wave pairing state ($T_c \simeq 90$ K, $2\Delta/k_BT_c \simeq 4.1$). The notation is the same as in Fig. 5. (Taken from [25].)

The existence of circulatory thermal conductivity was first pointed out by Ginzburg [26] back in 1944. Due to the fact that in traditional superconductors this effect plays virtually no role and is beyond the means of experimental verification, the circulatory contribution to the thermal conductivity has been shrouded in obscurity. The essential features of the effect are as follows.

When measuring thermal conductivity, it is convenient to put the specimen on open electrical circuit, i.e. maintain the current $j=0$. In this case, the diffusion of electrons down the temperature gradient is being opposed by the thermoelectric voltage. The measured electronic thermal conductivity, κ_e, is thus smaller than the thermal conductivity which would arise if the electric field E, rather than the current, were kept equal to zero and the thermoelectric voltage was not opposing the electron diffusion. Designating the extra heat conductivity when $E=0$ as κ_j, it is easy to show, starting from the phenomenological equations for generalized fluxes and forces [27], that the ratio

$$\frac{\kappa_j}{\kappa_e}=\frac{S^2}{L_o}=\frac{3e^2S^2}{\pi^2k_B^2} \tag{11}$$

where S is thermopower and L_0 is the Sommerfeld value of the Lorenz ratio. For typical metal near room temperature with $S\sim 5\ \mu\mathrm{VK}^{-1}$, the extra heat conductivity is $\kappa_j\sim 10^{-3}\kappa_e$, with much smaller values predicted at lower temperatures.

In superconductors, the situation is somewhat different. While measurements of $\kappa(T)$ are still done subject to the condition $j=0$, there is no thermoelectric voltage present, i.e., $E=0$ at the same time. The diffusion of electrons down the temperature gradient is thus unopposed by the electric field. The overall zero current condition is maintained by a counterflow of superconducting current so that

$$j=j_n+j_s=0 \tag{12}$$

Diffusion of the normal carriers is, then, subject to the boundary conditions $E=0$ and $j_n\neq 0$. Therefore, the thermal conductivity is enhanced over the value $\kappa_e(j=0)$. The extra heat conduction is, in this case, called the circulatory thermal conductivity, κ_j. Since the normal carriers each carry energy $\Delta(T)$ relative to the superconducting carriers, the contribution κ_j can now be larger than the value implied by Eq. (11) (for normal metals) at the same temperature. The factor $S/(k_B/e)$ for the normal metal case (representing the weighted mean energy of carriers relative to the thermal energy) is replaced by $\Delta(T)/k_BT$ so that Eq. (11), applicable now to superconductors, becomes

$$\frac{\kappa_j}{\kappa_e}=\frac{3eS_n\Delta(T)}{\pi^2k_B^2T} \tag{13}$$

where S_n is the thermopower for the normal electrons alone. Equation (13) is essentially the formula used in the recent paper by Ginzburg [28]. Again, inserting typical values for conventional superconductors ($T_c\sim 10$ K), the ratio κ_j/κ_e is of the order of 10^{-3}. For high-T_c superconductors, the energy difference between normal and superconducting carriers ($\sim k_BT_c$) is much larger, so, in principle, the potential for a significant contribution from κ_j to the thermal conductivity arises. Ginzburg uses the free electron model, i.e., approximates Eq. (13) by $\Delta(T)/\varepsilon_F$ ($\approx k_BT_c/\varepsilon_F$) which, for $T_c\sim 100$ K and $\varepsilon_F\sim 0.1$ eV, yields $\kappa_j/\kappa_e\sim 0.1$. Although κ_j now represents a significant enhancement of the electronic thermal conductivity, the term κ_e itself is typically only about 10% of the total thermal conductivity in sintered high-T_c materials and, thus, κ_j has little effect on the overall thermal conductivity. In any case, the estimate of κ_j provided by Ginzburg (based on the free electron model) is probably too large. It seems more appropriate to use Eq. (13) directly and substitute in the value of the thermopower, a transport coefficient that has been extensively studied [29]. Taking a typical value of $S_n\sim 2\ \mu\mathrm{VK}^{-1}$ for $YBa_2Cu_3O_7$ just above T_c yields the ratio $\kappa_j/\kappa_e\leq 0.01$. Assuming that the thermopower of the normal carriers below T_c is similar to that just above T_c, the ratio κ_j/κ_e should be proportional to the thermopower. Even though the electronic thermal conductivity, κ_e, in high-T_c single crystals is larger than that in sintered ceramics (estimates range from 30–50% of the total thermal conductivity), the thermopower remains small and the circulatory thermal conductivity is not likely to make an important contribution to the total heat transport. I therefore do not believe that any of the specific features of the heat transport in high-T_c superconductors that will be discussed in Section 4 can be accounted for by this circulatory heat contribution.

3.3. Thermal Conductivity of Superconductors in a Magnetic Field

It is well known that a magnetic field tends to destroy the superconducting state at $T<T_c$ via a

first-order phase transition. The way in which the field affects kinetic coefficients such as the thermal conductivity is rather complex and depends on how the flux enters a superconductor, i.e., what type of a superconductor is under observation. In type-I materials, in the intermediate state, the thermal conductivity is influenced not only by the presence of normal and superconducting lamellae [30] that have different thermal conductivities but also by Andreev-type reflection [31] of electron excitations at the boundaries between the normal and superconducting regions. In general, the existence of the lamellar structure leads to a reduction in the thermal conductivity because the phonon mean-free path decreases as the phonons pass from the superconducting into the normal phase. In the case of the Andreev process, it is the peculiar nature of the reflection of electron excitations that affects the heat transfer process. Discussion of these rather complicated phenomena can be found in a monograph by Saint-James *et al.* [32] and references therein. Since the vast majority of practical superconductors are type-II materials, high-T_c perovskites included, we now consider the effect of a magnetic field on these structures.

A characteristic feature of type-II superconductors is a particular kind of mixed state in which single-quanta flux lines (Abrikosov's vortex filaments [33] or fluxoids) penetrate the superconductor in a regular two-dimensional lattice once the magnetic field exceeds a certain limiting value called the lower critical field, H_{c_1}. For fields close to H_{c_1}, the flux lines are widely separated (~penetration depth). As the field increases, the density of fluxoids increases and their average separation decreases as $d \sim H^{-1/2}$. The superconducting phase is thus gradually squeezed out and, at $H = H_{c_2}$, where the normal regions overlap, superconductivity cannot be sustained anywhere in the sample volume. The presence of fluxoids in the mixed state alters the heat conduction of traditional superconductors in the following ways: The fluxoid structure serves as an additional scattering center for both phonons (usually at temperatures well below T_c where phonons dominate the transport) and electronic excitations (typically near T_c where the electronic excitations are plentiful). This additional scattering degrades the thermal conductivity. On the other hand, in fields approaching H_{c_2}, the single particle excitations associated with the normal core of the vortex begin to enhance the thermal conductivity. It is thus a well documented fact [34–36] (see Fig. 7) that the thermal conductivity of a conventional type-II superconductor in its mixed state shows a distinct

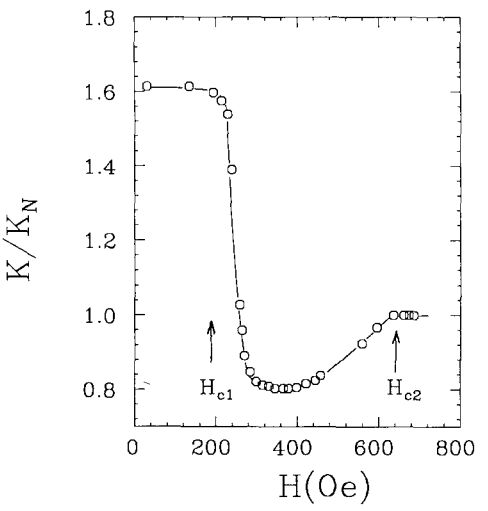

Fig. 7. The magnetic field dependence of the thermal conductivity of In–4 at.% Bi normalized to the normal-state conductivity. The lower, H_{c1}, and the upper, H_{c2}, critical fields are indicated. (Adapted from [34].)

minimum for magnetic fields in the range $H_{c_1} < H < H_{c_2}$. It should be noted that in the Meissner state, i.e., for $H < H_{c_1}$ where the field does not penetrate the sample, the thermal conductivity is field independent. As the fluxoids enter the sample at $H > H_{c_1}$, scattering of heat carriers sets in. Obviously, in all "practical" conventional superconductors (those with high H_{c_2} where pinning is strong and the electronic mean-free path, l_e, is necessarily small) l_e is likely to be smaller than the spacing between fluxoids and, therefore, the fluxoids cannot play a significant role as scatterers of electrons. For phonons the situation is entirely different. Since the mean-free path of phonons is usually larger than the spacing between the fluxoids even for rather low magnetic fields, phonon interaction with the fluxoid structure leads to a significant reduction in the thermal conductivity. Fluxoids can act as geometrical scattering centers of phonons provided the phonon wavelength is comparable to the size of the vortex core (~coherence length, ξ). This situation arises in conventional superconductors typically near and above 10 K. At very low temperatures, the phonon wavelength may exceed the coherence length and fluxoids lose their effectiveness as geometrical scattering centers for phonons. Nevertheless, the interaction of phonons with electronic excitations within the vortex cores may intensify and, in this context, the fluxoids can still cause a reduction in the phonon thermal conductivity of a superconductor in its mixed state.

Although an increasing magnetic field reduces the average spacing between fluxoids, the interaction among the vortices tends to stabilize the structure into a regular network. Thus, on average, the sample may look more homogeneous, i.e., potentially less resistive to the heat flow. At the same time, as the number of electronic excitations increases and the fluxoids come closer together, there exists the possibility [37] that single-particle excitations may tunnel from core to core. Consequently, as the magnetic field increases, the increasing contribution from electronic excitations results in a minimum followed by a rapid rise in the thermal conductivity that continues up to $H = H_{c_2}$. For $H > H_{c_2}$, the thermal conductivity is, again, essentially field independent. How the normal state conductivity is approached from below H_{c_2} depends on the ratio of the electronic mean-free path to the coherence length, l_e/ξ, i.e., on whether the superconductor is in the "clean" or "dirty" limit. While a general theory describing the behavior of the thermal conductivity in the mixed state does not yet exist, theoretical models pertaining to variations in the conductivity near H_{c_1} and H_{c_2} have been developed. The thermal conductivity of a "clean" type-II superconductor near H_{c_1} was considered by Cleary [38], and the behavior of the conductivity near H_{c_2} was treated by Caroli and Cyrot [39] in the "dirty" limit approximation and by Maki [40] and Houghton and Maki [41] in the "clean" limit. Without going into much detail, it is worth pointing out the distinctly different manner in which the thermal conductivity approaches the normal state as $H \to H_{c_2}$ in the clean and dirty cases. In dirty type-II superconductors ($l_e \ll \xi$) the thermal conductivity rises linearly as H approaches H_{c_2}. In the clean limit, on the other hand, the theory of Maki predicts a $(H_{c_2}\text{-}H)^{1/2}$ behavior near H_{c_2} and thus the conductivity approaches the normal state with a very large (essentially infinite) slope. While these predictions have been substantially confirmed in a number of measurements on elemental (niobium, vanadium) as well as alloyed type-II superconductors, the experimental situation is frequently complicated by additional effects. Among the most interesting are fluxoid pinning [34-36], which gives rise to a hysteresis in the field dependence of the thermal conductivity, and the fact that the conductivity usually shows a significant degree of anisotropy [34,36] when it is measured parallel and perpendicular to the fluxoid lattice. For details the reader is referred to the original papers.

What effect can one expect if high-T_c superconductors are subjected to an external magnetic field while their thermal conductivity is being measured? Since the free carrier contribution to the thermal conductivity in sintered samples is on the order of or less than 10% of the total conductivity, carrier-fluxoid scattering will be difficult to observe even for magnetic fields close to H_{c_2} and at high temperatures. On the other hand, the compact fluxoid cores in high-T_c materials ($\xi \sim 10$-30 Å) may act as efficient scattering centers for phonons near T_c where the phonon wavelength is comparable to ξ. Since H_{c_1} is very low, significant phonon-fluxoid scattering might take place at fairly low external fields. As the field increases, interactions with fluxoids should intensify and, because the electronic (hole) excitations are not expected to contribute in a significant way, this may result in a decrease in the thermal conductivity over a wide range of magnetic fields $H > H_{c_1}$. Another effect could possibly arise from the fact that in the temperature range below T_c, the zero-field thermal conductivity actually increases with decreasing temperature and reaches a maximum near $T_c/2$ that depends sensitively on the frequency of phonon-carrier processes relative to all other dissipative mechanisms. The introduction of an additional phonon scattering channel via fluxoids might lead to a marked reduction in the thermal conductivity peak. Latest experimental data illustrating the role of fluxoid scattering in single crystals of $YBa_2Cu_3O_7$ are presented in Section 4.2.1.

Finally, a couple of comments regarding the possibility of utilizing superconductors as thermal switches. Prior to the widespread use of dilution refrigerators, much interest centered on a practical use of the very high ratio in pure superconductors (Pb, Sn, Ta, Zn) of the thermal conductivity in the superconducting and normal states, the latter realized below T_c using an external field $H > H_c$. The high ratio arises from very different temperature dependences for the phonon and electron scattering mechanisms at low temperatures, namely a T^3 variation characteristic of boundary scattering of phonons as opposed to the T-linear behavior of electron-defect interactions. The conductivity ratio, $\kappa_{e,d}/\kappa_{p,b}$, is then proportional to T^{-2} and can reach magnitudes in the tens of thousands. Thermal switches of this kind were first explored by Heer and Daunt [42]. In high-T_c superconductors it is impossible to realize such a situation. Apart from the fact that the electronic thermal conductivity is small, high-T_c materials are type-II superconductors with an extremely high upper critical field and a large temperature derivative of H_{c_2}. This leaves only a few

degrees below T_c where the sample can be driven normal using typical laboratory magnets. Within this limited temperature range the reduced temperature, T/T_c, changes very little.

3.4. Tunneling States and Thermal Conductivity

It is well known [43] that glasses and amorphous systems in general have highly anomalous thermal properties at low temperatures, the origin of which can be traced to structural or orientational disorder in the system. Recently, a surprising observation of a glassy character in the thermal properties of mixed crystals of $KBr_{1-x}(CN)_x$ for a wide range of x was made by De Yoreo *et al.* [44]. In this case, the disorder arises from the random orientation of the CN impurity in the KBr crystal. Thus, the glassy character in the thermal transport need not be limited to an amorphous medium only, but may, under certain circumstances, extend to systems that one would normally view as crystalline solids.

It is no secret that numerous aspects of the physical properties of high-T_c superconductors are puzzling. Among such intriguing results are the data on sound velocity, ultrasonic attenuation, and internal friction that could be interpreted in terms of tunneling processes taking place in these materials [45–47]. Possible tunneling entities suggested include oxygen, oxygen vacancies, and even atomic disorder in the twin domains. Indeed, the T^2-temperature dependence of the thermal conductivity [48] of single crystalline $YBa_2Cu_3O_{7-\delta}$ below 1 K and sintered $La_{2-x}Sr_xCuO_4$ in the 1–10 K range [49] was viewed as an indication of the presence of two-level tunneling systems. While it is far from certain that this is the only possible interpretation of the data, the question of the existence of tunneling states in the high-T_c superconductors is, perhaps, worth considering. I, therefore, briefly outline the fundamental ingredients of the tunneling state model and how such tunneling states might influence phonon transport.

A remarkable aspect of amorphous solids is the fact that they dramatically demonstrate the shortcomings of the Debye model of solids. For a number of decades, solid state physicists were accustomed to treating atomic size disorder at low temperatures as being of no consequence to the flow of phonons. The argument was simple and well understood: because the phonon wavelength at low temperatures is very large (for $T < 1$ K typically $\lambda > 1000$ Å), the atomic scale structural disorder should have no effect on the lattice thermal conductivity of solids. According to Debye, a solid should, in this case, be viewed as an elastic continuum with a specific heat proportional to T^3 and a thermal conductivity limited by the scattering of phonons on crystallite boundaries. It was a stunning revelation then when Zeller and Pohl [50] drew attention to the fact that for a wide range of amorphous systems, the specific heat and thermal conductivity at low temperatures do not conform to the Debye model. An unexpectedly large specific heat with a linear T-dependence combined with an unusual T^2-variation in the thermal conductivity was observed in a broad range of amorphous materials (glasses, plastics, greases), suggesting that these properties were universal for this class of solids. Numerous attempts have been made to explain this so-called glassy character, usually by invoking some kind of microscopic inhomogeneity that affects phonon scattering. The model that is believed to describe the essential physics and that is most frequently called upon to explain the data is the tunneling state model (TS) developed independently by Phillips [51] and by Anderson *et al.* [52]. This phenomenological model is based on the idea that in a disordered solid, unlike a crystalline one, certain atoms or groups of atoms can occupy two different configurational states represented by a double-well potential (see Fig. 8). While the tunneling entities are never precisely identified, their tunneling through the barrier of the double-well results in an energy splitting of the ground state. At sufficiently low temperatures, higher energy states need not be considered. Assuming a barrier asymmetry Δ, it can be shown [51] that the energy splitting is

$$E = (\Delta^2 + \Delta_0^2)^{1/2} \tag{14}$$

where Δ_0 is the splitting in the absence of asymmetry ($\Delta = 0$). Because of the disordered nature of the

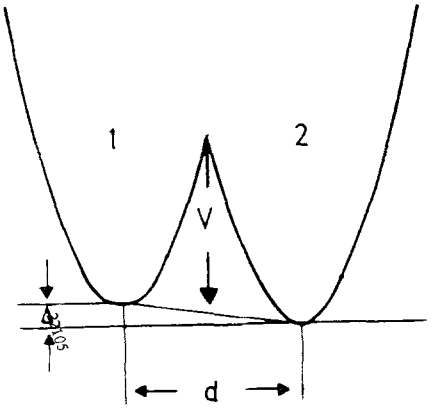

Fig. 8. Conceptual model of the asymmetric double-well potential.

amorphous state, one expects a broad distribution of potential barriers and asymmetries and, consequently, a wide range of TS relaxation times. Under these conditions it is reasonable to assume that the density of TS, $n(E)$, is approximately constant. This is required in order to explain the observed linear specific heat at low temperatures [43]. The quadratic temperature dependence of the thermal conductivity below 1 K is believed to arise from the resonant scattering of phonons on localized two-level states. In this case, the relaxation time for the ith phonon mode can be written as [53]

$$\tau_i^{-1} = \frac{\pi\gamma_i^2}{\hbar\rho v_i^2}\left(\frac{\Delta_o}{E}\right)^2 n(E)\hbar\omega \tanh\left(\frac{E}{2k_BT}\right) \quad (15)$$

where γ is the TS-phonon coupling constant, v_i is the ith mode velocity, and ρ is the density. Assuming, for simplicity, a perfectly symmetric double-well (i.e., $\Delta = 0$ and, hence, $\Delta_0/E = 1$), the phonon mean-free path due to resonant scattering on TS becomes

$$l_i^{-1}(T,\omega) = \frac{\pi\gamma_i^2}{\hbar\rho v_i^3}\bar{P}\hbar\omega \tanh\left(\frac{\hbar\omega}{2k_BT}\right) \quad (16)$$

where $\bar{P}$ is the density of TS in a symmetric double-well. Substituting Eq. (16) into Eq. (5) yields the quadratic temperature dependence of the thermal conductivity,

$$\kappa(T) = 4.93\left(\frac{k_B}{\pi^3\hbar^2}\right)\left(\frac{\rho v}{\bar{P}\gamma^2}\right)T^2 \quad (17)$$

It should be noted that the thermal conductivity of glasses, apart from its characteristic T^2 variation at low temperatures, is also notable for a "plateau" region near 10 K. This plateau does not arise as a direct consequence of the presence of tunneling states. Rather, it is believed that it has its origin in strong frequency-dependent phonon scattering that makes an amorphous solid act essentially as a low-pass phonon filter [43]. Whether tunneling states are the governing factor in the low-temperature thermal properties of high-T_c superconductors is a much debated issue. The model certainly has an aesthetic appeal, but it is not yet certain if it can withstand rigorous scientific scrutiny. I shall note relevant experimental situations when discussing specific high-T_c materials in the next section.

4. HEAT CONDUCTION IN HIGH-T_c SUPERCONDUCTORS

In the previous section I have outlined the key features that characterize thermal transport in superconductors in general. We now turn our attention to the behavior of the thermal conductivity in high-T_c superconductors. I shall illustrate their typical features, point out common elements in their heat transport processes, and highlight differences in their thermal conductivity as compared to traditional superconductors. I shall also discuss the information provided by the magnitude and temperature dependence of the thermal conductivity that pertains to the mechanism responsible for superconductivity in the 100 K range, and the physical parameters that can be extracted from such data.

The phenomenon that is referred to as high-T_c superconductivity occurs in a class of materials called perovskites. While the vast majority of perovskites are insulators (ferroelectrics), an intensive search over the past couple of years has led to the discovery of several superconducting perovskite systems with transition temperatures exceeding 23 K, the plateau reached by conventional superconductors. The high-T_c perovskites can be broadly grouped into the following families:

1. $La_{2-x}M_xCuO_4$ (M = Ca,Sr,Ba) with T_c's up to 40 K,
2. $MBa_2Cu_3O_{7-\delta}$ (M = Y or rare earth) with a typical T_c of 92 K,
3. $Bi_2(Ca,Sr)_{n+1}Cu_nO_{2n+4}$ with T_c as high as 115 K depending on the index n,
4. $Tl_2(Ca,Ba)_{n+1}Cu_nO_{2n+4}$ with the highest T_c reaching 125 K.

A characteristic feature of all the above perovskites is the presence of nearly two-dimensional Cu–O sheets believed to contain the essential ingredients of superconductivity. The first two groups, namely the 40 K and 92 K superconducting families, are somewhat special in that they are sensitive to oxygen stoichiometry. This is reflected in the dependence of both the superconducting and normal-state properties on the conditions of synthesis (namely the annealing treatment) as well as in their sensitivity to environmental factors such as humidity.

To the four groups above we could add Cu-free perovskites based on $Ba(Pb_{1-x}Bi_x)O_3$ which were found [54] in 1975 to be superconducting in the 13 K range, and the recently identified [55,56] $Ba_{1-x}K_xBiO_3$ compound which exhibits superconductivity at temperatures up to 30 K. These two systems are interesting not only for their lack of Cu ions and their cubic crystal structure, but because they may form an important bridge between conventional and high-T_c superconductors.

To make this review more tractable, I group the experimental data according to the schema above, even if this division is somewhat artificial.

4.1. $La_{2-x}Sr_xCuO_4$

The La family of perovskites has a layered K_2NiF_4-type structure with quasi-two-dimensional Cu-O sheets where strong antiferromagnetic correlations play a prominent role. The parent material, La_2CuO_4, is an orthorhombic insulator that undergoes a phase transition to a tetragonal configuration near 530 K. La_2CuO_4 is strongly antiferromagnetic with a Néel temperature near 230 K and about 0.5 μ_B/Cu atom [57]. The existence of a long-range magnetic order in this system has stimulated considerable theoretical interest and several attempts have been made to describe superconductivity in this family of materials as being intimately related to the magnetic state of the system [58]. By slightly changing the ratio of La/Cu atoms or by applying high oxygen pressure during the preparation process, La_2CuO_4 itself was shown [59,60] to undergo a superconducting transition. Because of a very small Meissner volume ($< 10\%$), it is believed that this superconducting state of La_2CuO_4 is of a filamentary nature. With a standard valency of La(3+) and O(2−), the formal valence state of Cu in the parent structure is 2+, i.e., a d^9 configuration. As one dopes La_2CuO_4 with 2+ ions such as Sr or Ba, one effectively withdraws an electron or, equivalently, introduces a hole into the Cu-O band. Where exactly the hole is located or, more specifically, whether the d^8 configuration exists (implying the presence of a Cu^{3+} ion if the hole is attached to copper) was a matter of contention early in the game. For our purposes it suffices to note that as the amount of dopant increases, the interplanar magnetic coupling weakens dramatically and this leads to a sharp drop in the Néel temperature and a vanishing of the $3d$ magnetic order. At the same time, the material shows a progressively stronger metallic character and, near $x = 0.05$, superconductivity sets in. The maximum transition temperature (~40 K) is observed around $x = 0.15$. Doping to levels of $x \sim 0.15$–0.2 has virtually no effect on the oxygen stoichiometry. However, the formation of solid solutions with still higher concentrations of the divalent ions does alter the amount of oxygen present and the appropriate representation for such structures should be $La_{2-x}Sr_xCuO_{4-y}$, i.e. as oxygen deficient perovskites. It is likely that the oxygen stoichiometry comes into play because the oxidation state of Cu becomes saturated. As a practical consequence, the value of the parameter y influences the low-temperature thermal conductivity. The key thermodynamic features of the La-based superconducting perovskites are summarized in the phase diagram (Fig. 9) reproduced from [61].

The first reports on the thermal transport behavior of high-T_c superconductors surfaced early in the summer of 1987, within a few months of the discovery of high-T_c superconductivity. For obvious reasons the measurements were made on sintered, i.e., polycrystalline, samples and this trend persisted until very recently when single crystals large enough for thermal conductivity measurements became available. The process of sintering results in a material that is less than 100% dense. As I have already noted, the voids in such samples effect the thermal conductivity in two ways: they scatter phonons, and reduce

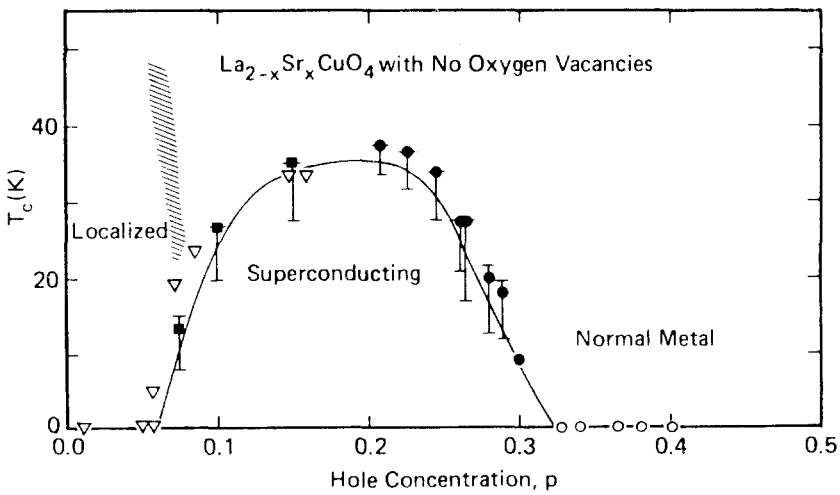

Fig. 9. Phase diagram of $La_{2-x}Sr_xCuO_4$. (Taken from [61].)

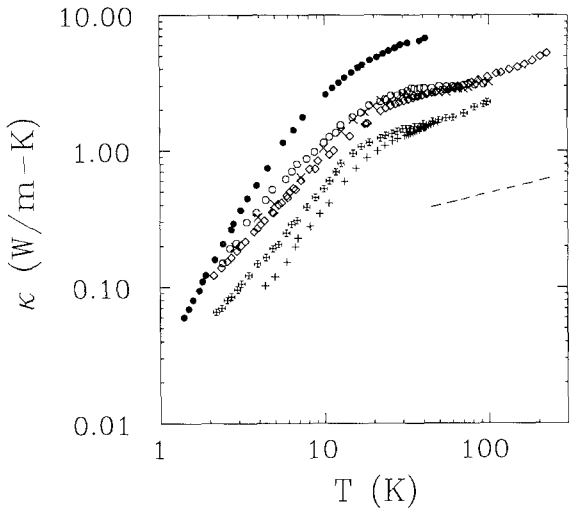

Fig. 10. Thermal conductivity of sintered $La_{2-x}Sr_xCuO_4$. ◇ Uher and Kaiser [62], $x=0.2$; +Bartkowski *et al.* [63], $x=0.2$; × Steglich *et al.* [65], $x=0.15$; ✣ Regueiro *et al.* [49], $x=0.15$; ○ Regueiro *et al.* [49], $x=0$; ● Bernasconi *et al.* [64], $x=0$. The estimated maximum electronic thermal conductivity for the sample of [62] is indicated by a broken line.

the volume fraction of the conducting medium, both adversely affecting the thermal conductivity. We thus expect a particular preparation process to be reflected in the magnitude of the thermal conductivity of the resulting samples, and this is clearly evident in Fig. 10 where the existing thermal conductivity data on sintered $La_{2-x}Sr_xCuO_4$ are collected. We note that while the temperature dependence of the conductivity is remarkably similar for all of the samples, regardless of the actual Sr content, we do see differences in the magnitude of up to a factor of 3 between sets of measurements where samples with nominally the same Sr concentration were investigated. This undoubtedly reflects the different sample density, porosity, and microstructure. As such information is not always provided in the original papers, its effect on the thermal conductivity is difficult to quantify. However, one does see quite clearly, comparing the data of Regueiro *et al.* for pure La_2CuO_4 with the 15% Sr-doped samples prepared under identical sintering conditions, the effect of additional scattering as the solid solution is formed. In general, the magnitude of the thermal conductivity is not large. To help to orient the reader one should note that above 50 K the heat conductivity is comparable to that of stainless steel.

In Section 3, I have pointed out that the transport of heat in the normal state of conventional superconductors is dominated by free charge carriers and that phonons play a secondary role. Is this also typical of high-T_c superconductors? The answer is no and this fact has overwhelming consequences for the behavior of the thermal conductivity at and below the superconducting transition temperature. This point will be particularly apparent when we discuss the thermal conductivity of the 1-2-3 compounds.

The lattice thermal conductivity, and, by Eq. (2), the electronic thermal conductivity as well, have been traditionally determined by one of two methods: by extrapolating the lattice thermal conductivity of alloys as a function of impurity content to zero impurity concentration, or, more elegantly, by making use of a strong transverse magnetic field and eliminating the charge carriers from the heat flow via a thermal equivalent of the Hall effect (Maggi-Righi-Leduc effect). Neither of these two methods is practical for high-T_c superconductors. I have noted the difficulty of making reproducible samples using sintering processes, and the magnetic field technique seems entirely out of the question due to the extremely low mobility of the charge carriers, only a few $cm^2V^{-1}sec^{-1}$ at best [66], even for single crystals. We can, however, make an estimate of the electronic thermal conductivity that can provide an upper bound on its magnitude. Assuming that the transport processes in perovskite superconductors are not so exotic that they totally invalidate the Wiedemann-Franz law, i.e., the relation between the electrical conductivity and the electronic part of the thermal conductivity,

$$L=\frac{\kappa_e}{\sigma T}=\frac{\rho\kappa_e}{T} \tag{18}$$

we can estimate the maximum possible value of κ_e from the measured electrical resistivity ρ and the Sommerfeld value of the Lorenz number $L_o = 2.44\times10^{-8}\,V^2\,K^{-2}$. I stress that this estimate yields only an upper bound on κ_e since L, and hence κ_e, will be lower if the relaxation times for the electrical and thermal processes are not equivalent, as is usually the case when the electron-phonon interaction is an important dissipative process.

Using data from [62], where electrical resistivity and κ were measured for the same samples, the estimated maximum electronic thermal conductivity is indicated in Fig. 10 by a broken line. We shall see later that a similar trend is observed in other high-T_c superconductors. Clearly, a distinguishing feature of high-T_c materials is the strong dominance of phonons over charge carriers in the normal-state heat transport of these structures. Approximately 80–90% of the heat

is carried by the lattice, in sharp contrast to conventional superconductors. The small carrier contribution to the thermal conductivity is a consequence not only of a short carrier mean-free path due to scattering on phonons and on the microstructure of the sample, but, primarily, of a significantly reduced free carrier density that is characteristic of these perovskite systems. Typical carrier densities here are some one to two orders of magnitude below the density is conventional superconductors.

With the lattice conductivity dominating the heat transport, and with the assumption of at least moderate phonon-carrier interaction, one would expect highly unusual behavior in the thermal conductivity as the sample is cooled through the superconducting transition temperature, T_c. While this is certainly true for high-T_c perovskites such as $YBa_2Cu_3O_7$ and Bi-based and Tl-based structures, all one can detect in ceramic forms of $La_{2-x}Sr_xCuO_4$ is a change in slope in the neighborhood of T_c. We note, however (see Fig. 15), that a modest rise in the thermal conductivity below T_c is observed in measurements on high-quality single crystals of $La_{1.96}Sr_{0.04}CuO_4$ when the heat flow is parallel to the copper-oxygen planes. In ceramic samples of the La family, the anomalous behavior near T_c is not well developed for two reasons: at these relatively low temperatures ($T_c \leq 40$ K), the rapid decline in the phonon population compensates for an increase in the phonon mean-free path, l_p, as the carriers condense, and strong phonon-defect scattering in ceramics sets a limit on the possible enhancement in l_p.

Let us now consider the temperature dependence of the thermal conductivity below T_c. The power law exponent in the low-temperature range depicted in Fig. 10 is about 1.4, a significantly slower variation than one would expect if boundary scattering dominates the phonon transport. A comparison of the mean-free path l_p [calculated from Eq. (7) using the experimental data for the specific heat and the speed of sound] with the typical grain size in the samples (10–100 μm) confirms that intragrain phonon scattering is an important, and, in some cases, dominant, limiting process, and explains why the boundary scattering T^3 contribution is not detected. The question then arises: what is the mechanism by which phonons are scattered within the grains? Regueiro *et al.* [49] argued that the thermal properties of $La_{2-x}Sr_xCuO_4$ superconductors essentially reflect an amorphous system with two-level tunneling states (TS), and they proposed the existence of a polaronic glass where the key ingredient is oxygen vacancies. According to these authors, the disorder originates from oxygen vacancies and associated polarons that are responsible for a constant mean-free path at high temperatures, while the randomness in vacancy distribution gives rise to the tunneling states that scatter phonons at low temperatures. Supporting evidence for this point of view comes from sound velocity and internal friction measurements [67] that mimic some of the characteristic features of typical amorphous materials. As I have noted in Section 3.4, provided the distribution of the relaxation times is sufficiently broad, the total relaxation time for phonon scattering on TS is inversely proportional to phonon frequency ω and, hence, this process leads to the T^2 temperature dependence at low temperatures. Furthermore, relaxational scattering of phonons on TS would provide an explanation for the logarithmic temperature dependence of the sound velocity and could presumably also account for a linear term in the specific heat. The nonzero linear term ($\gamma \neq 0$) in the specific heat has been a very controversial issue both from an experimental standpoint (intrinsic effect or artifact of the preparation process?) and from a theoretical one. This issue is well covered in a review article published recently in this journal [68] and also in an overview by Stupp and Ginsberg [69].

I should point out that in spite of the strong appeal of possible tunneling states in high T_c perovskites similar to the TS in amorphous systems, one should exercise caution because the similarity may turn out to be more intuitive than substantive. As far as the thermal conductivity data are concerned, the temperature range covered in Fig. 10 is too narrow to allow a conclusive determination of the power law of the temperature dependence. Furthermore, even the primary experimental evidence (internal friction, sound velocity, specific heat) that led to the proposal of a TS picture contain features that differ significantly from those observed in classical amorphous systems. For instance, the TS-phonon interaction is expected to lead to a T^3 dependence of the internal friction, rather than the observed $T^{1.8}$ power law, and the γ-term in the specific heat of La-based superconducting perovskites in some one to two orders of magnitude larger than the values observed in typical amorphous metals and insulators. While some of these discrepancies may be the result of the presence of impurity phases (either metallic or insulating) in the ceramic structure, I do not believe that the overall picture is fully clarified and further detailed studies are certainly needed to shed more light on this problem.

Two areas of thermal transport investigation that may be particularly relevant to the question of phonon scattering in La-based high-T_c superconductors are measurements on ceramic samples at temperatures below 1 K, and the study of the thermal conductivity of single crystals of both pure and Sr-doped La_2CuO_4. Recently such investigations have been undertaken. Figure 11 shows low-temperature thermal conductivities obtained by Uher and Cohn [70] on ceramic, Sr-doped samples with $x = 0.2$ (similar to the sample of Fig. 10), $x = 0.1$, and $x = 0.25$, the latter with a T_c of 15 K (for transition to the zero resistance state), prepared under identical conditions. Before I proceed to discuss the data, a comment on the sample with $x = 0.1$ is required. The 10% Sr content should have resulted in bulk superconductivity in this sample. Apparently due to imperfect homogenization, rather than showing a zero resistance transition, this sample displayed activated behavior that could be fitted [71] to Mott's variable-range hopping equation (see inset in Fig. 11) with an exponent of 1/4 and $T_0 \sim 432$ K. This implies a localization length in the range 20–35 Å, i.e., the system is near the metal-insulator transition. Furthermore, susceptibility and magnetoresistance studies on this sample clearly indicate the existence of superconducting islands up to 35 K, but these entities remain unconnected at all temperatures.

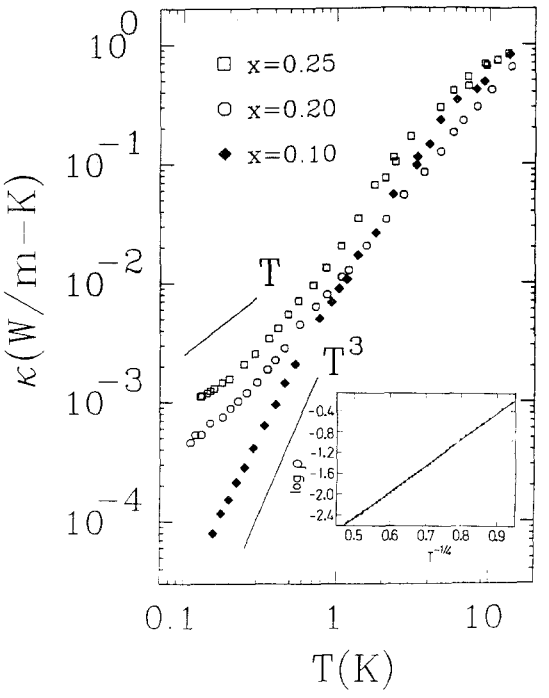

Fig. 11. Low-temperature thermal conductivity of $La_{2-x}Sr_xCuO_4$ compounds. The inset shows variable-range hopping behavior for the sample with $x = 0.1$. (Adapted from [70].)

Referring to Fig. 11, we note that in the temperature range $2 \leq T \leq 15$ K, the behavior of the thermal conductivity is comparable in all the samples (but clearly weaker than T^2). Dramatic differences become apparent at temperatures below about 0.5 K. The two samples with high Sr content, $x = 0.2$ and $x = 0.25$, show a weakening of their temperature dependence and a T-linear limiting behavior. On the other hand, the conductivity for the sample with $x = 0.1$ decreases proportional to T^3, suggesting that the phonon mean-free path is fixed by boundary scattering. As a result, near 100 mK, the two highly doped samples are more than an order of magnitude better at conducting heat than the sample with a Sr content of $x = 0.1$. This is a very surprising result since the temperature is two orders of magnitude below T_c and, according to the theoretical ideas of Section 3, the condensed carriers should be entirely removed from the heat conduction process, leaving only phonons for heat transport. Since the phonon spectrum should not change significantly when the Sr concentration is varied from 0.1 to 0.25, and since at $T \ll T_c$, the phonons should not care whether or not the superconducting condensate is spatially restricted, why do such markedly different behaviors arise at the lowest temperatures?

To clarify this point, the sample with a Sr content of $x = 0.2$ was vacuum annealed (900°C for 4 h) to eliminate any trace of superconductivity, and its thermal conductivity was measured again. The data are presented in Fig. 12 which, for comparison, also

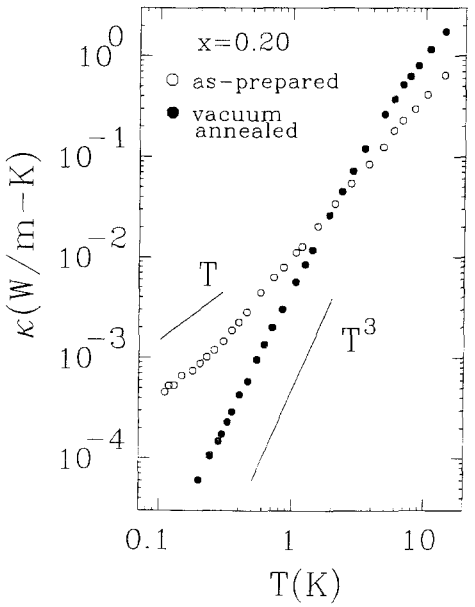

Fig. 12. Thermal conductivity of sintered $La_{1.8}Sr_{0.2}CuO_4$ before and after vacuum annealing. (Taken from [70].)

shows the original results on $x = 0.2$ given in Fig. 11. As one can readily see, the vacuum-annealed sample shows no low-temperature "pulling" as did the original material; it obeys a T^3 variation below 1 K and, in general, its thermal conductivity is very similar to the sample with $x = 0.1$ shown in the previous figure. It should be stressed that the microstructure of the vacuum-annealed sample is indistinguishable from the original sample that exhibited superconductivity, as one can see by inspecting scanning electron micrographs (see Fig. 13). This experiment then indicates that, for ceramic forms of $La_{2-x}Sr_xCuO_4$ that are insulating or where superconductivity is restricted to unconnected grains, the thermal conductivity is ultimately limited by phonon scattering on the crystal boundaries. Within the Debye model, the mean-free path, l_p, can be estimated [72] from the expression

$$\kappa_p = \frac{2\pi^2 k_B^4 l_p}{15\hbar^3 v^2} T^3 \tag{19}$$

where v is the velocity of sound. Taking $v = 5000\ \mathrm{ms}^{-1}$, the resulting $l_p \sim 9$–$10\ \mu$m is in good agreement with the range of grain and pore sizes evident in the SEM micrographs.

The weak temperature dependence and the crossover to a T-linear variation below about 0.3 K that are observed in the low-temperature thermal conductivity of superconducting $La_{2-x}Sr_xCuO_4$ ceramics suggest that an additional heat-conducting mechanism is operating in these structures. It is interesting to note that this behavior is reminiscent of that in low-carrier-density semimetals such as Bi [73] or graphite [74]. At very low temperatures, where the phonon contribution decreases rapidly, even a small number of carriers (in the case of Bi only about 10^{17} carriers/cm^3) may dominate the heat transport. A linear variation in the thermal conductivity is expected in the regime where carriers are scattered by impurities and defects. It has been proposed in [70] that a similar situation occurs in superconducting La-based ceramics. As we shall see later, this scenario has also been put forward to account for the behavior of 1-2-3 compounds [62,75]. The question arises, what is the origin of these normal carriers at temperatures far below T_c, where quasiparticle excitations should be entirely negligible? One possibility is that the carriers are of extrinsic origin due to compositional inhomogeneities, for example, impurity phases at interfaces and grain boundaries. An argument against this interpretation is the behavior of the $x = 0.1$ sample, which is undoubtedly inhomogeneous in the above sense, yet shows no evidence of free-carrier transport in its thermal conductivity. A more intriguing possibility is that normal carriers well below T_c are intrinsic to the superconducting phase. This could be, in principle, a consequence of coexisting superconducting and normal bands. Hall measurements [76,77] provide evidence for hole conduction in a single band for $x \leq 0.15$. Higher Sr doping leads to the formation of oxygen vacancies, an apparent decrease in hole concentration, and multi-band conduction involving some negative carriers. In this context, the thermal conductivity at very low temperatures can be understood if the electrons arising

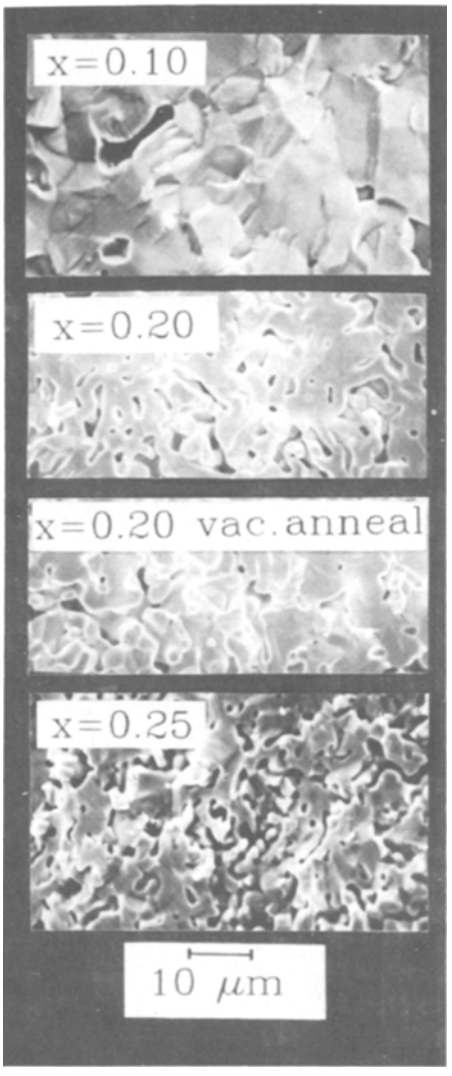

Fig. 13. Scanning electron micrographs of three samples of $La_{2-x}Sr_xCuO_4$ for which thermal conductivities are shown in Fig. 11, and of the vacuum annealed $x = 0.2$ specimen from Fig. 12. (Taken from [70].)

at higher Sr concentrations do not participate in superconductivity and thus contribute to the heat transport even well below T_c. The insulating behavior of the vacuum-annealed $x = 0.2$ sample is presumably a consequence of a shift of the Fermi level to a region of localized electronic states which eliminates the carrier contribution. The striking similarity in the behavior of the thermal conductivity of the vacuum-annealed sample with $x = 0.2$ and the sample with $x = 0.1$ (showing superconductivity within the unconnected grains) supports this interpretation.

What fraction of normal carriers is implied by the low-temperature thermal conductivity data? An approximate estimate can be obtained by calculating an effective residual resistivity, ρ_0^{eff}, (applying the Wiedemann–Franz law to the data of Fig. 11), and comparing it with a linear extrapolation of the normal-state resistivity to zero temperature, ρ_0^{extr} (for details see [70]). The ratio $\rho_0^{extr}/\rho_0^{eff}$ turns out to be about 0.15 and provides a rough estimate of the fraction of normal carriers contributing to the low-temperature heat transport in these superconducting samples. It is interesting to note that this uncondensed carrier fraction offers an explanation for the T-linear γ term in the specific heat of these samples at low temperatures as well. According to [70], this normal carrier fraction can yield the experimental values of the γ term (typically 5 mJ mol^{-1} K^{-2}) if one makes the reasonable choice of about $3m_e$ for the effective mass.

While this picture is certainly plausible, it would be nice to have an independent experimental verification of the existence of normal carriers at temperatures far below T_c. Perhaps high-frequency or optical studies carried out at low temperatures might provide information on the plasma edge of such carriers, if they indeed exist. As far as $La_{2-x}Sr_xCuO_4$ is concerned, it would be interesting to inquire into the behavior of the thermal conductivity at low temperatures for Sr concentrations in the range $0.05 \leq x \leq 0.15$, where bulk superconductivity exists yet only a single carrier band (holes) is believed to contribute to the transport. Such investigations have just been completed in my laboratory and they do not show any low-temperature "linear pulling" in low-level-doped $La_{2-x}Sr_xCuO_4$ superconducting single crystals. These results are presented in the following paragraphs where the behavior of single crystals is discussed in detail.

I should also note that an alternative explanation for the T-dependent thermal conductivity at low temperatures has been proposed by Salce *et al.* [78], who argue that the T-linear term arises from phonon scattering on lower-dimensional defects. Specifically, two-dimensional imperfections such as twins can lead to a mean-free path $l_p \sim T^{-2}$ which, combined with the assumed cubic variation in the specific heat, yields, via Eq. (7), a linearly dependent κ_p. The problem here is that the actual specific heat does not vary as T^3 at low temperatures but shows a large T-linear term and this invalidates the above argument.

High-T_c single crystals can yield more information than sintered samples for a variety of reasons. In addition to their high purity and grain-free structure, single crystals provide a perfect medium for the study of one of the key parameters of high-T_c superconductors, anisotropy. The degree of anisotropy is particularly relevant in layered structures as it has a bearing on the whole gamut of coupling parameters that determine the transport and magnetic and superconducting properties of the material in the two fundamental directions, along the layers and across the planes. Thanks to the dedicated efforts of our crystal-growing colleagues, single crystals of several families of high-T_c materials suitable for thermal transport studies have recently become available. Single crystals of La cuprates are among the largest successfully prepared, and thermal conductivity data are now available on both pristine La_2CuO_4 and Sr-doped crystals.

In Fig. 14 are shown the data obtained by Morelli *et al.* [79] on single crystals of La_2CuO_4 in three crystallographic orientations: along the [221] axis (the longest edge of the sample), and along two mutually perpendicular orientations, [001] and [110], obtained by cutting the sample into a parallelepiped. Since the spins localized on the copper sites have their moments aligned nearly parallel to the [110] axis, the above two orientations of the sample correspond to measurements of the thermal conductivity both perpendicular ([001]) and parallel ([110]) to the copper magnetic moment direction. The inset in Fig. 14 shows the structure in terms of a tetragonal coordinate system.

One immediately notes a substantially higher thermal conductivity for this crystalline medium as compared to the sintered version of the material (the dashed line represents the data of [49]). Moreover, the temperature dependence is very dramatic with a large peak near 40 K and a minimum at higher temperatures that depends on the orientation of the crystal. The authors point out that the 40 K peak provides strong evidence for the crystalline character of the heat transport and they suggest that the amorphous-

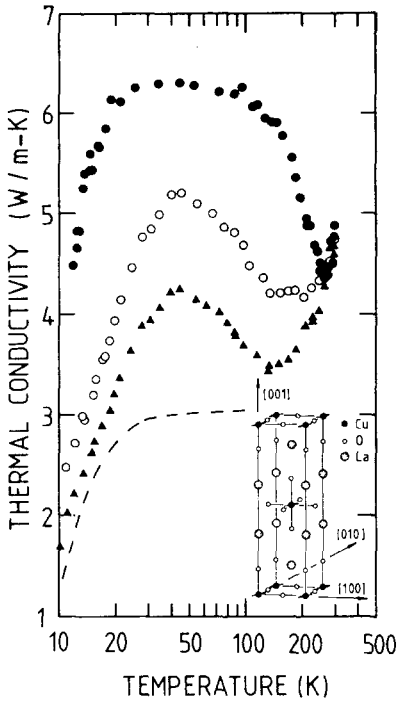

Fig. 14. Thermal conductivity of La_2CuO_4 single crystals: ● heat flow parallel to [001]; ○ heat flow parallel to [221]; ▲ heat flow parallel to [110]. The dashed line is data of [49] for sintered La_2CuO_4. (Taken from [79].)

like behavior of sintered La_2CuO_4 [49] is only an artifact of its polycrystalline nature which masks the intrinsic effects revealed on single crystal specimens. From a direct correlation (in the location, sharpness, and broadness of the features) between the susceptibility measurements and the thermal conductivity data, the authors argue that the lattice modes in La_2CuO_4 strongly interact with magnetic spin waves. Since the estimated umklapp-process-limited conductivity near the Debye temperature is about a factor of 2 larger than the measured thermal conductivity, Morelli *et al.* propose that above the Néel temperature (~250 K), the dominant phonon scatterers are disordered spins. The minimum on the curves in Fig. 14 then follows from phonon-spin scattering that scales with the magnetic order parameter. Specifically, above T_N, the phonon-disordered spin scattering rate is essentially temperature and frequency independent and the thermal conductivity increases as a result of a continued rise in the specific heat. On the other hand, for $T \leq T_N$, the number of disordered spins decreases and, provided the magnetic order parameter increases faster than the specific heat falls, the thermal conductivity will rise. The sharpness and location of the minima in the two mutually perpendicular directions then reflects, according to the authors, the nature of the magnetic ordering in each antiferromagnetic sublattice.

The proposal that the mechanism of the heat transport is closely coupled to the magnetic state of the crystal lattice is reasonable for pristine La_2CuO_4, and might even account for the surprising anisotropy in the heat flow where the thermal conductivity across the copper–oxygen planes appeared to be 50% larger than that along the planes (was the sample orientation correct?). We would expect, however, that the influence of magnetic effects would be considerably dampened in the Sr-doped crystals. This indeed seems to be borne out by the latest measurements of Morelli *et al.* [80] on nominally 4% Sr-substituted lanthanum cuprates. The above work represents one of two attempts to investigate the anisotropy of the thermal conductivity on a superconducting high-T_c single crystal. The sample had dimensions $1 \times 4 \times 8$ mm with the shortest and the longest axes along the [001] and [100] directions, respectively. The thermal conductivity was measured both across the copper–oxygen planes ($\kappa_\perp$), i.e., in the [001] direction, and along the copper–oxygen planes ($\kappa_\parallel$), in the [100] orientation. The sample indicated an onset of superconductivity around 25 K and reached the zero resistance state near 10 K. The thermal conductivity data for both orientations of the heat flow are reproduced in Fig. 15. A notable feature of the single crystal data is the large anisotropy in the thermal conductivity. The ratio $\kappa_\parallel/\kappa_\perp$ increases from 3 at room temperature to about 16 near 10 K. I wish to point out that the anisotropy here is opposite to that in pristine La_2CuO_4 single

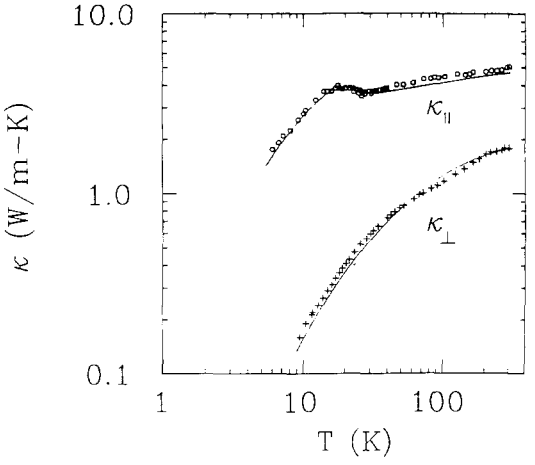

Fig. 15. Thermal conductivity of a $La_{1.96}Sr_{0.04}CuO_4$ single crystal measured parallel ($\kappa_\parallel$) and perpendicular ($\kappa_\perp$) to the Cu–O planes. Solid lines are fits to the BRT theory. (Taken from [80].)

crystals, and in greater accord with the intuitive expectation that phonons will propagate more readily along the planes than across the somewhat loosely coupled Cu-O stacks. It is satisfying to observe a hump in the in-plane conductivity below the onset critical temperature that was masked on the corresponding ceramic structures. It signifies that the heat transport mechanism at temperatures near T_c is essentially identical for all high-T_c perovskites and one does not need tunneling states to explain the change in slope near T_c in the sintered $La_{2-x}Sr_xCuO_4$. This change is simply a remnant of the intrinsic peak, much attenuated by the substantial phonon-defect scattering in these compounds, as was already pointed out [62]. Interestingly, evidence of the onset of superconductivity in the out-of-plane component of the thermal conductivity ($\kappa_\perp$) is largely washed out. This suggests that the transport of phonons across the Cu-O planes is disturbed by structural imperfections to a greater extent than the in-plane transport is. This is supported by the analysis of these data by Morelli *et al.* using the BRT theory modified to include scattering by crystal defects, essentially the model that was applied recently by Tewordt and Wölkhausen in [24] to analyze the thermal conductivity of 1-2-3 compounds (see the section on $YBa_2Cu_3O_7$ for details). As Morelli *et al.* show, phonon-carrier scattering plays an important role in the in-plane thermal transport. On the other hand, heat transport across the planes is dominated by phonon scattering from stacking faults and this overwhelms all other dissipative processes. In particular, the phonon-carrier contribution is negligible here. From the strength of the stacking fault scattering, expressed through the coefficient

$$\beta = 0.7(6\pi^2)^{2/3}\gamma_G^2 N_s \qquad (20)$$

where γ_G is the Grüneisen constant and N_s is the number of stacking faults per unit length, Morelli *et al.* obtain 7×10^7 stacking faults per meter which corresponds to a sheet fault spacing of some 140 Å. The authors ascribe the faults to misaligned CuO_2 planes which then suggests that about every 10th CuO_2 sheet is not in complete registry with the crystal structure. No supporting evidence for such structural disorder is provided, however, and it would be very useful to have these crystals examined by appropriate techniques of high-resolution electron microscopy. The fitting procedure applied to the in-plane thermal conductivity data yields a phonon-carrier coupling parameter of $\lambda \sim 0.6$, a value which is very similar to the one found by Tewordt and Wölkhausen [24] for sintered 1-2-3 compounds, and one which implies weak coupling. It is truly unfortunate that the thermal transport perpendicular to the Cu-O planes is so drastically affected by scattering on the stacking faults since this prevents an estimate of the phonon-carrier coupling in this direction and thus does not allow one to investigate anisotropy in the coupling. Perhaps with further improvements in crystal quality it may be possible to extract this important information. In this context, I mention a recently developed thermomechanical detwinning procedure [81] that yields twin-free single crystals of $YBa_2Cu_3O_7$ and that in principle should be applicable to all layered perovskite superconductors. It is possible that a similar approach relying on the ferroelastic behavior of these crystals could be used to improve their overall quality.

In collaboration with Dr. Morelli, thermal conductivity measurements on single crystals of $La_{2-x}Sr_xCuO_4$ with $x = 0$, 0.05, and 0.1 have been extended [82] to subkelvin temperatures in my laboratory in order to ascertain the limiting temperature dependence of the thermal conductivity. The in-plane component of the thermal conductivity for samples of the above Sr concentration, together with the out-of-plane thermal conductivity for the sample with $x = 0$, are shown in Fig. 16. The doped samples were too small and difficulties associated with the contact resistance precluded determination of the out-of-plane thermal conductivity on these specimens at very

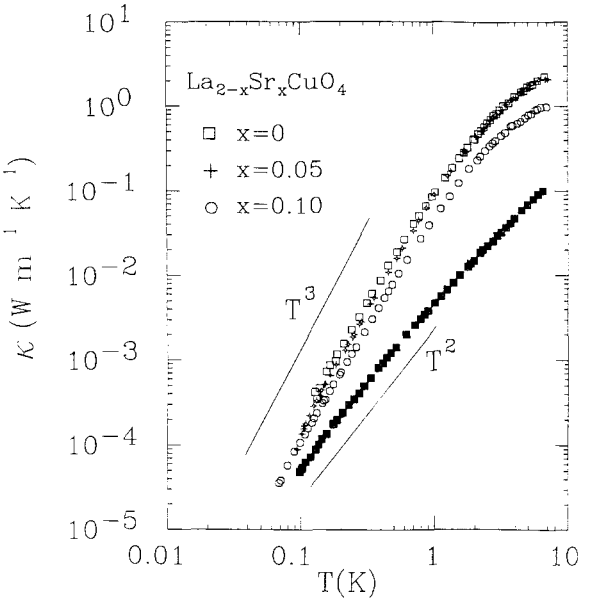

Fig. 16. Low-temperature thermal conductivity of $La_{2-x}Sr_xCuO_4$ single crystals measured parallel ($\kappa_\parallel$) to the Cu-O planes. Solid squares represent the out-of-plane thermal conductivity for the sample with $x = 0$. (Taken from [82].)

low temperatures. At 10 K, the anisotropy ratios were on the order of 20. There is little dependence of the in-plane κ on the Sr content; the samples with $x = 0$ and $x = 0.05$ have almost identical thermal conductivity. The sample with $x = 0.1$ has a slightly lower thermal conductivity, perhaps due to greater disorder in this material. The temperature dependence of the in-plane conductivity approaches a T^3 variation, a behavior which is in sharp contrast with $\kappa(T)$ of sintered samples (see Fig. 11) where the conductivity tended towards a T-linear limiting dependence. The data of Fig. 16 also differ from those on single crystals of 1-2-3 compounds shown in Fig. 31 and Bi-Ca-Sr-Cu-O crystals (see Fig. 51) where a quadratic temperature dependence was a good description of the data. The nearly T^3 variation in the 2-1-4 compounds suggests an ordinary crystalline character with phonon transport limited by boundary scattering.

The data for the out-of-plane conductivity for the sample with $x = 0$ show a somewhat weaker power law dependence, with exponent values closer to 2. Such behavior is reminescent of the thermal conductivity of oriented graphite where the in-plane dependence exhibits a $T^{2.8}$ law [83], while the out-of-plane variation is predominantly T^2 [84]. The quasi-two dimensional character of the graphite lattice is believed to be the determining factor here. It is tempting to suggest that dimensional effects may also play an important role in the thermal conductivity of high-T_c materials. Since the layering of Cu-O planes is more pronounced in Y-Ba-Cu-O and in Bi-Ca-Sr-Cu-O compounds than in La-Sr-Cu-O superconductors, one might expect the thermal conductivity of these former materials to have a greater tendency toward a T^2 power law dependence. Of course, this conjecture needs to be bolstered by further experiments.

4.2. $YBa_2Cu_3O_{7-\delta}$

4.2.1. Pristine Material

The raising of the superconducting transition temperature to over 90 K within a couple of months of the discovery of high-T_c superconductivity not only attests to the feverish round-the-clock effort that material scientists put forth in the early months of 1987, but also stands as an important milestone in the history of scientific inquiry. In rapid succession, the crystallographic phase responsible for $T_c \sim 90$ K was isolated, its structure identified as the oxygen-deficient perovskite of composition $YBa_2Cu_3O_{7-\delta}$ (the so-called 1-2-3 structure), and its basic thermodynamic parameters established. As in the case of doped La_2CuO_4, superconductivity appears confined to the orthorhombic phase of the system that, at 530 K, undergoes a transition to a tetrahedral structure. In terms of atomic arrangement, the orthorhombic-tetragonal transition is represented by the loss of Cu-O chains that, together with CuO_2 planes, form the backbone of the superconducting phase. Early folklore linking superconductivity with Cu-O chains has, however, since been disproved. In spite of their differing crystal structures, the similarities between the La-based and Y-based superconductors are actually quite substantive. In both of these perovskite systems, magnetic interactions are very prominent. $YBa_2Cu_3O_6$ plays the same role in the 1-2-3 family of superconductors that La_2CuO_4 does in the La family; it represents an antiferromagnetic insulating ground state. Doping by divalent ions—the road to superconductivity in lanthanum cuprates—is here replaced by increasing the oxygen content toward an O_7 stoichiometry. In fact, several intermediate phases with well-defined T_c's and oxygen stoichiometries between O_6 and O_7 have been synthesized, including an interesting one [85] with copper-oxygen chains perpendicular to each other on alternate (001) sheets.

With some regularity, papers appear in the literature describing sharply anomalous behavior in some physical property of the 1-2-3 compounds at temperatures as high as 240 K and above. The authors associate such behavior with trace amounts of a mysterious very high-T_c phase. The latest contribution in this regard is the interesting work of Chen *et al.* [86] on a mixed-phase Y-Ba-Cu-O material that was subjected to a low-temperature (< 150°C) oxygenation process. The samples were enclosed in an oxygen atmosphere and electrical and magnetic measurements were performed. Under these conditions, the authors observed a thermally recyclable zero-resistance state with a transition temperature as high as 265 K. Even though these particular measurements appear considerably more reproducible than is typical for these kinds of studies, fundamental difficulties with the identification of a super-high-T_c phase remain.

The fact that the T_c for $YBa_2Cu_3O_{7-\delta}$ is more than double that for $La_{2-x}Sr_xCuO_4$ has understandably resulted in a much closer scrutiny of the former material's physical parameters. Thermal conductivity studies are no exception and there are available a large number of reports dealing with heat transport in 1-2-3 compounds.

The early papers [62,75,87-90], submitted within a month or so of each other, established the general trend in the thermal conductivity of sintered $YBa_2Cu_3O_{7-\delta}$: a dominant phonon contribution and significant phonon-carrier scattering. Subsequent experiments confirmed this behaviour and explored important specific topics such as the role of microstructure, the effect of oxygen stoichiometry, changes resulting from neutron irradiation, the temperature dependence of the thermal conductivity in the extreme low-temperature range, and, of special interest, the anisotropy of heat conduction. We shall discuss these studies in turn.

In Fig. 17 are collected representative data illustrating the range of the magnitude and temperature dependence of the thermal conductivity. Again, a spread in the value of the conductivity of up to an order of magnitude is a direct consequence of the varying compactness of the sintered pellets. In particular, the sample of [89] must have had a very high porosity. One can judge this independently from its unusually high electrical resistivity of 19 mΩ-cm at 300 K. A contributing factor to a wide range of magnitudes observed in the thermal conductivity is the varied oxygen content of the samples, a parameter that is not always rigorously monitored. I shall point out later that the thermal conductivity is quite sensitive to oxygen stoichiometry. As in the La-based perovskites, 80-90% of the heat is carried by phonons and the overall thermal conductivity is rather low. A contrasting feature between the data of Fig. 17 and those in Fig. 10 is a sudden rise and pronounced maximum observed in the thermal conductivity of $YBa_2Cu_3O_{7-\delta}$ below T_c. This is a clear signature of a phonon-carrier interaction. The reason why it is so evident in the case of 1-2-3 compounds is their much higher T_c (less rapidly varying phonon population) and also perhaps a more favorable ratio between the phonon-carrier and phonon-defect scattering rates. Note also that, for the semiconducting sample of $YBa_2Cu_3O_{7-\delta}$ ($\delta \sim 1$) displayed in Fig. 17, the thermal conductivity decreases monotonically and no maximum is observed. I have already indicated in Section 3.2 that I do not believe circulatory thermal conductivity can explain any of the above features in the thermal conductivity because its contribution is very small.

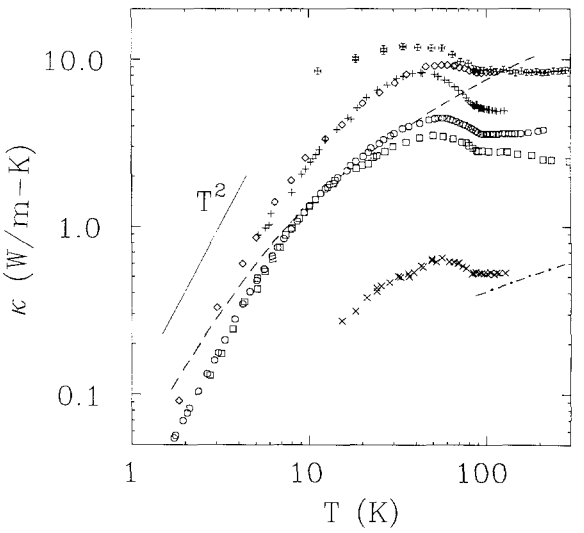

Fig. 17. Thermal conductivity of $YBa_2Cu_3O_7$. +Jezowski *et al.* [87]; × Morelli *et al.* [89]; ○ Uher and Kaiser [62]; □ Bayot *et al.* [88]; ◇ Gottwick *et al.* [75]. All measurements refer to superconducting ceramics. The broken curve represents the sintered $YBa_2Cu_3O_6$ insulator of Salce *et al.* [78]. ✣ data of Hagen *et al.* [96] for the *ab* plane of a single crystal. The dash-dot line indicates the maximum electronic thermal conductivity for the sample of [62].

One of the interesting aspects of the data in Fig. 17 is the temperature dependence of the thermal conductivity well above T_c. As one can note from the data, the trend is not unique: in some cases the thermal conductivity rises with temperature, in others it is constant or even decreases. In materials where about 90% of the heat is carried by phonons, one would expect phonon-phonon umklapp processes to become an important (dominant) dissipative mechanism at elevated temperatures. Consequently, the thermal conductivity should, eventually, decrease as T^{-1}. Most of the authors mention that radiation losses start to become a serious problem in their investigations near 150 K and some have attempted to correct their high-temperature data. Indeed, it is important to keep in mind that the steady-state longitudinal method (the preferred technique for thermal conductivity studies in virtually all of the investigations discussed in this review) is inherently inaccurate when used at high temperatures on materials of poor thermal conductivity unless special precautions are taken to limit the loss of heat by radiation. If one does not properly account for the radiation loss, the measured thermal conductivity is artificially large and the error grows with increasing temperature. It is possible then that the disagreement in the temperature dependence of κ above 100 K in Fig. 17 is partly due to an increase in radiation effects.

Some insight into the intrinsic variation of the thermal conductivity of Y-Ba-Cu-O ceramics above T_c has been made recently by Merisov *et al.* [91] and by Buravoi *et al.* [92]. The former group makes use

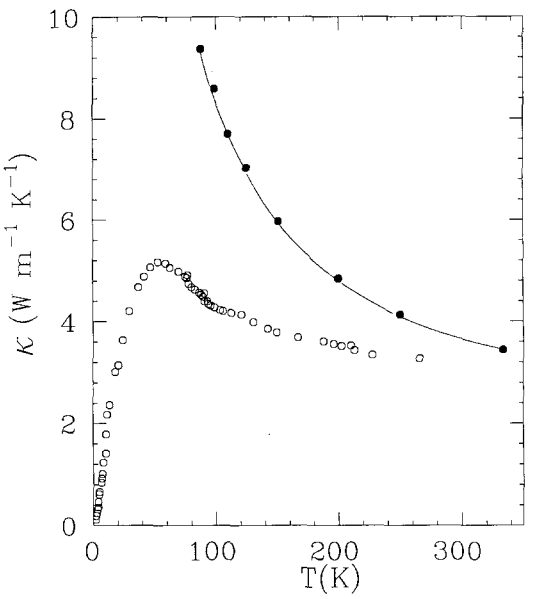

Fig. 18. Thermal conductivity of multiphase ceramics of Y-Ba-Cu-O. Open circles are the data of Merisov *et al.* [91] obtained with the use of a radiation shield to minimize the heat loss by radiation. Solid circles are the results of Buravoi *et al.* [92] collected with the aid of a thermal comparator.

of a radiation shield, the temperature profile along which is made to match the temperature profile along the sample. The latter authors avoided the use of the longitudinal method altogether and, instead, employed a comparative method of measurement wherein the sample, in the form of a disk, is sandwiched with a disk of the material having a known thermal conductivity. The geometry of this experimental setup minimizes the radiation heat loss. The data are shown in Fig. 18. The high-temperature behavior indicates a T^{-1} dependence of the thermal conductivity, suggesting that phonon-phonon umklapp scattering is dominant. A word of caution is in order here before one attempts to generalize this behavior as being typical of the 1-2-3 compounds. Both groups note that the T^{-1} dependence shown in Fig. 18 applies only to multiphase Y-Ba-Cu-O ceramics where, in addition to the superconducting phase, the so-called green phase, Y_2BaCuO_5, represents a large volume fraction of the sample (in [92] it is 20% by volume). As the amount of the green phase decreases, Buravoi *et al.* observe a dramatic reduction in the magnitude of the thermal conductivity and a change in the temperature dependence from T^{-1} to a situation where $\kappa(T)$ has a small positive slope above 100 K.

The issue of the normal-state temperature dependence of κ is also addressed in the recent work of Cohn *et al.* [93]. These authors have measured the *ab*-plane thermal conductivity of grain-oriented $YBa_2Cu_3O_{7-\delta}$ grown by liquid-phase processing [94]. This material is composed of rather large, twinned crystalline grains (up to 5 mm extent in the *ab*-plane and 20-30 μm thick) which are highly oriented along the *c* axis during growth. The misorientation of the *c* axes is less than 5°. Small amounts of other phases may exist as distinct entities between grains. The crystalline integrity of this material is evidenced by low *ab*-plane electrical resistivity, transport critical currents comparable to those measured in single crystals [95], and sharp superconducting transitions ($\Delta T_c \leq 0.5$ K). Two relatively large specimens ($8 \times 2 \times 1$ mm) having resistivities $\rho(300\text{ K}) = 350$ and 1000 $\mu\Omega$-cm have been measured. The heat conductivity (see Fig. 19) near room temperature is larger in magnitude than the data shown in Fig. 17, κ_{ab} increases as $1/T$ with decreasing temperature, and $\kappa_{ab}(92\text{ K})/\kappa_{ab}(280\text{ K}) = 1.3$. The peaks below T_c are substantial, resulting in conductivities at the maxima that are among the highest reported for a 1-2-3 material to date. The authors argue that the results provide a strong support for the $1/T$ behavior as a characteristic variation of a high-quality lattice, consistent with a thermal resistivity dominated by intrinsic phonon-phonon Umklapp scattering at high

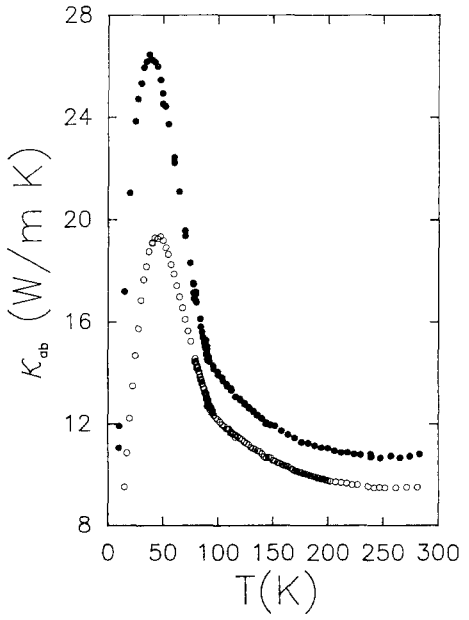

Fig. 19. The *ab*-plane thermal conductivity versus temperature for two specimens of $YBa_2Cu_3O_{7-\delta}$, grown by liquid-phase processing. The specimens are distinguished by the values of their electrical resistivity at room temperature: solid circles, 350 $\mu\Omega$-cm; open circles, 1000 $\mu\Omega$-cm. (Taken from [93].)

temperatures. In my opinion, the question concerning the intrinsic temperature dependence of κ for the 1-2-3 phase above 100 K remains an unsettled issue and more work is to be done before this behavior is fully understood. It would be particularly useful if single crystals could be studied at temperatures up to 300 K using thermal conductivity techniques that are substantially immune to or require only minimal corrections for radiation loss. This may prove to be a rather difficult task.

Let us now turn our attention to the theoretical implications of the thermal conductivity behavior near T_c. Referring to Fig. 17, we note that, at T_c, the thermal conductivity shows a sharp rise followed by a maximum in the range 50-60 K. As I have noted, it is widely believed that this behavior is the consequence of an enhancement in the phonon mean-free path as the carriers start to condense at T_c. An attempt to quantify the phonon-carrier interaction was made by Tewordt and Wölkhausen [24], who employed the BRT theory for phonon conductivity limited by carrier scattering and fitted it to the data of [62,65,78]. To make the model more realistic, they also included additional dissipative processes—scattering of phonons by static imperfections such as point defects, grain boundaries, and sheetlike faults. The strategy used was to first fit their theory to the $\kappa(T)$ of insulating samples to gain information on such parameters as the concentration of point defects, the number of sheetlike faults crossing a line of unit length, etc. Following this, the thermal conductivity of superconducting samples was fitted by switching on the phonon-carrier interaction. To facilitate the fitting procedure, Tewordt and Wölkhausen used Eq. (9). The resulting fits to the experimental data for both the semiconducting and superconducting samples of sintered $YBa_2Cu_3O_{7-\delta}$ are shown in Figs. 20 and 21. The agreement with experiment is quite good except very near T_c where the theoretical curves rise much more sharply than the experimental data. The authors suggest that this may be due to an averaging effect of CuO_2-plane orientations with respect to the temperature gradient. Experimentally, of course, it is necessary to establish a finite temperature difference across the sample and this may also contribute to the smearing of the onset of the rise. The data of Uher and Kaiser [62] (dashed line) are fitted by taking $A = 3.5\ \mathrm{W\,cm^{-1}}$, $\alpha = 50$, $\beta = 60$, and $\gamma = 100$. The data of Gottwick *et al.* [75] are fitted by using $A = 5\ \mathrm{W\,cm^{-1}\,K^{-1}}$, $\alpha = 50$, $\beta = 70$, and $\gamma = 0$ for the semiconducting sample (dash-dot line) and $A = 5\ \mathrm{W\,cm^{-1}\,K^{-1}}$, $\alpha = 60$, $\beta = 35$, and $\gamma = 100$ for the superconducting specimen. For the experimental curves of Salce *et al.* [78] the best fits are obtained with $A = 3\ \mathrm{W\,cm^{-1}\,K^{-1}}$, $\alpha = 40$, $\beta = 50$, and $\gamma = 0$ for the semiconducting sample (dash-dot line), and $A = 5\ \mathrm{W\,cm^{-1}\,K^{-1}}$, $\alpha = 60$, $\beta = 50$, and $\gamma = 80$ for the superconductor. In all cases, the scaling parameter, $\chi = \Delta(0)/\Delta_{BCS}(0)$, is taken to be unity, corresponding to a weak-coupling BCS gap. From the values of $\gamma \sim 100$, Tewordt and Wölkhausen estimate the phonon-carrier coupling constant due to the contribution of longitudinal acoustic phonons to be $\lambda \sim 0.5$, a magnitude that falls within the weak-coupling regime.

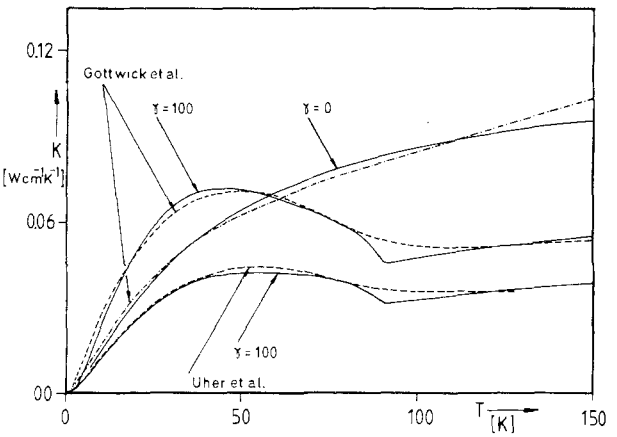

Fig. 20. Theoretical fits (solid lines) to the experimental thermal conductivity of sintered $YBa_2Cu_3O_{7-\delta}$ with: $\delta \approx 0$ (dashed lines), [62] and [75]; $\delta \approx 1$ (dash-dot lines), [75]. (Taken from [24].)

As I have pointed out when discussing the behavior of $La_{2-x}Sr_xCuO_4$ superconductors, it would be highly desirable to measure the degree of

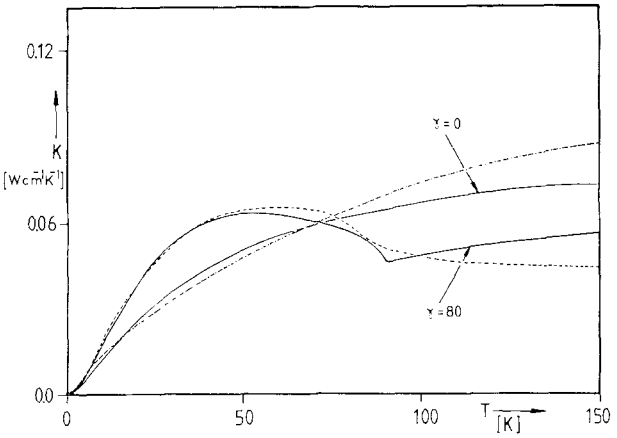

Fig. 21. Theoretical fits (solid lines) to the thermal conductivity data of [78] for superconducting (dashed line) and insulating (dash-dot line) $YBa_2Cu_3O_{7-\delta}$ ceramics. (Taken from [24].)

anisotropy of the phonon-carrier coupling constant as this has a direct impact on the question of the mechanism of superconductivity. The first attempt to do so has recently been undertaken by Hagen *et al.* [96] who investigated both the in-plane, κ_{ab}, and the across-the-plane, κ_c, thermal conductivities on superconducting as well as insulating single crystals of $YBa_2Cu_3O_{7-\delta}$ from 10 to 330 K. It should be pointed out that such measurements are highly delicate as one deals with very small crystals of typical dimensions $1 \times 0.5 \times 0.1$ mm. The experimental data are reproduced in Fig. 22. The in-plane conductivity, redrawn from the original linear-linear plot into a log-log display to facilitate comparison with the sintered samples, is shown in Fig. 17. The magnitude of the conductivity is somewhat larger than that of the 1-2-3 ceramics but otherwise the data are very similar. In particular, a sharp rise and a pronounced peak in κ at about $T_c/2$ is a feature of the superconducting state regardless of the degree of crystallinity. As expected, no anomaly is observed near 90 K on insulating single crystals, in contrast to superconducting specimens. The thermal conductivity, κ_{ab}, is, in this case, a smooth and essentially monotonic function of temperature and the magnitude of the conductivity above 90 K is comparable to its superconducting counterpart.

The results for the across-the-plane conductivity, κ_c, of the superconducting samples are shown in Fig. 22b. Here we note a distinctly different behavior than we observed for heat flow along the planes. The thermal conductivity is some 4-5 times smaller, increases slowly with decreasing temperature, and exhibits a broad peak in the range 50-80 K beyond which it falls sharply with decreasing temperature. There is no hint of any anomalous behavior at or very near the transition temperature T_c. The authors employ the Wiedemann-Franz ratio, using the value of the electrical resistivity at 300 K ($\sim 150\ \mu\Omega$-cm), and conclude that the charge carriers are responsible for about one-half of the total heat current above T_c in the *ab* direction, a value substantially larger than was seen in sintered specimens. From the fact that κ_{ab} is comparable in magnitude in the superconducting and insulating crystals, they then deduce that scattering of phonons on the charge carriers halves the lattice contribution, i.e., in the normal state of superconducting crystals, the phonon-umklapp and phonon-carrier scattering processes have a roughly equal effect. Proceeding with this argument and employing the fact that the anisotropy in the electrical resistivity, ρ_c/ρ_{ab}, is approximately 200-300 at 100 K,

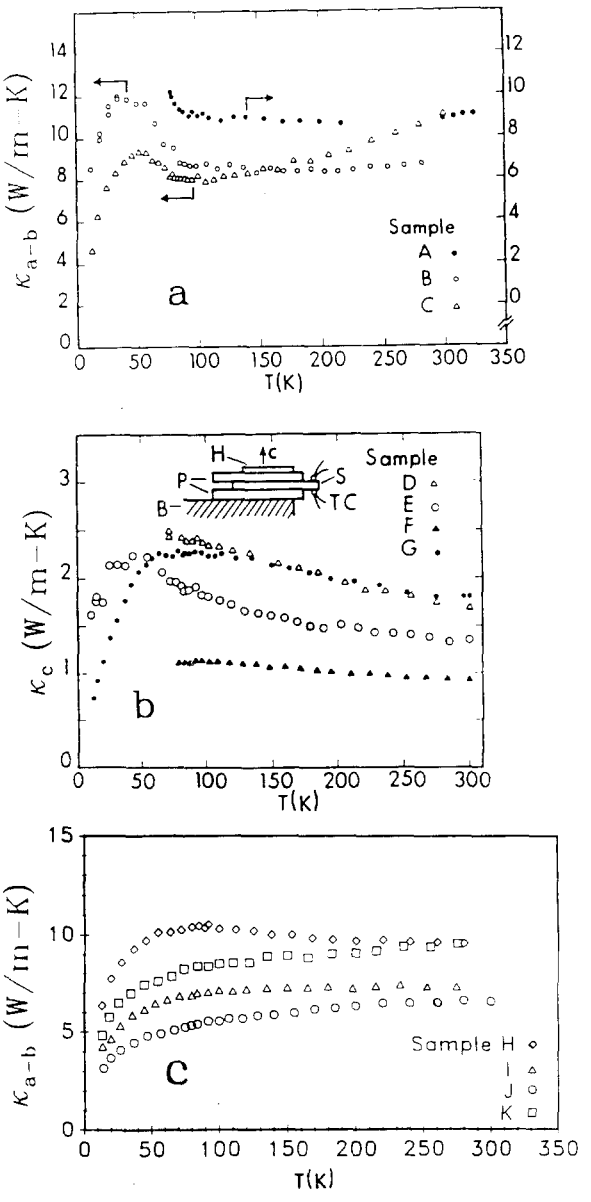

Fig. 22. (a) The in-plane thermal conductivity, κ_{ab}, for superconducting single crystals of $YBa_2Cu_3O_{7-\delta}$. (b) The out-of-plane thermal conductivity, κ_c, for superconducting single crystals of $YBa_2Cu_3O_{7-\delta}$. (c) The in-plane thermal conductivity, κ_{ab}, for insulating crystals of $YBa_2Cu_eO_{7-\delta}$ (with T_c below 4 K). (Taken from [96].)

Hagen *et al.* conclude that the phonon-carrier scattering is strong in the *ab* plane but very weak in the *c* direction, if present at all. They then suggest that such a large anisotropy in the coupling constant makes phonon-mediated superconductivity unlikely. While this conclusion is widely accepted, the actual estimate of the carrier contribution to the thermal conductivity which the authors arrive at should be viewed with

some caution as it may be somewhat too high. The reason for this is that their estimate hinges on the assumption of perfectly elastic carrier scattering (or, alternatively, on a common scattering time for the electrical and thermal processes) that would yield the Sommerfeld value, $L_0 = 2.44 \times 10^{-8}\ \mathrm{V^2\ K^{-2}}$, for the Lorenz ratio. In pure single crystals, at temperatures $T < \Theta_D$, where it is generally presumed that the in-plane phonon-carrier interaction is strong, it is inconceivable that the scattering would not have a substantially inelastic character. Consequently, the Lorenz ratio is likely to be less than L_0 and this should lower the carrier thermal conductivity fraction significantly.

Evidence of anisotropy in the thermal conductivity is also found in the measurements of Kirk *et al.* [97] on hot-pressed specimens of $YBa_2Cu_3O_{7-\delta}$. Figure 23 shows the data for samples #3 and #4 that were cut from the same hot-pressed cylindrical ingot. Sample #3, with dimensions $2.4 \times 2.67 \times 11.8$ mm, had its longest axis parallel to the pressing direction, while sample #4, with dimensions $2.5 \times 2.9 \times 10.7$ mm, had its longest axis perpendicular to the pressing direction. In addition, Fig. 23 also displays the data for sample #1 which was similar to sample #4 but cut from a different ingot. We note that the thermal conductivity is about 20% higher for sample #4 than sample #3 in spite of the two having identical chemical composition, compactness, and oxygen content. Such a difference is far beyond the experimental uncertainty of the data and suggests that κ is anisotropic and depends on the direction of the heat flow with respect to the pressing direction. The observed anisotropy apparently arises from an aspect of the hot-pressing technique that promotes partial alignment of the crystallites in the sample. The hot-pressing process is accompanied by internal stress which results in faster crystallite growth along the axis that maximises relief of this stress. In the case of $YBa_2Cu_3O_{7-\delta}$, hot-pressing causes crystallites to orient preferentially with their c axis along the pressing direction and the ab plane perpendicular to it. As the authors of [97] note, support for this picture is provided by SEM micrographs that show distinctly different microstructures depending on whether one views the sample parallel (smaller and more uniform grains) or perpendicular (larger, somewhat intergrown grains) to the pressing direction. Of course, an independent and simple test of possible anisotropy originating from the processing treatment would consist of measurements of the electrical resistivity of the hot-pressed material. Unfortunately, such measurements have not yet been carried out on the samples of [97].

A rather surprising feature of the data of Kirk *et al.* is the relatively small magnitude of the thermal conductivity. One would expect that compact (density exceeding 5 g/cm^3) and partially oriented hot-pressed samples would have thermal conductivities exceeding those measured on sintered specimens. Instead, Kirk *et al.* find substantially smaller (by at least a factor of 2) magnitudes of κ and it is not clear why this is so.

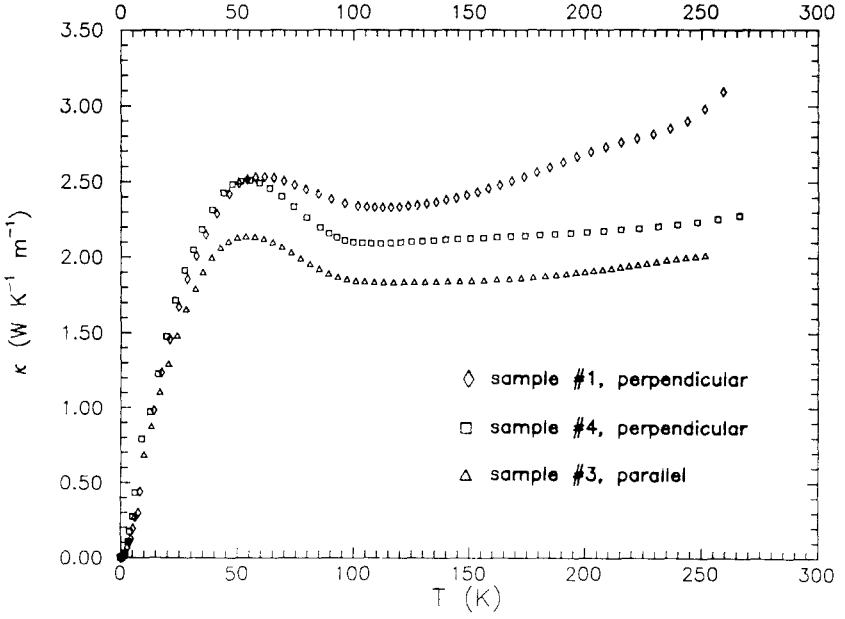

Fig. 23. Thermal conductivity of hot-pressed samples of $YBa_2Cu_3O_7$. Designations perpendicular and parallel refer to the direction of the heat current relative to the direction of hot-pressing. Samples #4 and #3 were cut from the same cylindrical ingot, sample #1 was prepared from a different ingot. (Taken from [97].)

Oxygen content is the crucial parameter determining whether a 1-2-3 compound behaves as a superconductor or an insulator. As we illustrate below, oxygen content also greatly influences the thermal transport properties, most notably the thermoelectric power and thermal conductivity. Several experimental studies document this point quite clearly.

Zavaritskii *et al.* [98] studied the thermal conductivity of $YBa_2Cu_3O_{7-\delta}$ as a function of oxygen deficiency δ by successively annealing their sample in vacuum or in an oxygen atmosphere. The oxygen content was established by gravimetric means before and after annealing and compared with the expected changes in the lattice parameters determined from x-ray diffraction measurements. The thermal conductivity at various stages of the annealing process is displayed in Fig. 24. As the oxygen concentration is reduced from $\delta \sim 0$ to $\delta = 0.3$, the maximum in the conductivity shifts to lower temperatures and the magnitude of the thermal conductivity decreases. Further vacuum annealing to values of $\delta \geq 0.5$ results in a nonsuperconducting material with still lower thermal conductivity. The authors argue that the removal of oxygen creates vacancies at both the chain and plane sites and these, in turn, act as very strong scatterers of short-wavelength phonons. Since the superconductivity can be reestablished by annealing in oxygen, this implies that, indeed, the changing oxygen content rather than changes in the connectivity of grains is the relevant factor behind variations in the thermal conductivity with varying δ. The authors make the interesting and important observation that a sample with $\delta = 1$, i.e., the O_6 stoichiometry obtained by prolonged vacuum annealing at 675°C, has a thermal conductivity which, above 120 K, is nearly a factor of 2 larger than values obtained in all other cases where $\delta < 1$, including the as-prepared superconductor. Since the heat capacities of the materials with O_6 and O_7 oxygen stoichiometries are approximately the same and the sound velocity [99] in $YBa_2Cu_3O_6$ is only larger than that in $YBa_2Cu_3O_7$ by about 9%, the structural transformation from the orthorhombic to the tetragonal configuration cannot account for such a large enhancement in the thermal conductivity of $YBa_2Cu_3O_6$. Instead, Zavaritskii *et al.* suggest that the conductivity is large because free carriers and oxygen vacancies are virtually absent and therefore cannot dissipate the energy and momentum of the phonon system. They estimate, by comparing the thermal conductivities of the as-prepared ($\delta \sim 0$) and vacuum annealed ($\delta = 1$) samples, that the phonon relaxation time for scattering by charge carriers, τ_{p-c}, is on the order of 10^{-12} sec, which is similar to that for ordinary superconductors above T_c. Since it is not at all clear to what extent the absence of charge carriers rather than the absence of oxygen vacancies is responsible for the excess in the thermal conductivity of $YBa_2Cu_3O_6$, the above estimate of τ_{p-c} is likely to be too large. After all, in the highly oxygen-deficient, insulating sample with $\delta = 0.69$, the phonon-carrier scattering rate must be much smaller than in the original superconducting sample yet, in spite of this, its thermal conductivity is substantially degraded rather than enhanced. The oxygen dependence of the thermal conductivity has also been investigated by Yefimov *et al.* [100], who observed for their range of the δ parameter (0.1-0.8) a similar trend in $\kappa(T)$.

Jezowski *et al.* [101] have measured the thermal conductivity of two single-phase superconducting ceramics of composition $\delta = 0.19$ ($T_c = 89.5$ K) and $\delta = 0.46$ ($T_c = 58$ K) and of an insulating sample with an oxygen deficiency $\delta = 0.9$. Again, lowering the oxygen content leads to a substantial decrease in the thermal conductivity. The authors propose that this may be connected with a change in the degree of orthorhombicity, perhaps by a breaking of the Cu-O chains. Since disruption of the chains leads to the

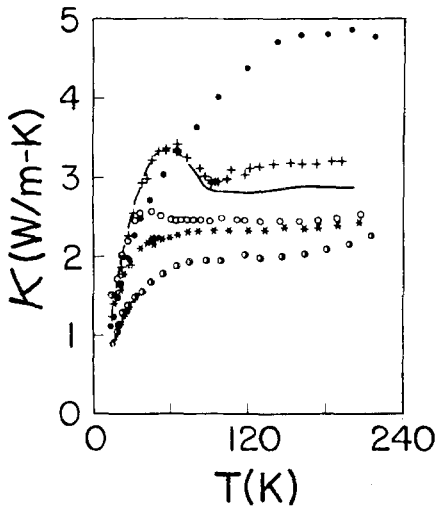

Fig. 24. Thermal conductivity of $YBa_2Cu_3O_{7-\delta}$ at various stages of vacuum or oxygen annealing. + original material with $\delta \approx 0$; ○ after annealing for 6 h at 435°C, $\delta = 0.3$, $T_c = 70$ K; * further annealing in vacuum for 6 h at 455°C, $\delta = 0.47$, $T_c = 56$ K; ◑ after further annealing for 6 h at 470°C, $\delta = 0.69$, nonsuperconducting; solid line—reannealed in oxygen for 21 h at 540°C, $\delta = 0.23$, $T_c = 91$ K; ● following vacuum annealing for 40 h at 675°C, $\delta = 1$, nonsuperconducting. (Taken from [98].)

creation of oxygen vacancies, the mechanism responsible for the decrease in the thermal conductivity with increasing δ is, in essence, phonon-defect (vacancy) scattering. The increase in phonon-defect interactions in samples with lower oxygen content also contributes to the diminished height of the maximum in the thermal conductivity curves. The authors of [10] stress the point that the thermal conductivity apparently exhibits a T^2 dependence in the low-temperature regime. What they are actually seeing is a continuously changing power law dependence that happens to mimic a quadratic variation in a very narrow temperature range from 4–7 K. As I shall discuss later, sintered specimens of $YBa_2Cu_3O_{7-\delta}$ do not obey a quadratic temperature dependence in the low-temperature limit, regardless of the value of δ.

An interesting aspect of the paper by Jezowski *et al.* is a detailed study of hysteresis in the thermal conductivity of their nonsuperconducting (tetrahedral) sample $YBa_2Cu_3O_{6.1}$ (see Fig. 25). In particular, they note that thermal conductivity anomalies appear in a temperature range (80–240 K) close to that where "mysterious" anomalies are occasionally observed in some physical properties of superconducting materials. This, coupled with the fact that, in the electrical transport, these anomalies are either absent or very weak (suggesting that they are not electronically driven), leads the authors to conclude that the underlying mechanism does not depend on oxygen content but is associated with instabilities in the crystal structure. They suggest a scenario whereby, for nonzero values of δ, the 1-2-3 phase may be considered a spinodal decomposition mixture of two phases of somewhat differing oxygen stoichiometry. The effect of spinodal decomposition on the thermal

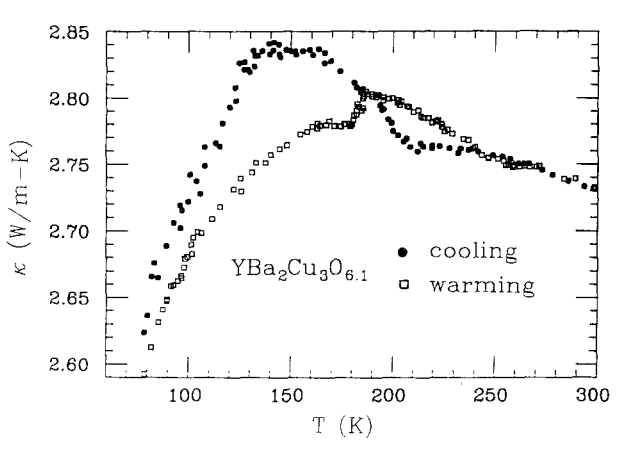

Fig. 25. Hysteresis in the thermal conductivity of a nonsuperconducting sample of $YBa_2Cu_3O_{6.1}$. (Taken from [101].)

conductivity of superconducting Y-Ba-Cu-O samples was further studied by Jezowski [102]. Using very high precision measurements of $\kappa(T)$, he found hysteresis of about 1–3% between the cooling and warming cycles above T_c. The temperature range where hysteresis is observed depends on the oxygen content of the sample. A discussion pertaining to spinodal decomposition, as well as the phase diagram for a two-phase mixture of materials with different oxygen ordering, can be found in the work of Khachaturian and Morris [103].

Let us now consider the behavior of the thermal conductivity of $YBa_2Cu_3O_{7-\delta}$ at low temperatures. Just as in the case of $La_{2-x}Sr_xCuO_4$, the temperature dependence and therefore the mechanism of the heat transport below 1 K remains a controversial issue. I have already mentioned that some authors who have investigated the thermal conductivity of the sintered 1-2-3 compounds down to the liquid-helium range have asserted that κ approaches a quadratic temperature variation, with tunneling states being hypothesized as the cause of this behavior. I have cautioned that this claim is based on a very narrow temperature range where the T^2 dependence is only a rough approximation to a continuously changing slope. In order to learn anything truly meaningful about the scattering processes affecting the conductivity or to establish the limiting temperature dependence, one must extend measurements to subkelvin temperatures. Such a task is accomplished most conveniently with the aid of a dilution refrigerator.

In the first measurements of κ that extended well below 1 K, Gottwick *et al.* [75] found a surprising weakening of the power law dependence below 0.5 K (see Fig. 26). According to the theoretical ideas of Section 3, at temperatures $T \ll T_c$, elementary excitations should be vanishingly small and the heat transport should be entirely of phonon origin. In practice this means that one would expect either a T^3 variation, reflecting phonon scattering on grain boundaries or crystal faces, or some other fixed power law dependence (such as T^2 for TS) if the scale of scatterers is somewhat shorter than the grain size of the microstructure. In this regard the "pulling" in the data of Fig. 26 is highly anomalous. Gottwick *et al.* were able to fit their data remarkably well (see the solid line through the points in Fig. 26) by writing the thermal conductivity as the sum of a linear and a cubic contribution:

$$\kappa(T) = aT + bT^3 \tag{21}$$

The T^3 term represents the expected boundary scat-

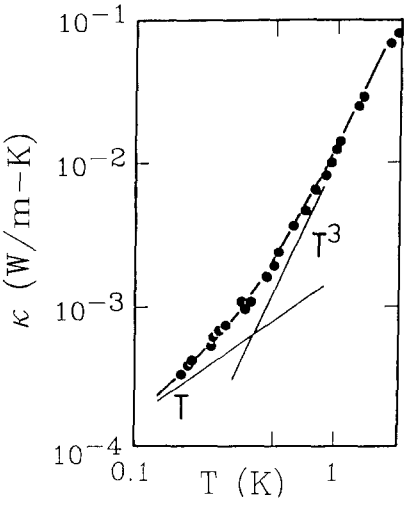

Fig. 26. Thermal conductivity of a sintered sample of $YBa_2Cu_3O_7$. Solid line through the data points is the sum of terms aT ($a = 16 \times 10^{-4}$ Wm^{-1} K^{-2}) and bT^3 ($b = 47 \times 10^{-4}$ Wm^{-1} K^{-4}). (Taken from [75].)

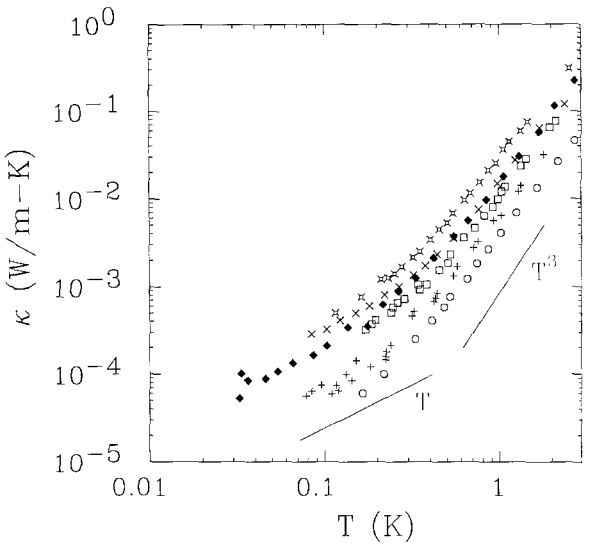

Fig. 27. Thermal conductivity of sintered $YBa_2Cu_3O_{7-\delta}$ at low temperatures. □ Gottwick *et al.* [75], × Salce *et al.* [78], ○ Freeman *et al.* [90], ◆ Graebner *et al.* [48], ⁎ Sparn *et al.* [104], + Kirk *et al.* [97].

tering of phonons with the fitted co-efficient $b = 47 \times 10^{-4}$ W/m-K^4. The authors associate the linear term with the presence of uncondensed carriers, and from the fitted magnitude of the coefficient $a = 16 \times 10^{-4}$ W/m-K^2, they estimate that about 15% of the carriers do not belong to the condensate. In their subsequent work [104] that included additional measurements on the superconducting and insulating phases of $YBa_2Cu_3O_{7-\delta}$, this group confirmed the T-linear asymptotic behavior in superconducting ceramics and contrasted it with the nearly cubic temperature dependence observed in their insulating samples. The coefficients of the linear and cubic terms of Eq. (21) that fit the data are summarized in Table I. Similar trends in the conductivity of the ceramic 1-2-3 compounds have been observed by Bernasconi *et al.* [64], Freeman *et al.* [90], Salce *et al.* [78], and Graebner *et al.* [48] (see Fig. 27), but these teams propose entirely different physical pictures. Bernasconi *et al.* fit Eq. (21) to their data below 0.3 K and point out that while the coefficient a decreases with increasing grain size and filling factor, the coefficient b increases (see Table I). Freeman *et al.* draw attention to the similar behavior of insulating sintered ceramic materials in general. They stress the importance of pores, which scatter phonons very efficiently in highly porous structures such as their specimen (70% theoretical density). Assuming the pores can be viewed as spheres of radius R in a material of porosity r, they write for the thermal conductivity (in units of W/m-K)

$$\kappa \simeq 2.72 \times 10^{10} \frac{R}{v^2 r} T^3 \qquad (22)$$

where v is the phonon velocity and v^2 is to be taken

Table I. Coefficients a and b in Eq. (21) for Sintered $YBa_2Cu_3O_{7-\delta}$

	Reference							
Coefficient	[75]	[90]	[48]	[104]	[107][c]	[107][d]	[64][a]	[64] (Sample 2)[b]
$a(10^{-4}$ Wm^{-1} $K^{-2})$	16	36	22	29	14	9.2	28	17
$b(10^{-4}$ Wm^{-1} $K^{-4})$	47	360	200	152	87	135	137	253

[a] Grain size in this sample ~20 μm.
[b] Grain size in this sample ~150 μm.
[c] As-prepared material.
[d] Reannealed on O_2 following destruction of superconductivity during vacuum annealing.

as an average over all modes. Using a porosity of $r = 0.3$ and a longitudinal phonon velocity (extrapolated to 0 K) of 7×10^3 m/s, they employ the model of Meredith and Tobias [105] for the conductivity of a porous medium and estimate that the 100% dense material should have nearly twice the thermal conductivity of the porous structure. From their own experimental data and Eq. (22) they find the radius of the (spherical) pores, R, to be 2 μm, consistent with SEM pictures and in reasonable agreement with a computed phonon mean-free path of about 4 μm. Although Freeman *et al.* draw a curve representing a T^2 variation through their lowest two points (between 150–200 mK), its curvature suggests a progressive weakening of the temperature dependence. Their data can be fitted with Eq. (21) with values of the parameters a and b given in Table I.

The measurements of Salce *et al.* and of Graebner *et al.* that extend down to ~70 mK and 30 mK, respectively, demonstrate that a linear temperature dependence is an excellent representation of the thermal conductivity behavior of sintered 1-2-3 compounds below about 100 mK. However, in contrast to the model of normal carriers as responsible for the T-linear variation in κ, these two groups suggest that the unusual crossover to a limiting T-linear dependence arises from structural defects. Salce *et al.* believe that the culprits are the walls between tetragonal domains (twins) in the superconducting samples. When the phonon wavelength becomes comparable to the characteristic size of these defects, they argue that a "pseudo-linear" term could appear in the high-temperature part of the crossover. As supporting evidence they call upon a theoretical work [106] where a linear variation in $\kappa(T)$ was derived for scattering of phonons by two-dimensional imperfections such as twins. The difficulty with this interpretation is that the typical spacing of twins within the grains of a sintered material is less than 0.1 μm, while the dominant phonon wavelength,

$$\lambda_{\text{dom}} = 2.7hv/k_BT \tag{23}$$

at 0.1 K is about 5 μm, i.e., the crossover should already have occurred at temperatures well above 1 K. In the same vein, Graebner *et al.* attribute the "pulling" toward a T-linear dependence to Rayleigh scattering from the microstructure. This model runs into new difficulties with characteristic dimensions in that Rayleigh scattering requires all dimensions of the obstruction (grains in this case) to be much smaller than the phonon wavelength, which would only be true for temperatures below 10 mK. Apart from this, however, there is strong experimental evidence to suggest that the Rayleigh scattering model can be ruled out of consideration. Very simply, there are no changes in the grain size on annealing the samples in vacuum and rendering them insulating, yet these specimens show no crossover or any other anomalous feature in the thermal conductivity below 1 K.

Cohn *et al.* [107] have investigated in detail the changes in the low-temperature thermal conductivity of $YBa_2Cu_3O_{7-\delta}$ by cycling a sample between its superconducting and insulating states using successive vacuum and oxygen annealing treatments. The superconducting state of the sample was monitored by field-cooled magnetization (Meissner effect) in a 30-Oe external field, and the microstructure was inspected in an SEM following every heat treatment step. As the data in Fig. 28 indicate, no changes were detected either in the grain size or the porosity of the samples. The behavior of the thermal conductivity, however, clearly depends on whether the sample is annealed in oxygen (yielding superconducting material) or in vacuum (resulting in an insulating material), as illustrated in Fig. 29. Invariable, the sample in its superconducting state tends toward a T-linear dependence below 0.3 K while a roughly T^3 variation is observed in the insulating state with no hint of any anomalous behavior. The authors propose uncondensed carriers as the cause of the T-linear temperature dependence of the thermal conductivity in superconducting 1-2-3 ceramics and, applying the Wiedemann-Franz law, estimate the fraction of carriers not participating in superconductivity to be about 5%. This fraction is large enough to account for the γ-linear term in the specific heat (5–9 mJ/mole-K^2) with a reasonable value of the effective mass ($4m_e - 8m_e$). While these estimates are rather crude and rely on a free-electron approximation that is likely grossly inadequate, they nevertheless demonstrate a correspondence between the T-linear "pulling" in the low-temperature thermal conductivity and the large γ term in the specific heat. As we shall see later, this correlation is supported by the behavior of the Bi-based high-T_c superconductors, since these materials exhibit no T-linear dependence in κ and no γ term in their specific heat. It is not clear, assuming such uncondensed carriers exist, whether they are intrinsic to the La- and Y-based family of superconductors, or whether they are an artifact of a "dirty" synthesis. We shall return to this point later.

A preliminary study of the effect of heat treatment on the thermal conductivity measured near room

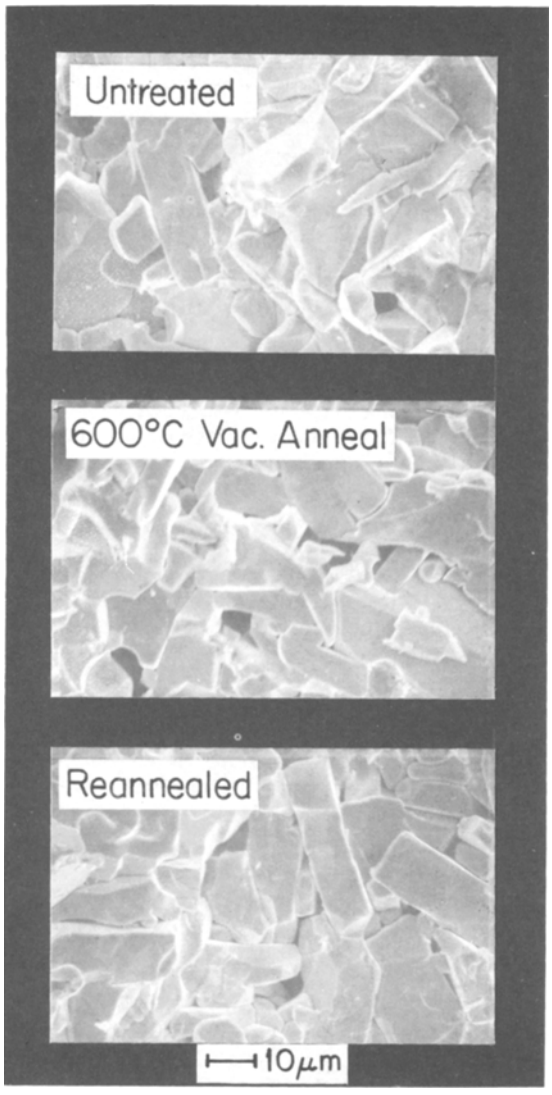

Fig. 28. Scanning electron micrographs of a specimen of $YBa_2Cu_3O_{7-\delta}$ before and after successive heat treatments. The view is perpendicular to the direction of heat flow on freshly cleaved material. (Taken from [107].)

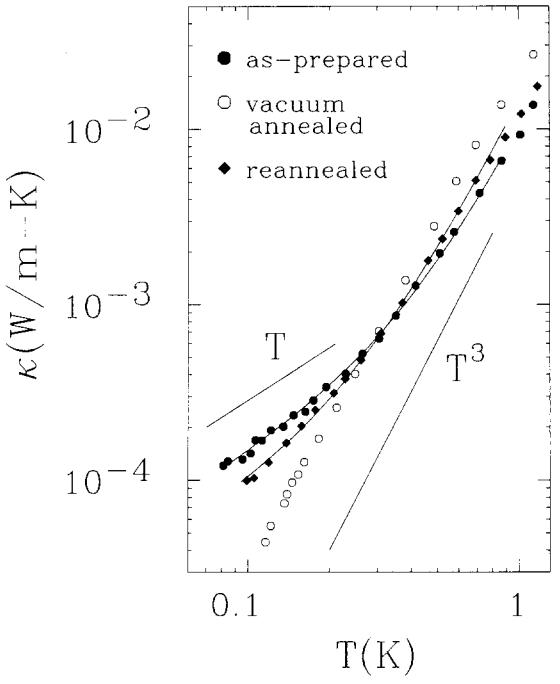

Fig. 29. Thermal conductivity of sintered $YBa_2Cu_3O_7$ in the as-prepared state and after successive heat treatments. Solid lines through the data are fits to the form $\kappa = aT + bT^3$ with coefficients a and b given in Table I. (Taken from [107].)

temperature was done recently by Williams *et al.* [108]. Using a comparative longitudinal heat flow apparatus, the authors determined κ in the range 300–360 K on a sample of $YBa_2Cu_3O_{7-\delta}$ in its as-prepared state and also following a heat treatment in oxygen at 950°C for 16 h. The data are reproduced in Fig. 30. In spite of a dramatic improvement in the room-temperature electrical resistivity from 10^{-3} Ωm for the as-prepared material to 3.4×10^{-5} Ωm following annealing, the thermal conductivity indicated a surprising degradation of about 20% as a result of the heat treatment. As the authors point out, such effect arises due to an enhancement in phonon scattering and they note several possible mechanisms that may be responsible, among them point-defect scattering and carrier–phonon interaction. Any definitive statement on the effect of heat treatment on the magnitude or temperature dependence of the thermal conductivity must await a more thorough investigation.

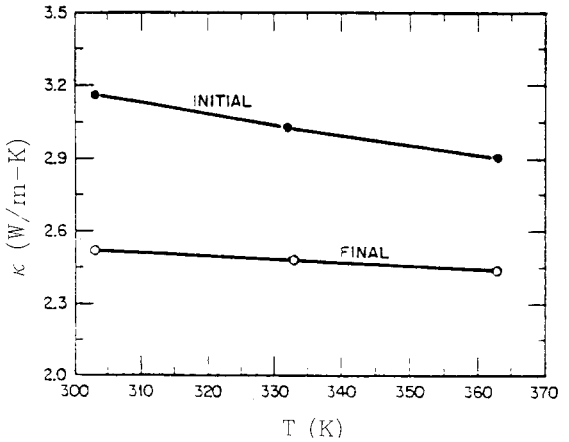

Fig. 30. Thermal conductivity of sintered $YBa_2Cu_3O_{7-\delta}$ in the as-prepared state and following heat treatment in oxygen at 950°C for 16 h. (Taken from [108].)

Let us turn our attention to the low-temperature behavior of single crystals. Obviously, thermal conductivity measurements on single crystals are likely to provide more information regarding the intrinsic mechanism of heat transport. Unfortunately, the experimental data here are by no means plentiful. Graebner *et al.* [48] have measured the in-plane thermal conductivity on small single crystals of $YBa_2Cu_3O_{7-\delta}$ down to 30 mK. Because of their greater structural integrity, one would expect the total scattering rate in single crystals to be smaller than in polycrystalline media. This, indeed, follows from Fig. 31 where single crystal data are compared to those for a sintered material. What is surprising, however, is the temperature dependence of the thermal conductivity. One would, perhaps, naively assume that the dominant dissipative mode in single crystals would be phonon scattering on the crystal boundaries and, therefore, a T^3 variation in the conductivity would follow. This is certainly not what the data of Fig. 31 indicate. Graebner *et al.* draw a $T^{1.8}$ line through the data points, indicating an approximate power law dependence which serves as a basis for their tunneling model of heat conduction. As I have noted in Section 3.4, this kind of phenomenological model has proved very useful in accounting for the low temperature thermal conductivity of some classic amorphous systems such as a-SiO_2. According to this model, phonons scatter resonantly from tunneling entities that occupy a double-well potential. Although the identity of these tunneling entities is frequently unknown, in the case of high-T_c superconductors, oxygen vacancies and tetragonally coordinated atoms are possible candidates. Comparing Eq. (17) with experimental results, Graebner *et al.* obtain $\bar{P}\gamma^2 = 4.8 \times 10^7\ \mathrm{erg^{-1}\,cm^{-3}}$, where $\bar{P}$ is the average density of tunneling states and γ is the coupling strength of TS to strain fields. This value is high, comparable to that for a-SiO_2, and in good agreement with values determined from measurements [46] of the sound velocity and damping below 1 K. Recall, however, that there is no evidence of a plateau above 1 K in the thermal conductivity of high-T_c superconductors, contrary to the situation in glasses where a plateau is a universal feature. While the tunneling picture has considerable appeal, closer inspection of the data of Fig. 31 reveals a continuous curvature and a distinct pull towards a lower power law exponent somewhere around 0.3 K. More recent experiments by Sparn *et al.* [109] on several single crystals of $YBa_2Cu_3O_7$ demonstrate quite convincingly the presence of a linear term in the in-plane thermal conductivity below 1 K (see Fig. 32). The authors note that, below 300 mK, the data obey Eq. (21) with a deviation of less than 5%, while a fit to a T^2 dependence results in a much larger (about 15%) and progressively increasing deviation as the temperature decreases. They argue that the presence of this linear term is persuasive evidence for the existence of intrinsic fermion low-energy excitations in high-T_c ceramics as

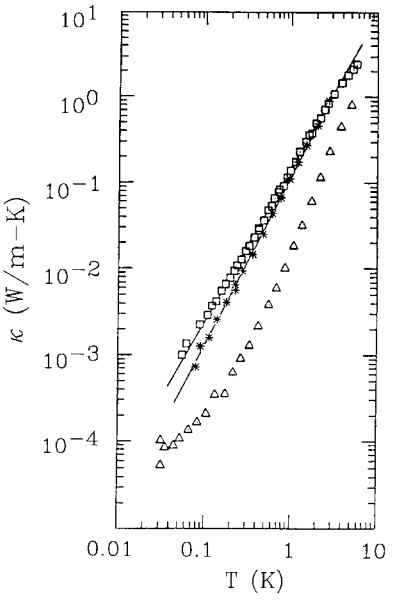

Fig. 31. In-plane thermal conductivity, κ_{ab}, for single crystal samples of □ $YBa_2Cu_3O_{7-\delta}$, and * $HoBa_2Cu_3O_{7-\delta}$. For comparison, open triangles indicate the thermal conductivity of sintered $YBa_2Cu_3O_{7-\delta}$. (Adapted from [48].)

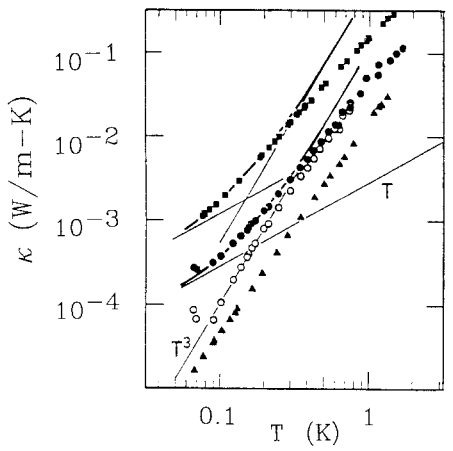

Fig. 32. Thermal conductivity of single crystals of $YBa_2Cu_3O_7$. ■ κ_{ab} of sample 1, ● κ_{ab} of sample 2, ○ κ_{ab} of sample 2 after subtracting the term aT, ▲ κ_c of sample 2. Lines through the data points are fits using Eq. (21) with coefficients given in Table II. (Taken from [109].)

Table II. Coefficients a and b in Eq. (21) for Single Crystals of $YBa_2Cu_3O_7$ from [109]

Coefficient	Sample I (κ_{ab})	Sample II (κ_{ab})	Sample III (κ_c)
$a(10^{-4}\,Wm^{-1}\,K^{-2})$	120	28	—
$b(10^{-4}\,Wm^{-1}\,K^{-4})$	5500	1030	600

well as single crystals. On one of the single crystals, designated in Fig. 32 by solid triangles, the authors also measured the thermal conductivity along the c direction. In this case, no linear term was apparent and the data indicated a T^3 asymptotic behavior. The observed difference in the thermal conductivity parallel and perpendicular to the Cu-O planes is explained as resulting from the reduced "characteristic dimension" for boundary scattering along the c axis. The thickness of this flux-grown sample is large (about 1.6 mm), and it is likely that layers of insulating flux material are interspersed within the crystal, parallel to the ab plane. Since magnetic fields of up to 8 T have no effect at all on the thermal conductivity in this very low temperature regime (i.e., on its aT term), Sparn *et al.* conclude that the assumed low-energy excitations cannot be spinon-type [110]. Clearly, the tendency toward a T-linear variation in $\kappa(T)$ is not as dramatic in single crystals as it is in sintered samples (compare the values of the coefficients a and b in Tables I and II), but it is developed to a degree that it casts considerable doubt on the TS picture.

It has been noted above that magnetic field has essentially no effect on the thermal conductivity of high-T_c superconductors at subkelvin temperatures. The reason for this is easily understood: the phonon wavelength at such low temperatures is very large and exceeds the characteristic flux core dimension ($\sim 2\xi$, where ξ is the coherence length) by several orders of magnitude. As a consequence, no significant phonon-fluxoid scattering takes place in this temperature range. In Section 3.3 I have pointed out that magnetic field might influence the thermal conductivity at temperatures where the phonon wavelength becomes comparable to the coherence length. For high-T_c materials this is expected in the temperature interval 10-100 K. The first hint of the effect of magnetic field on κ was detected by Zhu *et al.* [111] who observed a 4-10% decrease in the thermal conductivity of polycrystalline $YBa_2Cu_3O_7$ when the field of 3 T was directed perpendicular to the temperature gradient. More thorough investigations of suppression of the thermal conductivity by magnetic field were carried out recently by Palstra *et al.* [112] and by Florentiev *et al.* [113]. The former authors, as part of their studies of entropy transport due to vortex motion in single crystals of $YBa_2Cu_3O_7$, determined the change in κ_{ab} with the magnetic field oriented perpendicular to the ab plane, (Fig. 33). Florentiev *et al.* measured the ab plane thermal conductivity on 1-2-3 single crystals with the field rotated in the plane perpendicular to the temperature gradient. A decrease in κ_{ab} of up to 25% was observed in the field of 3.4 T (Fig. 34), and the data revealed large angular dependence (Fig. 35). The experimental observation indicating that below 20 K there is very little difference between the zero-field thermal conductivity and the thermal conductivity measured in 3.4 T is interpreted by the authors as a sign that the phonon wavelength begins to exceed the core diameter of the flux line. From the magnitude of the dominant phonon wavelength at 20 K they arrive at an independent estimate of the coherence length $\xi \sim 40$ Å which agrees well with estimates of ξ obtained by more direct techniques. As yet, no measurements exist of the effect of magnetic filed on the out-of-plane thermal conductivity, κ_c. The lack of such data amplifies difficulties associated with the c-axis thermal transport on thin, flakelike specimens.

4.2.2. *Substitutional $LaBa_2Cu_3O_{7-\delta}$ Superconductors*

Substitutional studies wherein one or more chemical constituents of a parent material are replaced either completely or partially by other elements is one of the most vigorously pursued areas of research on high-T_c superconductors. Apart from the fact that this route led to the discovery of high-T_c superconductivity, the importance of substitutional studies stems from their role as a powerful probe of the chemical and structural environment in a material which, in turn, determines whether or not the material will exhibit superconductivity. Furthermore, such investigations offer the tantalizing possibility of discovering related structures with even higher T_c's. Where in the crystal lattice the substitution takes place determines the degree to which the superconducting

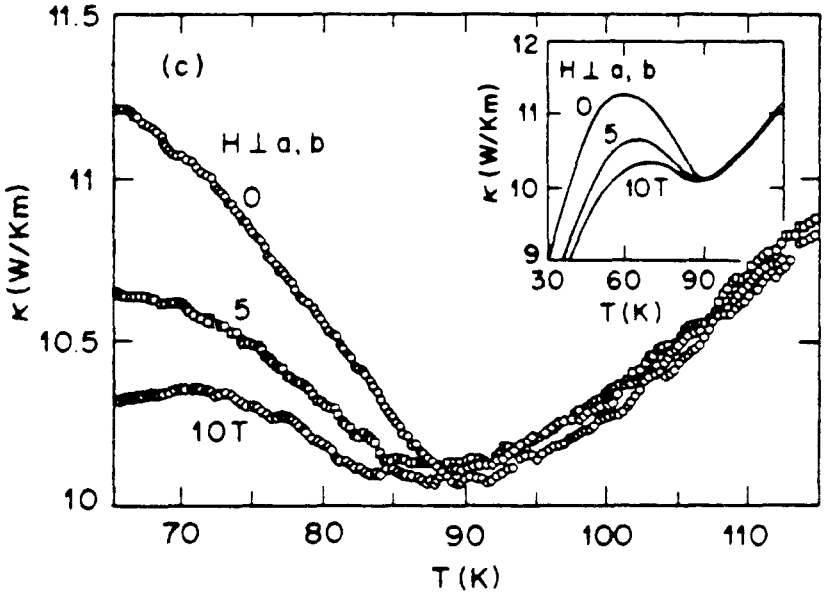

Fig. 33. Thermal conductivity, κ_{ab}, of a single crystal of $YBa_2Cu_3O_7$ measured at magnetic fields oriented perpendicular to the *ab* plane. (Taken from [112].)

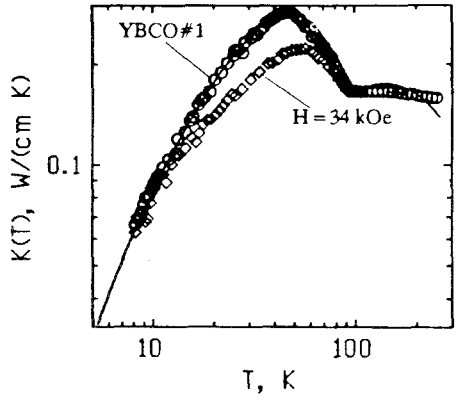

Fig. 34. In-plane thermal conductivity, κ_{ab}, of a single crystal of YBCO measured in zero magnetic field and in a field of 3.4 T oriented perpendicular to the *ab* plane. (Taken from [113].)

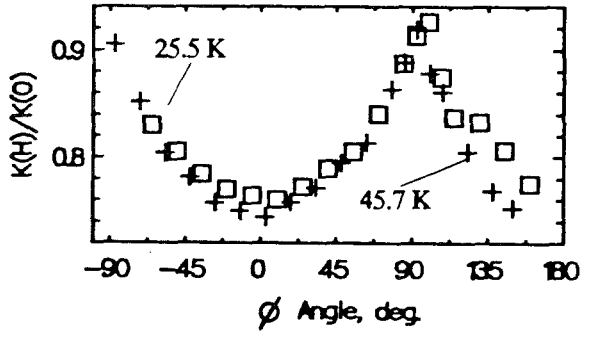

Fig. 35. Angular dependence of the in-plane thermal conductivity of a single crystal of YBCO determined in a magnetic field of 3.4 T oriented perpendicular to the heat flow and making an angle ϕ with the *c* axis of the crystal. (Taken from [113].)

parameters are affected. Substitution on a given lattice site is primarily controlled by three factors: (i) the ionic radii, (ii) the valence state, and (iii) the coordination number. The extent to which the dopant and host parameters match determines not only the level of substitution but also the strain fields arising from changes in local lattice constants. In cuprate superconductors, changes in the superconducting properties upon substitution are determined by the response of the Cu-O network. It is beyond the scope of this review to discuss the vast literature that has accumulated on the subject of substitution in high-T_c materials over the past couple of years. For this, the reader is referred to a review article [114] and references therein. I shall restrict our discussion to only those examples where thermal conductivity measurements were used to probe the effects of substitution. So far, all such studies have pertained to cation substitution at the Y site by an element from the lanthanide family. With the exception of Ce, Tb, and, most notably, Pr, complete replacement of Y by all other lanthanides has been achieved without significantly affecting T_c. This, of course, suggests that the Y site does not play a special role in superconductivity; it is there to stabilize the structure.

What is the effect of substitution on the thermal conductivity? In general, anion or cation substitution can affect the thermal conductivity in the following ways:

(i) A shift in T_c results in changes in the position of the thermal conductivity peak and its height.

If T_c is drastically degraded, it can be difficult to resolve the peak because the enhancement in the phonon mean-free path may not compensate for the rapidly diminishing phonon population at lower temperatures.

(ii) Impurity scattering may be enhanced if substitution leads to the formation of a multiphase structure.

(iii) If only partial substitution is achieved, κ can be affected by mass-defect scattering.

(iv) Scattering from strain fields and dislocations will increase if the dopant is dissimilar to the lattice ion.

(v) Both κ_e and κ_p will be affected if the substitution leads to changes in the carrier density or the degree of carrier localization.

(vi) Magnetic ordering may interfere if magnetic ions are substituted.

In the case that we consider here, Y site substitution by lanthanides, mechanisms (iii)-(vi) may in principle influence the thermal conductivity. However, since no thermal conductivity experiment has been performed on substituted single crystals, it is not possible to resolve specific features in the thermal conductivity data reflecting the chemical environment (bonding, strain, etc.) in which a substitutional ion is located. Variability in the structural integrity of sintered samples, namely different porosities, density, and grain size, are simply too large and their influence on the thermal conductivity overwhelms any changes arising from substitution. To illustrate this point, we compare the data of Jezowski *et al.* [115] where Y was replaced by both Sm and Gd (Fig. 36) with the measurements of Heremans *et al.* [116]

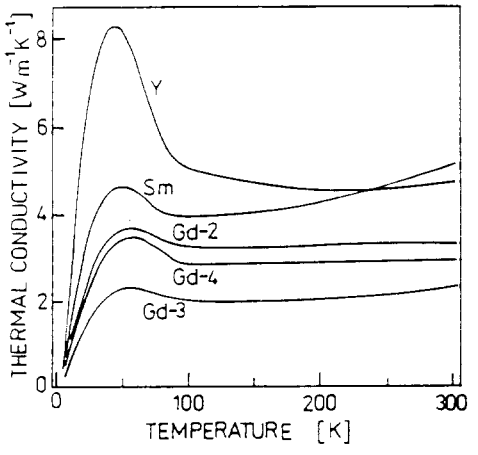

Fig. 36. Thermal conductivity of Sm and Gd-substituted 1-2-3 superconducting ceramics. (Taken from [115].)

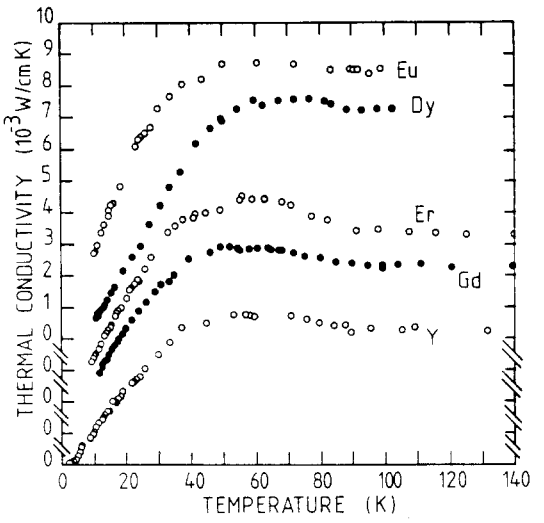

Fig. 37. Thermal conductivity of several rare-earth-substituted superconducting ceramics. For clarity, the vertical axis for each sample is displaced one unit. (Taken from [116].)

on a series of lanthanide-substituted 1-2-3 compounds (Fig. 37). The samples from these groups have comparable T_c's and display the same characteristic features in the thermal conductivity. One notes, however, that the thermal conductivities measured by the first group are, in general, an order of magnitude larger than the data of Heremans *et al.* obtained on rather porous structures. Furthermore, the Jezowski group finds the thermal conductivity of their parent material ($YBa_2Cu_3O_{7-\delta}$) to be far superior to that of their substituted 1-2-3 compounds. In contrast, the parent material of Heremans *et al.* shows a smaller κ than they observe for their substituted superconductors.

The high electrical resistivity of the samples studied by Heremans *et al.*, coupled with their assumption of a free electron mass, leads them to an extremely low estimate ($\sim 10^{-15}$ sec) of the carrier-phonon scattering time τ_{c-p}, as obtained from the expression for the phonon-limited resistivity, ρ_{c-p},

$$(\rho_{c-p})^{-1} = ne^2\tau_{c-p}/m^* \tag{24}$$

Interpreting such a short τ_{c-p} as an indication of strong coupling between the carrier and phonon systems, Heremans *et al.* proceed to calculate the carrier-phonon coupling constant, λ_{c-p}, using the lowest-order variational solution of the Bloch-Boltzmann transport equation

$$\hbar/\tau_{c-p} = 2\pi\lambda_{c-p}k_BT \tag{25}$$

The resulting coupling constants fall within the range 2.4-6 and seem to be unrealistically high.

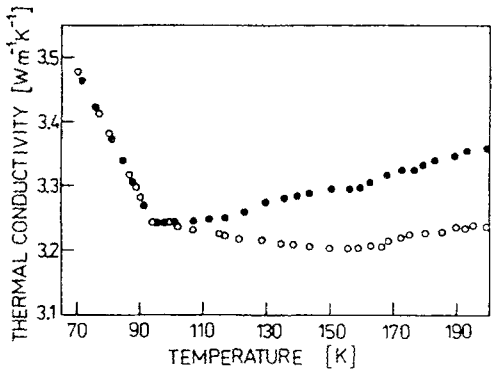

Fig. 38. Thermal conductivity of the sample Gd-2 before (open circles) and after (solid circles) heat treatment in helium gas above 150°C. (Taken from [115].)

Referring to Fig. 36, we note a pronounced increase in the thermal conductivity of the Sm-substituted 1-2-3 compound above T_c. Jezowski *et al.* propose that this behavior is connected with the presence of gas inside the pores of this sintered material. Gas recondensation from the hot to the cold wall of the pore then constitutes an additional heat-transporting mechanism. The authors provide further evidence for the role of gas in the pores of the microstructure by heating their Gd-substituted sample in a helium atmosphere above 150°C and comparing the thermal conductivity before and after the heat treatment (Fig. 38). At and below T_c the two curves coincide. For $T > T_c$, however, the heat-treated sample indicates a distinctly larger thermal conductivity which increases with increasing T. This happens in spite of no measurable effect on the electrical resistivity and no changes in the microstructure following the heat treatment. The question of why the gas should be samarium-specific when all of the samples were prepared under identical conditions remains a puzzle.

$GdBa_2Cu_3O_{7-\delta}$ is not only a high-T_c superconductor, but also an antiferromagnet with a Néel temperature $T_N \sim 2.2$ K. Below the ordering temperature of this material, superconductivity coexists with antiferromagnetism. Mori *et al.* [117] measured the thermal conductivity of a Gd-substituted ceramic sample between 1.5-7 K and observed a small upturn close to T_N as well as a change in the slope of the temperature dependence from approximately T^2 above the Néel temperature to closer to T^3 below T_N (Fig. 39). They suggested that the change in the conductivity may be due to decreasing phonon-paramagnon scattering below T_N. On application of an external magnetic field at 4.41 K, Mori *et al.* detected a 2.5%

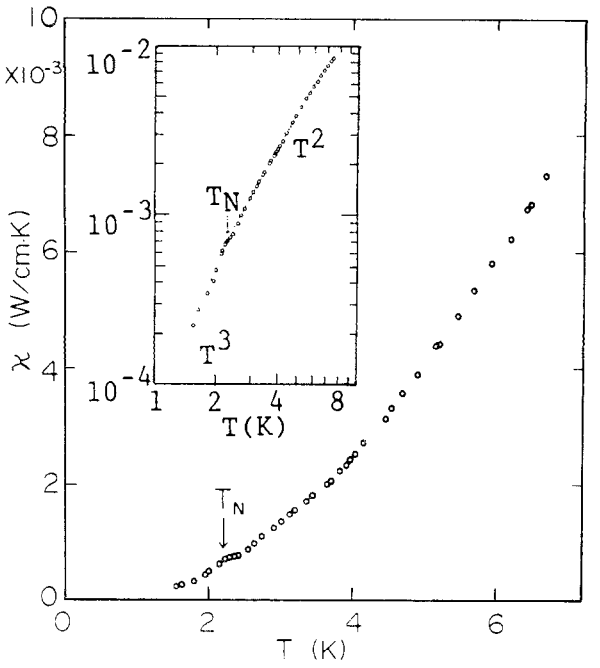

Fig. 39. Thermal conductivity of sintered $GdBa_2Cu_3O_{7-\delta}$. The inset shows the data plotted on the log-log scale to highlight the change in the temperature dependence below T_N. (Taken from [117].)

decrease in the thermal conductivity when the field strength was less than 1 kOe (see Fig. 40). The onset and completion of these changes correlated with a deviation from linearity and a minimum in the magnetization curve. They interpret the reduction in κ_p as arising from scattering of phonons within the normal regions of the sample or from normal-superconducting phase boundaries. This behavior is similar to

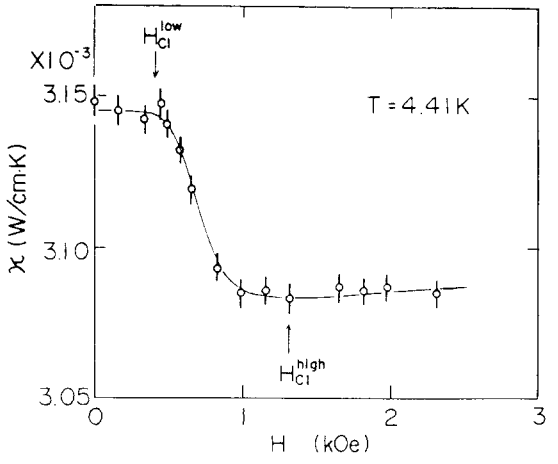

Fig. 40. Magnetic field dependence of the thermal conductivity of sintered $GdBa_2Cu_3O_{7-\delta}$. (Taken from [117].)

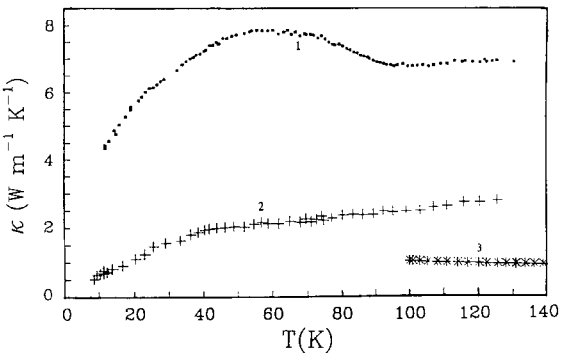

Fig. 41. Crosses indicate the thermal conductivity of a tetragonal crystal of $GdBa_2Cu_3O_x$. Solid squares represent the total thermal conductivity of a superconducting sample of $TmBa_2Cu_3O_x$ (about 50% of the sample is a single-domain region). Curve 3 indicates the electronic component of the thermal conductivity. (Adapted from [118].)

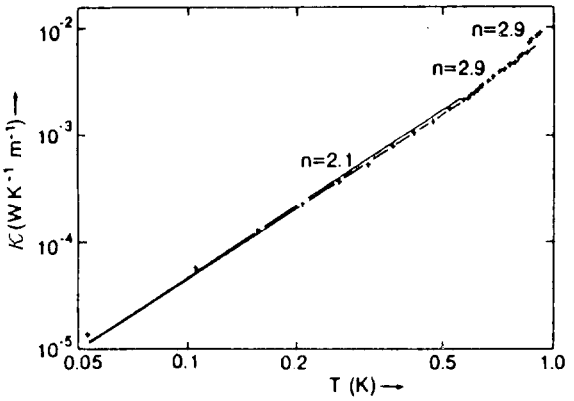

Fig. 42. Thermal conductivity of a polycrystalline, superconducting sample of $SmBa_2Cu_3O_7$ at very low temperatures. The index n indicates the power law exponent of the thermal conductivity. (Taken from [119].)

that seen in typical type-II superconductors, as discussed in Section 3.3. The in-plane thermal conductivity of a tetragonal single crystal of $GdBa_2Cu_3O_{7-\delta}$ ($0.7 \leq \delta \leq 1$) was investigated recently by Aliev *et al.* [118] in the temperature range 10–130 K. The data are presented in Fig. 41. The behavior of the thermal conductivity is similar to that seen in ceramic samples of $YBa_2Cu_3O_{7-\delta}$ with a comparable oxygen deficiency (see Fig. 24). Also displayed in Fig. 41 are the data for the in-plane thermal conductivity of a substantially single-domain, superconducting ($T_c \sim 90$ K) specimen of $TmBa_2Cu_3O_x$ studied by the same authors. These results agree qualitatively with the in-plane thermal conductivity of $YBa_2Cu_3O_7$ measured in [96].

Thermal conductivity measurements on Sm-substituted [119] and on Er- and Ho-substituted [120] high-T_c ceramics were extended recently down to 60 mK by Willekers *et al.* The authors investigated both superconducting and nonsuperconducting specimens and noted significantly different power law dependences, $\kappa \propto T^n$, between the two groups. The exponent for nonsuperconducting samples below 0.5 K is $n \simeq 2.7$, indicating almost purely phonon transport. The power law dependence for superconducting samples is not unique, varying, below 0.5 K, from $n \simeq 2.1$ for $SmBa_2Cu_3O_7$ to $n \simeq 2.2$ for $ErBa_2Cu_3O_7$ and to $n \simeq 2.9$ for superconducting $HoBa_2Cu_3O_7$. The authors indicate that for Sm- and Er-based ceramics they may, over a limited temperature range of 0.35–0.6 K, fit the data well with the form $\kappa = aT + bT^3$ where the coefficients a and b are comparable to those for $YBa_2Cu_3O_7$ given in Table I. For $HoBa_2Cu_3O_7$, however, such fitting procedure fails. Above 0.5 K, the exponents increase to $n \simeq 2.9$ for Sm-substituted sample and to $n \simeq 2.6$ for Er-based material. The low-temperature exponents of the power-law dependence of superconducting samples may be strongly affected by the magnetic state of substituted ions. Sharp magnetic-phase transitions are observed on the specific heat at 0.56 K for $SmBa_2Cu_3O_7$ and at 0.17 K for $HoBa_2Cu_3O_7$. In addition, the authors note that a Sm-based material (in both superconducting and nonsuperconducting states) shows a reproducible jump of about 20% near 0.84 K in its thermal conductivity measured in "field free" environment (Fig. 42). The earth's magnetic field is sufficient to suppress the jump and Willekers *et al.* assume that the jump is caused by a subtle magnetic process such as, for example, a one-dimensional ordering proposed by Simizu *et al.* [121]. Clearly, the thermal transport studies on high-T_c perovskites in which the rare earth sublattice orders magnetically are a delicate matter and one must have a good control of not only the temperature but also of external magnetic field.

One other lanthanide-substituted system for which the thermal conductivity was studied is $EuBa_2Cu_3O_{7-\delta}$. Izbizky *et al.* [122] investigated the heat transport of a high-density (6.35 g/cm^3) sintered sample with an average grain size ≥ 20 μm. The data (see Fig. 43) are very similar to those for $YBa_2Cu_3O_{7-\delta}$. The authors apply the BRT theory to determine the carrier-limited, κ_{p-c}, and the defect-limited, κ_{p-d}, phonon thermal conductivities which are shown in Fig. 43 by solid and broken lines, respectively. From the former they proceed to compute, using the formulas of [20], the superconducting

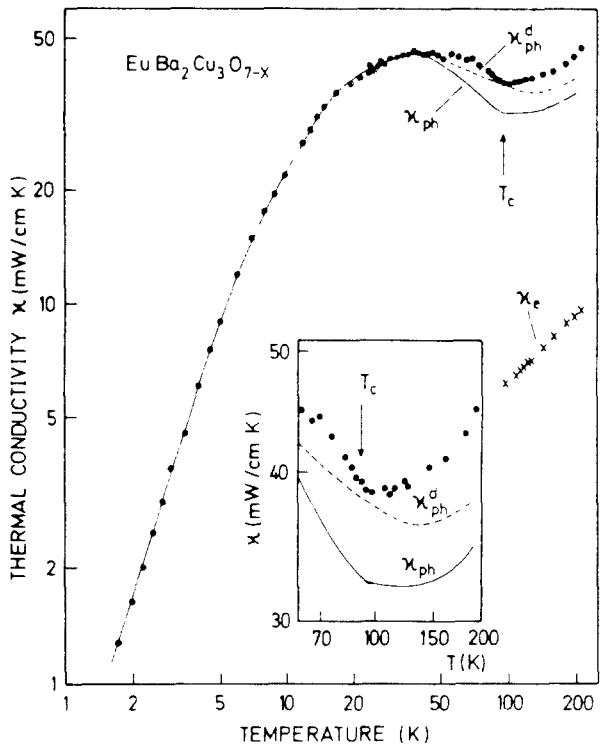

Fig. 43. Thermal conductivity of $EuBa_2Cu_3O_{7-\delta}$. The solid line represents the phonon thermal conductivity and the broken line the "defect" limited contribution. Crosses indicate the electronic thermal conductivity. The inset expands the region near T_c. (Taken from [122].)

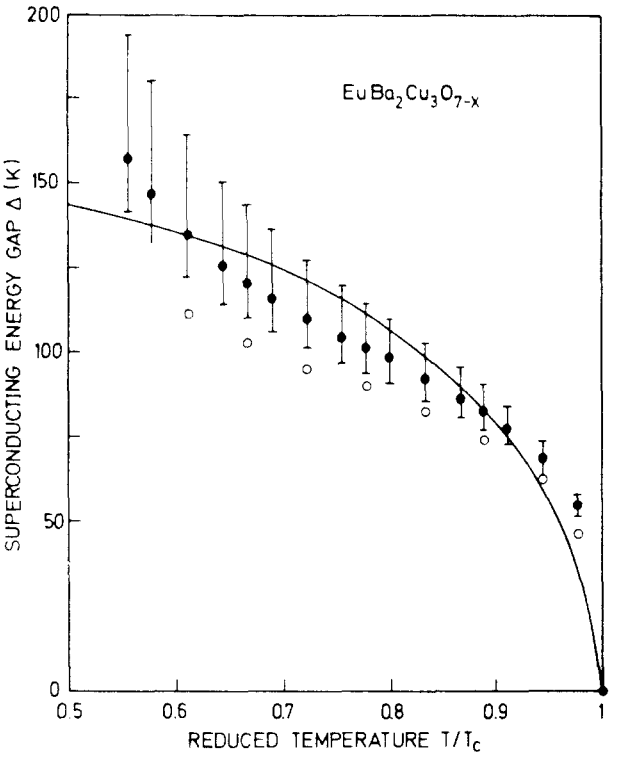

Fig. 44. Superconducting energy gap (in Kelvin) plotted against the reduced temperature. The error bars indicate the maximum estimated error arising from approximations and/or uncertainty in the geometrical factor. Open circles represent gap calculations that use as an input the thermal conductivity data of [87]. The BCS gap temperature dependence with $2\Delta(0)/k_BT_c = 3.3$ is shown by the solid curve. (Taken from [122].)

energy gap as a function of temperature. The results are reproduced in Fig. 44. For comparison, the energy gap of $YBa_2Cu_3O_{7-\delta}$, calculated using the thermal conductivity data of [87], is indicated by open circles, and the BCS gap temperature dependence with $2\Delta(0)/k_BT_c = 3.3$ is drawn by a solid line. There is reasonable agreement between the data and the weak coupling value of $2\Delta(0)/k_BT_c$, a trend that is generally confirmed by other kinds of experiments. Eu-based material of considerably lower density (4.5 g/cm^3), designated as $EuBa_2Cu_3O_{9-\delta}$, was investigated by Buravoi *et al.* [92] between 80–300 K.

4.2.3. Radiation-Damaged $YBa_2Cu_3O_{7-\delta}$

The ability of a material to undergo a certain level of radiation damage, e.g., by fast neutrons, without a serious degradation of its operational characteristics is an important consideration for a number of industrial applications. In superconductors, the studies of radiation-induced damage usually focus on two pivotal questions: how does the T_c change with the fluence of energetic particles and what is the effect of structural damage on the critical current density, J_c. Answers to these questions have been forthcoming from experiments started not long after the discovery of high-T_c superconductivity and they can be summarized as follows: For low radiation levels (fluences $\leq 10^{17}$ n cm^{-2}), T_c is essentially independent of the fluence. At higher levels of irradiation, T_c begins to decrease rapidly and at fluences $\sim 10^{19}$ n cm^{-2} superconductivity is suppressed to below 4 K. Overall, the sensitivity of high-T_c perovskites to fast-neutron damage is about a factor of 2 higher than for typical A15 compounds. While structural defects created by neutron bombardment have the effect of pinning the flux-line network and, therefore, enhancing J_c, there is concurrent damage done to the intergrain regions affecting the weak-link structure of the material which results in the resistively measured J_c decreasing with fluence.

Fast neutrons inflict structural damage by, among other things, creating and redistributing oxygen vacancies. The subsequent increase in scattering

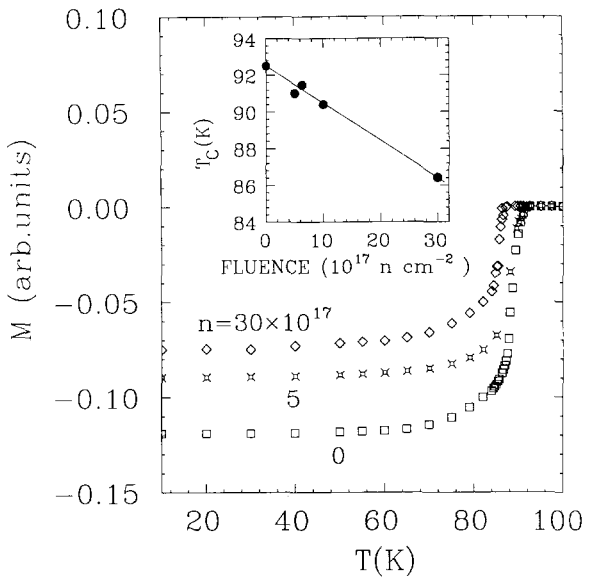

Fig. 45. Changes in the magnetic moment of sintered $YBa_2Cu_3O_7$ irradiated with fast neutrons. The inset shows degradation of T_c with fluence of neutrons. (Taken from [123].)

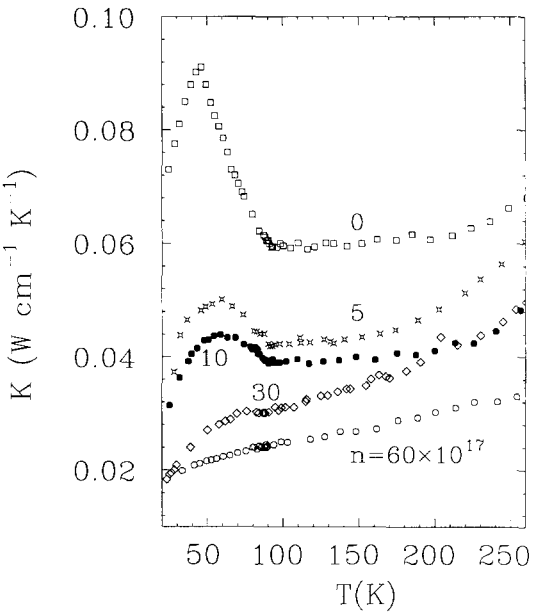

Fig. 46. Thermal conductivity of $YBa_2Cu_3O_7$ at various levels of irradiation. Fast-neutron fluence is indicated on each curve. (Taken from [123].)

has an effect on both the phonon and carrier distribution functions, which, in turn, leads to changes in the magnitude and temperature dependence of the thermal conductivity with increasing fluence. Such changes were detected in the measurements of Uher and Huang [123] on fast-neutron-irradiated sintered samples of $YBa_2Cu_3O_{7-\delta}$. The experiments were carried out on rectangular samples ($2\times2\times15$ mm) cut from the same disk and exposed at room temperature to fast neutrons ($E \geq 0.1$ MeV) with fluences between 10^{17} to 6×10^{18} n cm^{-2}. After the samples reached the desired level of damage, changes in T_c were examined by monitoring the magnetic moment and electrical resistivity (see Fig. 45). The thermal conductivity between 20–250 K was then measured by a steady-state technique. The data are reproduced in Fig. 46. As is apparent from the figure, exposure to fast neutrons has two major consequences: the overall thermal conductivity decreases with increasing fluence, and the maximum is strongly suppressed, vanishing altogether at the highest fluences. Since the electrical resistivity increases rapidly with fluence, the already small contribution of carriers to the thermal transport is further reduced upon irradiation. Hence, degradation of the thermal conductivity in neutron-irradiated samples arises primarily due to additional phonon scattering on radiation-induced defects. While a detailed analysis of structural damage in high-T_c superconductors is not yet available, it very likely consists of cascades of vacancies and interstitials. The fact that these defects give rise to additional phonon scattering is clearly revealed by the pronounced attenuation of the thermal conductivity peak. Undoubtedly, the progressively stronger phonon-defect scattering at high neutron fluences imposes a limit on the phonon mean-free path and, as a result, the influence of phonon-carrier interactions on the thermal conductivity is lessened. It should be noted that even at the highest fluence of 6×10^{18} n cm^{-2}, where the conductivity peak is totally washed out, the material still possesses a high transition temperature in excess of 80 K. This is, of course, consistent with the notion that the traditional phonon-mediated mechanism alone cannot account for superconductivity in the 90 K range. It would be of interest to measure the effect of radiation-induced damage on the thermal conductivity of single crystals and highly oriented epitaxial thin films and examine how these results differ from those for ceramic structures. Such studies should be accompanied by detailed high-resolution TEM investigations so that specific defect centers can be identified and a more quantitative analysis of the thermal transport properties can be undertaken.

4.2.4. Thermal Conductivity of $YBa_2Cu_3O_{7-\delta}$ Thin Films

In the Introduction I noted that thermal conductivity is a parameter of vital importance in a number

of applications of thin-film high-T_c superconductors. We have already seen that, at around 4 K, the phonon mean-free path, l_p, is on the order of 1 μm for polycrystalline ceramics and perhaps a factor of 2–5 larger for high-quality single crystals. Epitaxially oriented thin films are expected to have an l_p close to the value in single crystals. Thus, the free paths are comparable to the thicknesses of typical thin film superconductors and further reductions in film thickness should result in a size limitation on the phonon transport. While no experimental data are available as of yet to corroborate this prediction, the problem has recently been considered theoretically by Flik and Tien [6]. Using the kinetic theory approximation, they devised a simple method based solely on geometrical arguments to account for size effects in thin film structures. Their starting point is the Fuchs–Sondheimer model [124,125] which treats resistance due to scattering of phonons or electrons at the film surfaces. It is assumed that the carrier paths originate isotropically and scatter diffusely at the film boundaries, a reasonable assumption when one takes into account the small magnitude of the phonon wavelength (<0.5 μm above 10 K) as compared to the characteristic roughness [126] (~ 1 μm) at the surface of the film. Since the a and b lattice parameters of the 1-2-3 compounds are similar while the c-axis parameter has roughly three times their value, it is reasonable, from the point of view of transport effects, to consider the structure as tetragonal. The thermal conductivity, then, has two nonzero tensor components: κ_a for the in-plane conductivity and κ_c for the c-axis conductivity. The vast majority of high-quality films are made with the c axis normal to the film plane. In the notation of Flik and Tien this corresponds to the y axis coordinate. For a thick film then, $\kappa_x = \kappa_a$, $\kappa_y = \kappa_c$, and the material anisotropy, $A = \kappa_x/\kappa_y$, is the same as the crystal anisotropy, κ_a/κ_c. Assuming further that the relaxation time is independent of direction, the anisotropy is entirely due to the difference in the sound velocities, $v_a/v_c = A^{1/2}$. From Eq. (7) it immediately follows that $l_a/l_c = A^{1/2}$. Taking into account both size effects and crystal anisotropy, Flik and Tien obtain for the conductivities along and across a thin film of thickness d,

$$\kappa_x = 2\kappa_a F(\delta_1) \tag{26}$$

$$\kappa_y = \frac{2\kappa_a}{A} G(\delta_2) \tag{27}$$

where $\delta_1 = d/l_a$, $\delta_2 = dA^{1/2}/l_a$ and $F(\delta) = l_x/l$, $G(\delta) = l_y/l$ (the solutions for the size effect derived by the authors on the basis of the Fuchs–Sondheimer theory).

The anisotropy of the film follows immediately from

$$\frac{\kappa_y}{\kappa_x} = \frac{1}{A}\frac{G(\delta_2)}{F(\delta_1)} \tag{28}$$

Equation (28) represents the combined effect of the material anisotropy and the size effect on the anisotropy of a thin film. As Flik and Tien point out, the material anisotropy, A, influences the film anisotropy in two ways. It is a multiplication constant in Eq. (28), and it enters into the arguments of functions F and G where it differs by a factor of $A^{1/2}$ between the two directions. Physically this means that, for the same film thickness δ, the size effect is more prominent in the high-conductivity direction, i.e., in the direction where the intrinsic mean-free path is large.

Flik and Tien also consider the case where the c axis lies in the plane of the film, say parallel to the x axis. This orientation can be realized using certain methods of $YBa_2Cu_3O_{7-\delta}$ thin film deposition [127]. The material anisotropy now becomes $A = \kappa_c/\kappa_a$, Eqs. (26) and (27) apply again, and the influence of the size effect on the thermal conductivity along the z direction is given by

$$\kappa_z = \frac{2}{A}\kappa_c F(\delta_2) \tag{29}$$

Size-induced anisotropy in a thin film of otherwise isotropic material arises as a consequence of different reductions in the phonon mean-free path in the directions along and across the film. In very thin films, it is strong enough to convert an isotropic film into a highly anisotropic medium for thermal transport. Figure 47 is a graphic representation of Eq. (28) for several values of the material anisotropy A. The $A = 1$ case stands for a thin film of isotropic material. The curves reveal a very interesting trend. If the material anisotropy, A, is smaller than unity, the size effect has a strong influence, and for very small film thicknesses, it might even lead to a reversal of the anisotropy. Alternatively, a highly anisotropic material may, due to the size effect, become isotropic for a particular film thickness.

Size effects in thin films of high-T_c superconductors such as $YBa_2Cu_3O_{7-\delta}$ are even likely to come into play in the liquid-nitrogen temperature range for film thicknesses on the order of 1000 Å and below, particularly if epitaxial registry has been relied on to

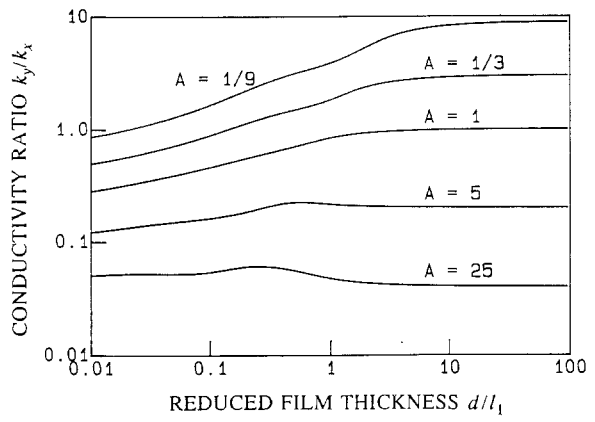

Fig. 47. Combined influence of size effect and material anisotropy on the thermal conductivity of a thin film. (Taken from [6].)

produce films of high quality. Much interesting work awaits experimentalists who care to explore thermal transport in thin-film high-T_c superconductors.

4.3. $Bi_2Sr_2Ca_{n-1}Cu_nO_{2n+4}$

Following an intensive search for superconductors with still higher T_c, Maeda *et al.* [3] reported in early 1988 the discovery of superconductivity in a quinary system based on Bi-Sr-Ca-Cu-O, the first high-T_c material synthesized without a rare-earth element. This work benefitted from the prior study of Michel *et al.* [128] on a quaternary Bi-Sr-Cu-O system where signs of superconductivity were detected in the 7-22 K range. As a result of a thorough structural analysis, two compositions (and subsequently a third, lower T_c phase) were identified as responsible for superconductivity: $Bi_2Sr_2CaCu_2O_8$, the so-called (2212) phase with a T_c of about 85 K, and $Bi_2Sr_2Ca_2Cu_3O_{10}$, the (2223) phase with $T_c \sim 110$ K. Due to the more complex structure of the quinary system and the widely varying reactivity and volatility of the individual constituents it is, in general, difficult to prepare single-phase specimens of this material. This has certainly proved to be the case with the (2223) phase, which is invariably intergrown with the lower-T_c, 85 K phase, in spite of great efforts to isolate the former. It is only because of success with partial substitution of Pb for Bi, a process which promotes the formation and improves the connectivity of the 110 K phase, that the zero-resistance state has routinely been achieved near 110 K.

A characteristic feature of the Bi-based material is the presence of pairs of BiO layers held together by a van der Waals type of bond. Pronounced anisotropy in the BiO bonding (in-plane bond length of 2.2 Å versus an across-the-plane bond length of 3.4 Å) coupled with a range of c axis periodicities that can be formed by adding Cu-O planes between the BiO double layers greatly enhances the layered aspect of the crystal structure in this material. There are several other notable differences from the 1-2-3 compounds that are considered important from a theoretical and practical viewpoint. The structure does not support Cu-O chains such as occur in the rhombohedral phase of $YBa_2Cu_3O_{7-\delta}$, and early speculations that these chains may play a key role in the mechanism of superconductivity appear unfounded. Likewise, since there is no tetragonal-orthorhombic transition in the Bi family of superconductors, there are no mirror-type (110) twins. This suggests that models of high-T_c superconductivity based on the existence of twins suffer from a lack of universality, among other things. For potential technological applications it is of interest that the Bi system is relatively insensitive to oxygen treatment. Finally, a very important feature of these materials is their apparent lack of a γ term in the low-temperature specific heat. This property may have an impact on the behavior of the thermal conductivity at low temperatures, as will be indicated below.

Currently, several reports exist in the literature that describe measurements of the thermal conductivity of Bi-based superconductors. Quantities that have been measured include the thermal conductivity of sintered samples and the in-plane thermal conductivity of single crystals.

Peacor and Uher [129] investigated the thermal transport from room temperature down to 70 mK on a sintered sample of nominally (2223) material [though it undoubtedly contained some (2212) phase], and two hot-pressed specimens of a nominal (2212) composition. The hot-pressed samples were cut from the same ingot parallel (sample C) and perpendicular (sample B) to the pressing direction. As I have mentioned before, hot-pressing promotes the alignment of crystallites during the processing stage and this gives rise to a certain degree of structural anisotropy. The processing-induced anisotropy is reflected in the resistivity data of Fig. 48 where one observes that the anisotropy ratio, R_C/R_B, is equal to about 4 at 300 K, and that the resistivity in the parallel direction shows a slightly activated character. Note also that the sintered specimen (sample A) has metallic properties superior to those of the hot-pressed material in spite of its lower density. As Murayama *et al.* [130] show, this seems to be the

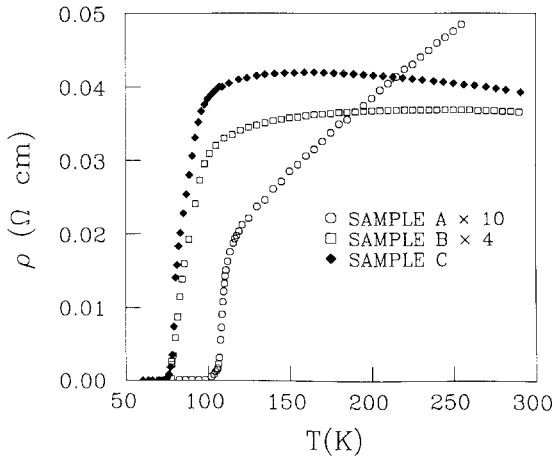

Fig. 48. Temperature dependence of the resistivity of sintered Bi-Sr-Ca-Cu-O. Note different scales for the samples and large anisotropy for the hot-pressed material, samples B and C. (Taken from [129].)

result of reduced oxygen diffusion in the more compact environment of the hot-pressed materials. Only after prolonged annealing in air does the normal-state resistance of a hot-pressed material fall below that of a sintered sample.

The temperature dependence of the thermal conductivity of the sintered sample of Peacor and Uher is shown in Fig. 49. The conductivity decreases gradually down to 110 K where a clear upturn, followed by a maximum near 75 K, is observed. Because of evidence for the existence of two intergrown phases in this sample, the authors searched for an additional upturn in the κ vs. T plot around 85 K that would signal a lengthening in the phonon mean-free path as the carriers of the (2212) phase condensed. None was detected. It is not surprising that it is difficult to resolve any small additional upturn in the already rising thermal conductivity, particularly if the (2223) phase occupies a large volume fraction. It is also possible that the number of normal carriers associated with the (2212) phase is small and/or these carriers couple weakly to the phonon system. The magnitude of the conductivity of this material is comparable to, though somewhat smaller than, that of a typical 1-2-3 compound. Using the Wiedemann-Franz law, the authors conclude that, at most, about 13% of the heat is carried by charge carriers. A virtually identical charge carrier contribution (10%) has been estimated by Mori *et al.* [131] in their measurements of sintered $Bi_{1.4}Pb_{0.6}Sr_2Ca_2Cu_3O_x$, (see Fig. 50), even though the magnitude of the total thermal conductivity of their samples is about 50% higher than the data of Fig. 49. These two sets of measurements also yield similar results for temperature dependence of $\kappa(T)$ in the superconducting state. On the other hand, investigations of the thermal conductivity of sintered $Bi_2(Ca_{0.5}Sr_{0.5})_3Cu_2O_x$ by Aliev *et al.* [132] reveal the existence of two peaks in $\kappa(T)$ (located near 115 K and 75 K) which suggests that the sample contains a two-phase mixture with a small volume fraction of the (2223) phase. In general, at temperatures above 10 K, the main features of the thermal conductivity

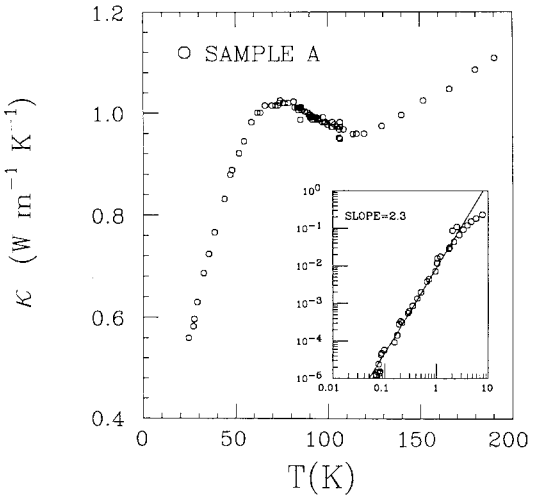

Fig. 49. Thermal conductivity of sintered $Bi_2Sr_2Ca_2Cu_3O_{10}$ (sample A). The inset shows the data at very low temperatures. (Taken from [129].)

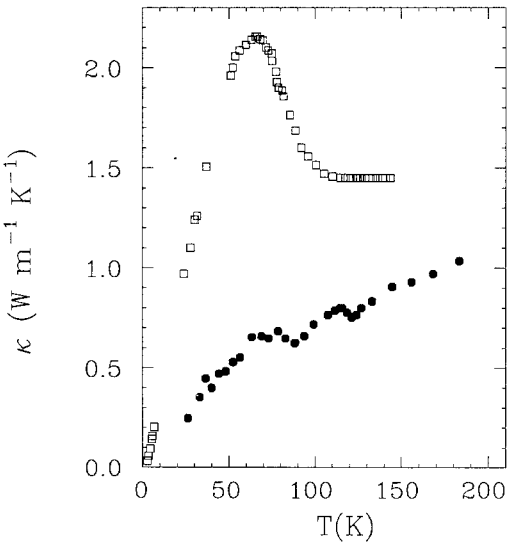

Fig. 50. Thermal conductivity of sintered Bi-Sr-Ca-Cu-O. Open squares are the data of Mori *et al.* [131] for $Bi_{1.4}Pb_{0.6}Sr_2Ca_2Cu_3O_x$; solid circles are the data of Aliev *et al.* [132] for $Bi_2(Ca_{0.5}Sr_{0.5})_3Cu_2O_x$.

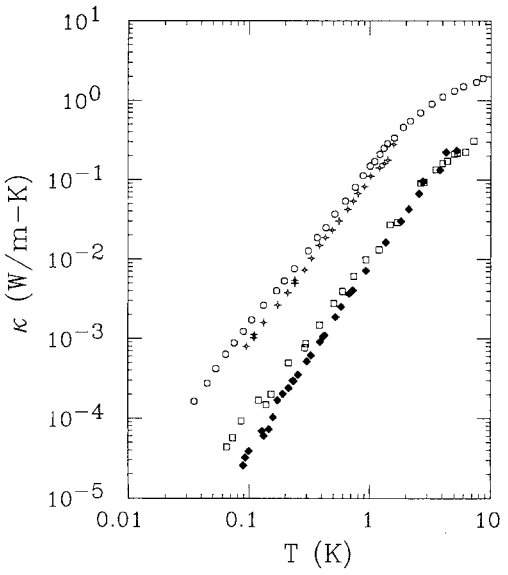

Fig. 51. Thermal conductivity of $Bi_2Sr_2Ca_1Cu_2O_8$ at very low temperatures. ◆ hot-pressed material (sample C) and □ hot-pressed material (sample B) of [129]; ○ single crystal, κ_{ab}, of [133]; ¤ single crystal, κ_{ab}, of [109].

of Bi-based ceramics are similar to those of 1-2-3 compounds. One would, therefore, expect that the behavior of the transport below 10 K would also be similar for these two families of high-T_c superconductors. This, however, is not so. As the data of Fig. 51 and the inset of Fig. 49 indicate, an approximately T^2-dependence sets in below about 2 K and proceeds unabated down to the lowest temperatures. This is in sharp contrast to the behavior of the thermal conductivity in sintered samples of $La_{2-x}Sr_xCuO_4$ and $YBa_2Cu_3O_{7-\delta}$ where, thus far without exception, the thermal conductivity obeys Eq. (21), i.e., a distinct linear term sets in below about 0.3 K. I have already noted that this linear "pull" in the thermal conductivity occurs in ceramic samples that show a large γ term in their specific heat. Since all attempts to detect a γ term in Bi-based superconductors have failed [68], the lack of a T-linear term in the thermal conductivity of these materials further corroborates the one-to-one relationship between the T-linear contributions to the heat transport and the specific heat. Just as the presence of a linear specific heat term is not a universal feature of high-T_c oxides, so a T-linear dependence of the thermal conductivity is not an intrinsic feature of the thermal transport in these ceramics. The sintered Bi-based material simply bucks the trend.

The thermal conductivity of $Bi_2Sr_2Ca_1Cu_2O_8$ single crystals is reported on by Zhu *et al.* [133], by Sparn *et al.* [109], by Aliev *et al.* [118], by Zavaritskii *et al.* [134], and by Crommie and Zettl [135]. The first two groups concentrate on in-plane measurements at very low temperatures with the aim being to determine the limiting temperature dependence of $\kappa(T)$ (see Fig. 51). The data of Zhu *et al.* extend down to 30 mK and indicate an approximately T^2 variation of $\kappa(T)$. Sparn *et al.* attempt to fit Eq. (21) to their data assigning the values $a = 63 \times 10^{-4}\ \mathrm{Wm^{-1}\,K^{-2}}$ and $b = 2500 \times 10^{-4}\ \mathrm{Wm^{-1}\,K^{-4}}$ to the coefficients, though one can also obtain a satisfactory fit assuming a quadratic temperature dependence. As can be seen from Fig. 51, these two measurements are, overall, in remarkably good agreement. If any tendency toward a T-linear variation at the lowest temperatures is present, it is certainly far less developed than in superconducting crystals of 1-2-3 compounds. It is interesting then and contrary to the case of La-Sr-Cu-O and Y-Ba-Cu-O superconductors, that the temperature dependence of Bi-Ca-Sr-Cu-O does not seem to depend on the particular morphology of the investigated samples; a T^2 variation in κ at low temperatures is a very good approximation to the behavior of both single crystals and sintered samples. Because of its pronounced layered character, it is possible that dimensional effects play an important role in the heat transport of Bi-Sr-Ca-Cu-O superconductors. Unfortunately, the thermal conductivity along the c direction has not yet been measured and, therefore, this assumption is only a speculation that awaits experimental scrutiny.

Aliev *et al.* describe measurements of the in-plane thermal conductivity in three single crystals of the (2212) phase in the temperature range from 10 K to about 130 K (see Fig. 52). These investigations display a degree of variability in the data for the three samples. Although the sample designated as No. 2 has features that closely resemble the data for ceramic samples, the other two samples studied, No. 1 and No. 3, show a peculiar upturn in the thermal conductivity that sets in below 15 K. The authors attempt to explain this upturn as essentially being a signature of the dielectric peak in the thermal conductivity. No such behavior is seen by any other group, including Zavaritskii *et al.* and Crommie and Zettl who recently measured the in-plane thermal conductivity in high-quality single crystals of $Bi_2Sr_2Ca_1Cu_2O_8$. Since the anomalous behavior reported in [118] is observed at the lower extreme of the temperature range investigated, it seems possible that it is an experimental artifact, perhaps having to do with thermometry.

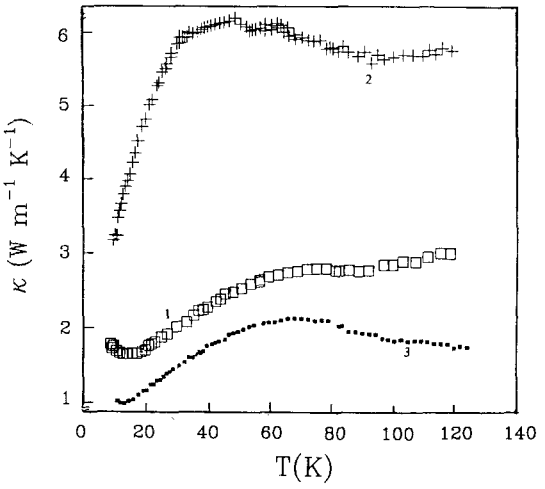

Fig. 52. Thermal conductivity of three single crystals of $Bi_2Sr_2Ca_1Cu_2O_x$. Numbers on the curves designate various samples. (Adapted from [118].)

The data of Zavaritskii *et al.* on four single crystals with an exceptionally high T_c (~95 K) for the (2212) phase are displayed in Fig. 53. The magnitude of the thermal conductivity above T_c falls in-between the data of Aliev *et al.* and is about a factor of 2-3 larger than for ceramic samples in Fig. 49. Using the Wiedemann-Franz law in conjunction with the electrical resistivity, the authors estimate that the carrier thermal conductivity at 100 K represents about 20% of the total heat conductivity for sample No. 1, 10% for samples Nos. 2 and 3, and 15% for sample No. 4. They also calculate the phonon mean-free path in these crystals at 100 K as being of the order of 40 Å.

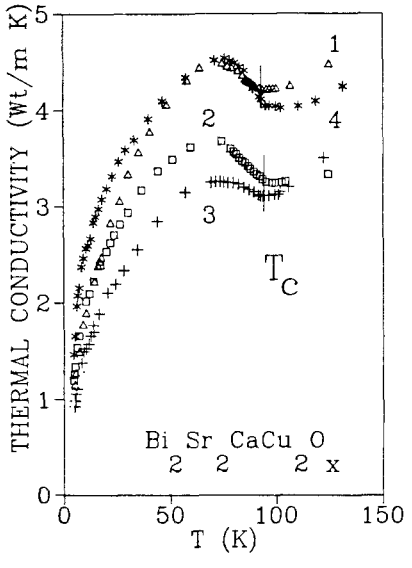

Fig. 53. In-plane thermal conductivity, κ_{ab}, for four single crystals of $Bi_2Sr_2Ca_1Cu_2O_x$. (Taken from [134].)

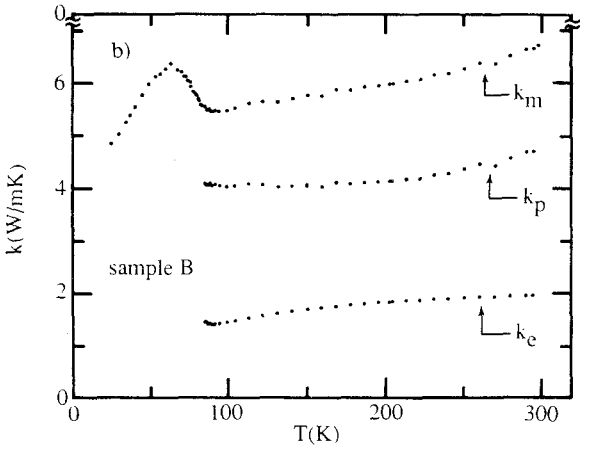

Fig. 54. In-plane thermal conductivity of a single crystal of $Bi_2Sr_2Ca_1Cu_2O_{8-x}$. The total, κ_m, the phonon, κ_p, and the carrier, κ_e, contributions are shown separately. (Taken from [135].)

Crommie and Zettl investigated the *ab*-plane thermal conductivity on the (2212) phase single crystals with the onset and completion of the superconducting transition at 89 K and 81 K, respectively. From the Wiedemann-Franz ratio they obtained about 33% carrier contribution with the rest of the heat being carried by phonons. Assuming the validity of the Mathiessen's rule, they analyzed the phonon thermal resistivity in terms of the phonon-carrier and phonon-defect scattering channels and concluded that the defect scattering contribution is roughly twice as large as the phonon-carrier term. The total thermal conductivity together with the deduced phonon and carrier components is shown in Fig. 54.

4.4. $Tl_mBa_2Ca_{n-1}Cu_nO_{2(n+1)+m}$

Tl-based high-T_c superconductors were discovered early in 1988 by Sheng and Hermann [4] and by Parkin *et al.* [136] and, at this point, are the perovskites with the highest reproducible transition temperature, $T_c \sim 125$ K. In its typical double Tl layer form ($m = 2$), the Tl-Ba-Ca-Cu-O system is very similar to the Bi-Sr-Ca-Cu-O system and both can be designated as $(B^{III})_2(A^{II})_2Ca_{n-1}Cu_nO_{2n+4}$, where B^{III} is Bi or Tl, and A^{II} is Sr or Ba. The index n represents the number of Cu-O planes sandwiched between the Tl layers and has a profound effect on the superconducting properties of this material. As n increases, the structure progresses from a Ca-free (2201) phase with $T_c \sim 10$ K, to a (2212) superconductor with T_c near 106 K, and, eventually, to a (2223) material that superconducts up to 125 K. Unfortunately, the prospect of obtaining a still higher T_c by

increasing n beyond $n=3$ is difficult to realize due to the metastable nature of the resulting layered structures. It is interesting to note that a double Tl layered structure is not necessarily required for the realization of high values of T_c. Among single Tl-O layer compounds, discovered originally by Parkin *et al.* [137], is included the (1234) phase, $TlBa_2Ca_3Cu_4O_{11}$, which has been identified by Ihara *et al.* [138] as a 120 K superconductor. Numerous other structural modifications have been discovered which attest to the difficulty of preparing single-phase samples in this family of perovskites. A word of caution regarding the handling of Tl is appropriate here. Tl is a highly toxic substance that presents a potentially serious hazard not only during the synthesis, where its high volatility is a concern, but also in its final compound form, since Tl is soluble in water and can permeate the skin.

Although Tl-based perovskite superconductors are appealing for their high transition temperature, reports on the thermal transport of these materials are few. The lack of interest stems partly from a hesitancy to handle this toxic material and partly from a prevailing sentiment that there is little radically new information to be gleaned from this system. Indeed, high temperature data (see Fig. 55) reveal the expected rise in $\kappa(T)$ below T_c followed by a maximum, just as has been seen in all other Cu-O plane high-T_c superconductors. The nominal stoichiometry of the samples depicted in Fig. 55 is $Tl_2Ba_2Ca_2Cu_3O_x$ but, undoubtedly, other minor

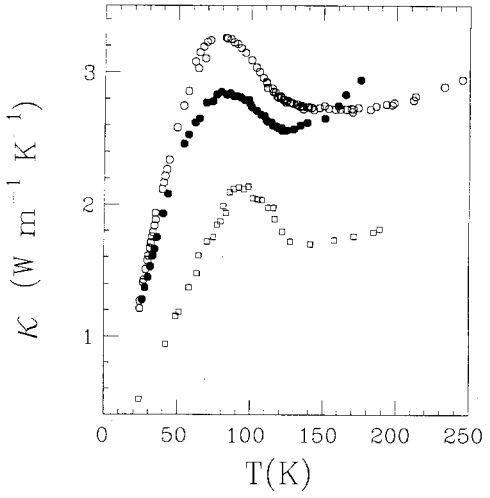

Fig. 55. Thermal conductivity of sintered $Tl_2Ba_2Ca_2Cu_3O_{10}$. Open squares are the data of Aliev *et al.* [132]. Solid and open circles are the data for two samples of Peacor *et al.* [139]. Transition temperatures of the above samples are near 120 K.

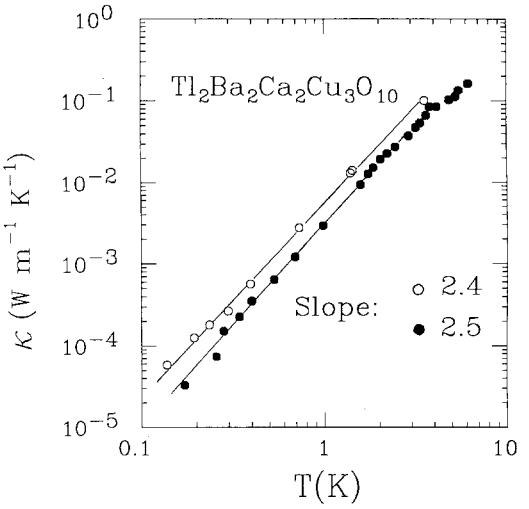

Fig. 56. Thermal conductivity of $Tl_2Ba_2Ca_2Cu_3O_{10}$ at very low temperatures. Data taken on the samples of [139]. The high-temperature range is shown in Fig. 55.

phases are present. The data of Aliev *et al.* [132] are designated by open squares and the two samples of Peacor *et al.* [139] by solid and open circles. The latter authors extended their measurements to temperatures near 100 mK in order to determine the limiting temperature dependence of the thermal conductivity. The preliminary results are displayed in Fig. 56 and indicate an approximately $T^{2.5}$ power law behavior. Down to 150 mK there is no indication of the presence of a linear variation in $\kappa(T)$. These preliminary measurements were made on rather large samples which were difficult to cool to below 100 mK due to the extremely long equilibration times that resulted from the high heat capacity and poor thermal conductivity of the material. Experiments on much smaller samples might allow a better estimate of the limiting temperature dependence. Of course, single crystal samples would be highly desirable and, if and when these become available, anisotropy of the thermal transport will be an important area to pursue.

4.5. Copperless Cubic Superconductors

In 1975, Sleight *et al.* [54] discovered superconductivity in the $Ba(Pb_{1-x}Bi_x)O_3$ system. Although this was an interesting discovery, it did not generate great excitement because the transition temperature ($T_c \sim$ 13 K) was well below that achieved in established metal-based superconductors. However, the discovery [55, 56] of superconductivity in the closely related system of $Ba_{1-x}K_xBiO_3$ with $T_c \sim 30$ K, i.e., well above the highest values seen in conventional

superconductors, has led to the realization that this copperless family of perovskites is an important class of materials that may form a bridge between conventional and Cu-O plane high-T_c superconductors.

$Ba_{1-x}K_xBiO_3$ is a ceramic which, with the exception of its bluish tinge, looks and feels like any other high-T_c ceramic. There are several notable features, however, which clearly distinguish this copperless perovskite from its Cu-O plane cousins:

(i) Copperless superconductors are cubic rather than layered perovskites.

(ii) There are wide $6s$ and $2p$ electron bands near the Fermi level, instead of d-electrons. Consequently, correlation effects are unimportant.

(iii) As expected, there is no magnetism found in the compound.

(iv) There is a large isotope effect ($T_c \sim M^{-\alpha}$) in $Ba_{1-x}K_xBiO_3$ with the coefficient $\alpha \sim 0.3$-0.4.

(v) The phase diagram of $Ba_{1-x}K_xBiO_3$ is typified by a metal-insulator transition with a rather abrupt onset of superconductivity [140] (see Fig. 57).

My group has recently undertaken a study [141] of the heat transport in the $Ba_{1-x}K_xBiO_3$ system with an aim toward comparing the behavior of $\kappa(T)$ with that observed in Cu-O plane high-T_c superconductors. As it has turned out, the results are most surprising in their departure from the data on Cu-O plane perovskites.

Experiments were carried out on samples prepared according to the procedure of Dabrowski *et al.* [142]. Two superconducting samples ($x = 0.4$) with

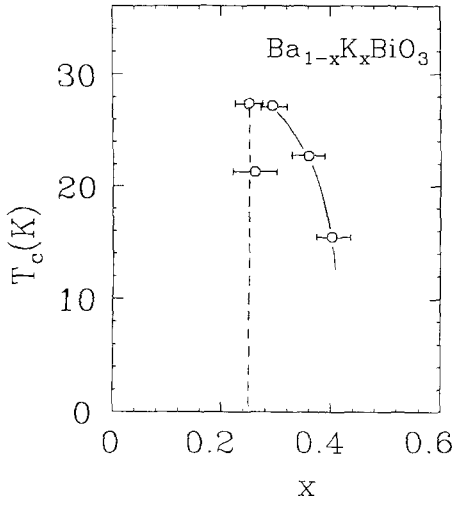

Fig. 57. Phase diagram (T_c vs. x) for $Ba_{1-x}K_xBiO_3$. (Adapted from [140].)

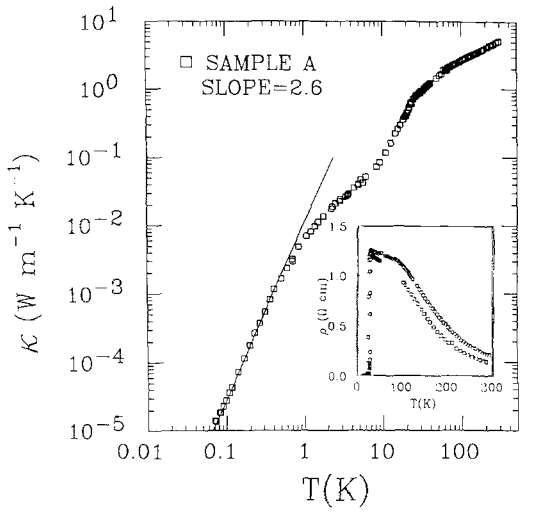

Fig. 58. Thermal conductivity of sample A of sintered $Ba_{1-x}K_xBiO_3$ with $x = 0.4$. The inset shows the electrical resistivity of samples A (open squares) and B (open circles). (Adapted from [141].)

$T_c = 25.2$ K and 27.5 K, respectively, and an insulating sample ($x = 0.2$) were chosen for study. All of the samples are single phase as indicated by X-ray diffraction patterns. The resistivity, shown in the inset of Fig. 58, is large and displays a nonmetallic character similar to that seen by other authors [142,143]. Above 190 K, the behavior of $\rho(T)$ is consistent with variable-range hopping, $\rho \sim \exp(T_0/T)^{1/4}$, with $T_0 = 2.7 \times 10^6$ K. The thermal conductivity of the samples is shown in Fig. 58. Although $\kappa(T)$ is somewhat smaller than that in sintered Y and La-based high-T_c's, it is huge compared to what would be expected from the application of the Wiedemann-Franz law to the electrical resistivity. Stated differently, the experimental Lorenz ratio of about 3×10^{-4} V^2 K^{-2} at 30 K is some four orders of magnitude larger than the Sommerfeld value $L_0 = 2.44 \times 10^{-8}$ V^2 K^{-2}. As we have seen in the previous sections, a Lorenz ratio an order of magnitude larger than L_0 is typical of high-T_c superconductors and indicates the dominance of phonons over the charge carriers to the extent that phonons generally carry ~90% of the total heat current. Does the exceptionally large Lorenz ratio seen in $Ba_{0.6}K_{0.4}BiO_3$ imply that here phonons account for 99.99% of all heat transported? Certainly not, and the increase in $\kappa(T)$ upon application of a magnetic field (at $T \leq T_c$; see Fig. 59), clearly demonstrates the presence of a large charge carrier contribution. In this regard, $Ba_{1-x}K_xBiO_3$ superconductors behave much like conventional superconductors in which charge carriers dominate the heat flow. There is

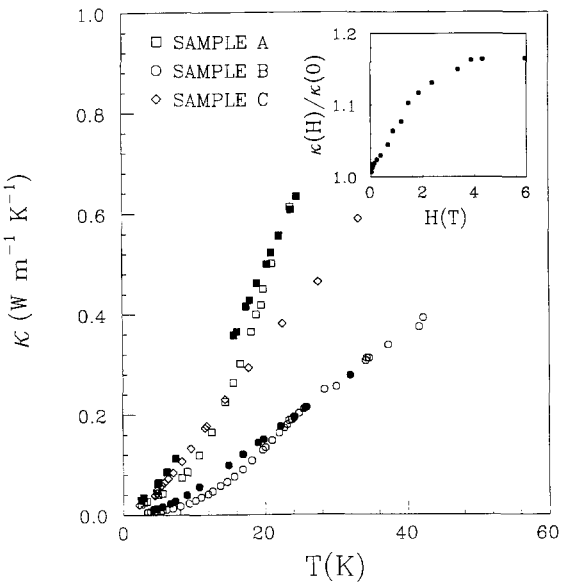

Fig. 59. Change in the thermal conductivity of $Ba_{0.6}K_{0.4}BiO_3$ on application of a magnetic field. The solid squares and circles are for measurements performed in a 6T field, open symbols represent zero field data. The inset shows the ratio of the thermal conductivity in a magnetic field to the thermal conductivity in zero field, $\kappa(H)/\kappa(0)$, for sample A as a function of field strength at a constant temperature of 20 K. (Taken from [141].)

definitely no hint of an increase in $\kappa(T)$ as the sample is cooled below T_c. On the contrary, the onset of superconductivity leads to a decrease in $\kappa(T)$. I should note that, in contrast to BaKBiO, the effect of a magnetic field on the thermal conductivity of ceramic Cu-O plane perovskites is small [111] and results in a decrease in the thermal conductivity believed to arise from phonon and carrier scattering on the fluxoid lattice.

To account for the huge values of the ratio L and the large electronic contribution to the thermal transport, Peacor *et al.* [141] propose a model based on the granular nature of the material. The system is modelled by metallic and semiconducting regions with the same cross-sectional area in series, so that the electrical resistivity is

$$\rho = (1-y)\rho_1 + y\rho_2 \tag{30}$$

and the thermal conductivity is given by

$$\kappa^{-1} = (1-y)(\kappa_{e1}+\kappa_{p1})^{-1} + y(\kappa_{e2}+\kappa_{p2})^{-1} \tag{31}$$

where y is the nonmetallic fraction of the path, κ_{e1} and κ_{p1} are the electronic and phonon thermal conductivities, respectively, in the metallic regions, and ρ_1 is the resistivity of the metallic region. Similar quantities with subscript 2 refer to the barrier regions. Overall, high resistivity can arise if $\rho_2 \gg \rho_1$, since the resistivity can be dominated by the semiconducting regions even if the barriers are thin. The electronic thermal conductivities for each region are related to the corresponding electrical resistivities by the appropriate Lorenz numbers, L_i (assumed $\sim L_0$ for elastic scattering). Thus, $\rho_2 \gg \rho_1$ implies $\kappa_{e2} \ll \kappa_{e1}$, but because one can have $\kappa_{e2} \ll \kappa_{p2}$ (i.e., phonons can propagate heat across the barriers with reasonable efficiency), the thermal resistance is not necessarily dominated by the barrier regions in the same way as the electrical resistance. Obviously, for the change in κ_{e1} due to superconductivity (see Fig. 59) to have a large effect on the total thermal conductivity, κ_{e1} must be of at least a similar size to κ_{p1}. It is also clear that y must be rather small, i.e., the barriers very thin so that they do not dominate the heat resistance. This thinness of the barriers is, of course, consistent with the achievement of the zero resistance state seen in the samples. Since, roughly, $\rho \sim y\rho_2 \gg \rho_1$ and κ is comparable in magnitude to κ_{e1}, the value of $L = \kappa\rho/T$ can be very large, as observed. Peacor *et al.* estimate the intrinsic resistivity of the metallic grains to be on the order of 120 $\mu\Omega$cm which is orders of magnitude smaller than the observed resistivity and 100 times smaller than the smallest resistivity observed thus far, that of the sample of Hinks *et al.* [143]. This implies that the existing ceramic samples of $Ba_{1-x}K_xBiO_3$ all have a similar granular structure that impedes the carrier transport. Furthermore, one cannot make use of the Wiedemann-Franz law to estimate the respective phonon and carrier thermal conductivity contributions as was routinely done in the case of Cu-O plane superconductors.

The uncertainty about the relative contribution of phonons and charge carriers to the thermal transport greatly complicates the analysis of $\kappa(T)$ below T_c. In Fig. 60 is plotted $\kappa_s(T)/\kappa_n(T)$, the ratio of the thermal conductivity in the superconducting and normal states, versus the reduced temperature, where $\kappa_n(T)$ is obtained with the aid of a 6-T magnetic field that shifts the superconducting boundary down to about $T/T_c \sim 0.7$. Also shown in Fig. 60 are the theoretical ratios of κ_{es}/κ_{en} for the weak and strong coupling models calculated under the assumption that defect scattering is dominant. Obviously, the presence of phonons is responsible for the fact that the experimental curve, $\kappa_s(T)/\kappa_n(T)$, lies above the two theoretical predictions. From Fig. 60 it might appear that the weak coupling limit is more appropriate than the strong coupling scenario. In reality, however, one must examine the size of the phonon contribution required in the two separate cases to obtain agreement with the κ_s/κ_n curve and decide which is more reason-

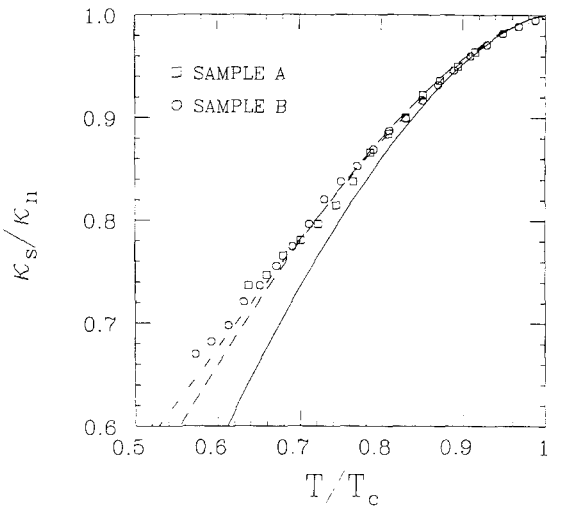

Fig. 60. The ratio $\kappa(H=0)/\kappa(H=6\text{T})$ plotted against the reduced temperature. Theoretical curves of κ_{es}/κ_{en} for the weak coupling (full curve) and strong coupling (dotted curve) cases are indicated. Also shown are two curves representing the predictions of the strong coupling model with the addition of a phonon contribution: $r_1=0.45$, $r_2=0$ (chain curve) and $r_1=0.25$, $r_2=0.25$ (dashed curve). See text for definition of r_1 and r_2. (Taken from [141].)

able. For instance, the weak coupling model requires the introduction of only a small phonon contribution to match the experimental results. Good agreement is achieved by taking the fractional phonon contribution to the conductivity in region 1 at T_c, $r_1=\kappa_{p1}/(\kappa_e+\kappa_{p1})$, to be 0.15 and neglecting the fraction of the thermal resistance due to region 2 phonons in series with the electronic thermal resistance in region 1 at T_c, $r_2=W_{p2}/(W_e+W_{p2})$. Another successful combination of parameters is $r_1=0.08$ and $r_2=0.08$. For the strong coupling case, significantly higher phonon contributions are needed ($r_1=0.45$, $r_2=0$ indicated by the chain curve, and $r_1=0.25$ and $r_2=0.25$ designated by the dashed curve). Based on the fact that the thermal conductivity of the insulating specimen (sample C) is comparable is magnitude to the total thermal conductivity for samples A and B, Peacor *et al.* argue that the phonon contribution to $\kappa(T)$ in samples A and B is rather large. Consequently, the size of the reduction observed in Fig. 60 is consistent with a strong coupling mechanism for the superconductivity. The authors point out that a much better estimate of the strength of the carrier-phonon interaction can be obtained once single crystals or very high quality sintered samples become available so that one can use the Wiedemann-Franz law in conjunction with the electrical resistivity to arrive at the $\kappa_e(T)$ and $\kappa_p(T)$ contributions directly. Regardless of this difficulty, the thermal conductivity of $Ba_{1-x}K_xBiO_3$, specifically its substantial charge carrier contribution and its behavior in a magnetic field, clearly stands in contrast to the thermal conductivity of all Cu-O plane superconductors. Thermal conductivity studies lend support to the widely held opinion that copperless, cubic perovskites are an interesting class of superconductors with normal and superconducting parameters substantially different from those of all other high-T_c materials. Closer scrutiny is needed to ascertain whether the mechanism of superconductivity in this system is of the classical, phonon-based type or of some other, more complex variety.

5. CONCLUSION

An impressive collection of experimental data on the thermal conductivity of high-T_c superconductors has been assembled over the past 3 years and much has been learned about the mechanism of heat transport in these materials. Although their total thermal conductivity is rather low, the Cu-O plane superconductors exhibit a surprisingly large phonon contribution to the heat flow that, in single crystals, amounts to some 60% and, in sintered samples, up to 90% of the total heat current. Small electronic contributions are the consequence of strong defect scattering (particularly in sintered samples) and, above all, of the reduced charge carrier density that is typical of Cu-O perovskite structures. The dominance of phonons, coupled with the effectiveness of the phonon-carrier scattering, is responsible for the spectacular rise in the thermal conductivity below T_c and the occurrence of a maximum near $T_c/2$. The height of the maximum varies from being barely detectable to being nearly twice the value of the conductivity at T_c and depends, primarily, on the relaxation time of phonon-carrier scattering in relation to other phonon dissipative processes. Experimental data can be approximated very successfully with the BRT theory modified to include defect scattering. The phonon-carrier coupling parameter obtained from the fitting procedure falls within the domain of weak to moderately strong coupling with $\lambda \sim 0.5$-0.6.

The thermal transport properties of all Cu-O plane superconductors show a considerable degree of anisotropy wherein the in-plane heat conduction greatly exceeds the conduction across the Cu-O sheet. Unfortunately, the dearth of data on the c axis heat conduction, in conjunction with the strong phonon-defect scattering in this direction, prevents the evaluation of the coupling constant anisotropy.

Although several investigations of the thermal conductivity have now been extended to temperatures below 100 mK, the limiting power law behavior of $\kappa(T)$ remains an unsettled issue. One finds a correlation between the occurrence (absence) of a limiting T-linear dependence in $\kappa(T)$ and the presence (absence) of a large γ term for the linear contributions to κ and c_v. Minute amounts of a normal phase dispersed in the high-T_c matrix (perhaps along the grain boundaries) could yield both the nonzero γ term and the T-linear contribution to κ. Since such impurity phases would be squeezed out of high-quality single crystals to a considerable degree, linear terms in the thermal conductivity of single crystals are expected to be greatly suppressed, as indeed they are. This line of argument suggests an approximately quadratic temperature dependence as the intrinsic power law variation for the low-temperature thermal conductivity of high-T_c superconductors. However, whether a T^2 variation of the thermal conductivity necessarily implies the existence of two-level tunneling states, such as apparently dominate the thermal transport in glassy materials, is, I believe, far from certain. Quite apart from the fact that a T^2 variation is frequently "forced" upon the data, the picture of good-quality single crystals of high-T_c superconductors as amorphous solids is conceptually troubling. It is worthwhile to note that experimental values of the γ term in $La_{2-x}Sr_xCuO_4$ and $YBa_2Cu_3O_{7-\delta}$ are at least an order of magnitude larger than values typical of amorphous materials.

More recent studies of the thermal conductivity of both sintered [107] and single crystal specimens [109], coupled with the latest analysis of the specific heat data [68,69], suggest that the nonzero values of γ and, therefore, the T-linear term in $\kappa(T)$ are of intrinsic origin. This, of course, implies that there cannot be a gap in the electronic density of states. Clearly, more experimental data are needed before one can make a final judgment on the low-temperature behavior of high-T_c superconductors. The issue is important as it has a bearing on the electronic structure of high-T_c superconductors and, hence, on the mechanism of superconductivity.

In general, experimental efforts should center on the study of high-quality single crystals where one can better observe the intrinsic behavior. In particular, information on the c axis thermal transport is rather limited, yet it is of great importance to the understanding of how and by what means heat propagates across the Cu-O sheets. More studies should also be done on thermal transport in Bi-Sr-Ca-Cu-O single crystals. This material can be prepared in the form of relatively large crystals and its pronounced layered structure provides for the possible observation of unusually high anisotropy values in the thermal conductivity. I believe that copperless cubic superconductors will attract more attention because of their unique normal and superconducting state properties. Investigations of single crystals of these materials, when they become available, may be particularly fruitful as they would avoid the complications that arise from the granular nature of sintered samples. Finally, innovative techniques are being developed to study the thermal response and the phonon-carrier interaction in high-T_c thin films. I expect that some of the most exciting results will come from the use of femtosecond laser methods to probe nonequilibrium carrier distributions and their relaxation rates [144] in these systems.

In writing a comprehensive review on any particular topic dealing with high-T_c superconductors, one runs the unavoidable risk of being quickly out of date or of inadvertently omitting relevant papers. While I aimed at an exhaustive presentation of the available literature on the thermal conductivity of high-T_c perovskites, I apologize to those colleagues whose work may have been overlooked. It is a challenge to keep abreast of the progress in this exciting and rapidly evolving field.

ACKNOWLEDGMENTS

It is my pleasure to thank my student, Ray Richardson, for his help in preparing this review. I also wish to acknowledge fruitful discussions with Dr. Alan Kaiser concerning heat transport in superconductors. I have greatly benefitted from interactions with my former students, Drs. Donald Morelli and Joshua Cohn, and from lively input and enthusiasm from my current student, Scott Peacor. I would like to thank all colleagues who allowed me to use their results in this review. The work was supported by U.S. Army Research Office Contract No. DAAL-03-87-K-0007.

REFERENCES

1. J. G. Bednorz and K. A. Müller, *Z. Phys. B* **64**, 189 (1986).
2. M. K. Wu, J. R. Asburn, C. J. Torng, P. H. Hor, R. L. Meng, L. Gao, Z. J. Huang, Y. Q. Wang, and C. W. Chu, *Phys. Rev. Lett.* **58**, 908 (1987).
3. H. Maeda, Y. Tanaka, M. Fukutomi, and T. Asano, *Jpn. J. Appl. Phys.* **27**, L209 (1988).

4. Z. Z. Sheng and A. M. Herman, *Nature (London)* **332**, 55 (1988).
5. P. L. Richards, J. Clarke, R. Leoni, Ph. Lerch, B. Verghese, M. R. Beasley, T. H. Geballe, R. H. Hammond, P. Rosenthal, and S. R. Spielmann, *Appl. Phys. Lett.* **54**, 283 (1989).
6. M. I. Flik and C. L. Tien, ASME Winter Annual Meeting, San Francisco, 1989, *J. Heat Transfer*, in press.
7. R. Gross, M. Hartmann, K. Hipler, R. P. Huebener, F. Kober, and D. Koelle, *IEEE Trans. Magn.* MAG-25, 2250 (1989).
8. R. P. Huebener, R. Gross, and J. Bosch, *Z. Phys. B* **70**, 425 (1988).
9. H. E. Fischer, S. K. Watson, and D. G. Cahill, *Comments Condens. Mater. Phys.* **14**, 65 (1988).
10. E. Gmelin, in *Studies of High-Temperature Superconductors*, A. Narlikar, ed. (Nova Science Publishers, New York, 1989), Vol. 2, Chap. 4.
11. C. Uher, 3rd Annual Conf. on Superconductivity and Applications, NYSIS, Buffalo, September 1989, in *Superconductivity and Applications*, H. S. Kwok, ed. (Plenum Press, New York, 1990) p. 217.
12. A. Inam, M. S. Hedge, X. D. Wu, T. Venkatesan, D. England, P. F. Miceli, E. W. Chase, C. C. Chang, J. M. Tarascon, and Y. B. Wachtman, *Appl. Phys. Lett.* **53**, 908 (1988).
13. J. G. Fanton, D. B. Mitzi, A. Kapitulnik, B. T. Khuri-Yakub, G. S. Kino, D. Gazit, and R. S. Feigelson, *Appl. Phys. Lett.* **55**, 598 (1989).
14. Y. Syono, M. Kikuchi, K. Oh-ishi, K. Hiraga, H. Arai, Y. Matsui, N. Kobayashi, T. Sasaoka, and Y. Muto, *Jpn. J. Appl. Phys.* **26**, L498 (1987).
15. C. S. Pande, A. K. Singh, L. E. Toth, D. U. Gubser, and S. A. Wolf, *Phys. Rev. B* **36**, 5669 (1987).
16. C. H. Chen, J. Kwo, and M. Hong, *Appl. Phys. Lett.* **52**, 841 (1988).
17. H. A. Hoff and C. S. Pande, in *Studies of High-Temperature Superconductors*, A. Narlikar, ed. (Nova Science Publishers, New York 1989), Vol. 3, Chap. 13.
18. R. Berman, *Thermal Conductivity in Solids* (Oxford University Press, 1976).
19. V. L. Gurevich, *Transport in Phonon Systems*, Vol. 18 of Series on Modern Problems in Condensed Matter Sciences, V. M. Agranovich and A. A. Maradudin, eds. (North-Holland, Amsterdam, 1986).
20. J. Bardeen, G. Rickayzen, and L. Tewordt, *Phys. Rev.* **113**, 982 (1959).
21. K. Maki, *Prog. Theor. Phys.* **31**, 378 (1964).
22. B. T. Geilikman and V. Z. Kresin, *Kinetic and Nonsteady-State Effects in Superconductors* (Wiley, New York, 1974).
23. K. Mendelssohn and J. Olsen, *Proc. Phys. Soc. A* **63**, 2 (1950).
24. L. Tewordt and Th. Wölkhausen, *Solid State Commun.* **70**, 839 (1989).
25. L. Tewordt and Th. Wölkhausen, *Solid State Commun.* **75**, 515 (1990).
26. *V. L. Ginzburg, J. Phys. (USSR)* **8**, 148 (1944).
27. J. M. Ziman in *Principles of the Theory of Solids*, 2nd edn. (Cambridge University Press, 1972).
28. V. L. Ginzburg, *J. Superconduct.* **2**, 323 (1989).
29. A. B. Kaiser and C. Uher in *Studies of High-Temperature Superconductors*, A. Narlikar, ed. (Nova Science Publishers, New York, 1990), Vol. 7, in press.
30. K. Mendelssohn and J. Olsen, *Phys. Rev.* **80**, 859 (1950).
31. A. F. Andreev, *Sov. Phys.-JETP* **19**, 1228 (1964).
32. D. Saint-James, G. Sarma, and E. J. Thomas, *Type II Superconductivity* (Pergamon Press, Oxford, 1969).
33. A. A. Abrikosov, *Sov. Phys.-JETP* **5**, 1174 (1957).
34. L. Dubeck, P. Lindenfeld, E. A. Lynton, and H. Rohrer, *Rev. Mod. Phys.* **36**, 110 (1964).
35. J. Lowell and J. B. Sousa, *J. Low Temp. Phys.* **3**, 65 (1970).
36. B. K. Chakalskii, N. A. Redko, S. S. Shalyt, and V. M. Azhazha, *Sov. Phys.-JETP* **48**, 665 (1978).
37. R. D. Parks, F. C. Zumsteg, and J. M. Mochel, *Phys. Rev. Lett.* **18**, 47 (1967).
38. R. M. Cleary, *Phys. Rev. B* **1**, 169 (1970).
39. C. Caroli and M. Cyrot, *Phys. Kondens. Mater.* **4**, 285 (1965).
40. K. Maki, *Phys. Rev.* **158**, 397 (1967).
41. A. Houghton and K. Maki, *Phys. Rev. B* **4**, 843 (1971).
42. C. V. Heer and J. G. Daunt, *Phys. Rev.* **76**, 854 (1949).
43. A. C. Anderson in *Amorphous Solids—Low Temperature Properties*, Vol. 24 of Topics in Current Physics, W. A. Phillips, ed. (Springer-Verlag, New York, 1981).
44. J. J. De Yoreo, W. Knaak, M. Meissner, and R. O. Pohl, *Phys. Rev. B* **34**, 8828 (1986).
45. P. Esquinazi, J. Luzuriaga, C. Duran, D. A. Esparza, and C. D'Ovidio, *Phys. Rev. B* **36**, 2316 (1987).
46. B. Golding, N. O. Birge, W. H. Haemmerle, R. J. Cava, and E. Rietman, *Phys. Rev. B* **36**, 5606 (1987).
47. M. Nùñez Regueiro, P. Esquinazi, M. A. Izbizky, C. Duran, D. Castello, J. Luzuriaga, and G. Nieva, *Physica C* **153–155**, 1016 (1988).
48. J. E. Graebner, L. F. Schneemeyer, R. J. Cava, J. V. Waszczak, and E. A. Rietman, *Symp. Proc. Mater. Res. Soc.* **99**, 745 (1988).
49. M. Nùñez Regueiro, D. Castello, M. A. Izbizky, D. Esparza, and C. D'Ovidio, *Phys. Rev. B* **36**, 8813 (1987).
50. R. C. Zeller and R. O. Pohl, *Phys. Rev. B* **4**, 2029 (1971).
51. W. A. Phillips, *J. Low Temp. Phys.* **7**, 351 (1972).
52. P. W. Anderson, B. I. Halperin, and C. M. Varma, *Philos. Mag.* **25**, 1 (1972).
53. J. M. Grace and A. C. Anderson, *Phys. Rev. B* **40**, 1901 (1989).
54. A. W. Sleight, J. L. Gillson, and P. E. Bierstedt, *Solid State Commun.* **17**, 27 (1975).
55. L. F. Mattheis, E. M. Gyorgy, and D. W. Johnson, Jr., *Phys. Rev. B* **37**, 3745 (1988).
56. R. J. Cava, B. Batlogg, J. J. Krajewski, R. C. Farrow, L. W. Rupp, Jr., A. E. White, K. T. Short, W. F. Peck, Jr., and T. Y. Kometani, *Nature (London)* **332**, 814 (1988).
57. D. Vaknin, S. K. Sinha, D. E. Moncton, D. C. Johnston, J. Newman, C. R. Safinya, and H. E. King, Jr., *Phys. Rev. Lett.* **58**, 2802 (1987).
58. R. J. Birgeneau and G. Shirane in *Physical Properties of High Temperature Superconductors*, D. M. Ginsberg, ed. (World Scientific Publishing, Singapore, 1989).
59. P. M. Grant, S. S. P. Parkin, V. Y. Lee, E. M. Engler, M. L. Ramirez, J. E. Vazquez, G. Lim, R. D. Jacowitz, and R. L. Greene, *Phys. Rev. Lett.* **58**, 2482 (1987).
60. S. A. Shaheen, N. Jisrawi, Y. H. Lee, Y. Z. Zhang, M. Croft, W. L. McLean, H. Zhen, L. Rebelsky, and S. Horn, *Phys. Rev. B* **36**, 7214 (1987).
61. J. B. Torrance, Y. Tokura, A. I. Nazzal, A. Bezinge, T. C. Huang, and S. S. P. Parkin, *Phys. Rev. Lett.* **61**, 1127 (1988).
62. C. Uher and A. B. Kaiser, *Phys. Rev. B* **36**, (1987).
63. K. Bartkowski, R. Horyn, A. J. Zaleski, Z. Bukowski, M. Horobiowski, C. Marucha, J. Rafalowicz, K. Rogacki, A. Stepien-Damm, C. Sulkowski, E. Trojnar, and J. Klamut, *Phys. Stat. Solidi (a)* **103**, K37 (1987).
64. A. Bernasconi, E. Felder, F. Hulliger, H. R. Ott, Z. Fisk, F. Greuter, and C. Schueler, *Physica C* **153–155**, 1034 (1988).
65. F. Steglich, U. Ahlheim, D. Ewert, U. Gottwick, R. Held, H. Kneissel, M. Lang, U. Rauchschwalbe, B. Renker, H. Rietschel, G. Sparn, and H. Spille, *Phys. Scr.* **37**, 901 (1988).
66. Y. Iye in *Studies of High-Temperature Superconductors*, A. Narlikar, ed. (Nova Science Publishers, New York, 1989), Vol. 2, Chap. 7, p. 199.
67. R. Srinivasan in *Studies of High-Temperature Superconductors*, A. Narlikar, ed. (Nova Science Publishers, New York, 1989), Vol. 1, Chap. 12, p. 267.
68. R. A. Fisher, J. E. Gordon, and N. E. Phillips, *J. Superconduct.* **1**, 231 (1988).
69. S. E. Stupp and D. M. Ginsberg, *Physica C* **158**, 299 (1989).
70. C. Uher and J. L. Cohn, *J. Phys. C* **21**, L957 (1988).

71. C. Uher and A. B. Kaiser, *Phys. Rev. B* **37**, 127 (1988).
72. R. Berman and J. C. F. Brock, *Proc. R. Soc. London Ser. A* **289**, 46 (1965).
73. W. P. Pratt, Jr. and C. Uher, *Phys. Lett. A* **68**, 74 (1978).
74. D. T. Morelli and C. Uher, *Phys. Rev. B* **31**, 6721 (1985).
75. U. Gottwick, R. Held, G. Sparn, F. Steglich, H. Rietschel, D. Ewert, B. Renker, W. Bauhoffer, S. von Molnar, M. Wilhelm, and H. E. Hoenig, *Europhys. Lett.* **4**, 1183 (1987).
76. C. Uher and A. B. Kaiser, *Phys. Lett. A* **125**, 421 (1987).
77. N. P. Ong, Z. Z. Wang, J. Clayhold, J. M. Tarascon, L. H. Greene, and W. R. McKinnon, *Phys. Rev. B* **35**, 8807 (1987).
78. B. Salce, R. Calemczuk, C. Ayache, E. Bonjour, J. Y. Henry, M. Raki, L. Forro, M. Couach, A. F. Khoder, B. Barbara, P. Burlet, M. J. M. Jurgens, and J. Rossat-Mignod, *Physica C* **153–155**, 1014 (1988).
79. D. T. Morelli, J. Heremans, G. Doll, P. J. Picone, H. P. Jenssen, and M. S. Dresselhaus, *Phys. Rev. B* **39**, 804 (1989).
80. D. R. Morelli, G. L. Doll, J. Heremans, M. S. Dresselhaus, A. Cassanho, D. R. Gabbe, and H. P. Jenssen, *Phys. Rev. B* **41**, 2520 (1990).
81. D. L. Kaiser, F. W. Gayle, R. S. Roth, and L. J. Swartzendruber, *J. Mater. Res.* **4**, 745 (1989).
82. D. T. Morelli, G. L. Doll, J. Heremans, M. S. Dresselhaus, A. Cassanho, H. P. Jenssen, S. D. Peacor, and C. Uher, to be published.
83. D. T. Morelli and C. Uher, *Phys. Rev. B* **31**, 6721 (1985).
84. C. Uher and D. T. Morelli, *Synth. Met.* **12**, 91 (1985).
85. G. Balestrino, S. Barbanera, A. Paoletti, P. Paroli, and M. V. Antisari, *Phys. Rev. B* **38**, 6609 (1988).
86. J. T. Chen, L-X. Qian, L-Q. Wang, L. E. Wenger, and E. M. Logothetis, *Mod. Phys. Lett. B* **3**, 1197 (1990).
87. A. Jezowski, J. Mucha, K. Rogacki, R. Horyn, Z. Bukovski, and M. Horobiowski, *Phys. Lett. A* **122**, 431 (1987).
88. V. Bayot, F. Delannay, C. Dewitte, J-P. Erauw, X. Gonze, J-P. Issi, A. Jonas, M. Kinany-Alaoui, M. Lambricht, J-P Michenaud, J-P. Minet, and L. Piraux, *Solid State Commun.* **63**, 983 (1987).
89. D. T. Morelli, J. Heremans, and D. E. Swets, *Phys. Rev. B* **36**, 3917 (1987).
90. J. J. Freeman, T. A. Friedmann, D. M. Ginsberg, J. Chen, and A. Zangvil, *Phys. Rev. B* **36**, 8786 (1987).
91. B.A. Merisov, G. Ya. Khadzhai, M. A. Obolenskii, and O. A. Gavrenko, *Sov. J. Superconduct.: Phys., Chem., Eng. (Russ. Ed.)* **2**, 19 (1989).
92. S. E. Buravoi, K. V. Nefebov, V. A. Samoletov, B. A. Tallerczik, and E. V. Kharitonov, *Sov. J. Superconduct.: Phys., Chem., Eng. (Russ. Ed.)* **2**, 32 (1989).
93. J. L. Cohn, V. Selvamanickam, and K. Salama, to be published.
94. K. Salama, V. Selvamanickam, L. Gao, and K. Sun, *Appl. Phys. Lett.* **54**, 2352 (1989).
95. T. L. Francavilla, V. Selvamanickam, K. Salama, and D. H. Liebenberg, *Cryogenics*, **30**, 606 (1990).
96. S. J. Hagen, Z. Z. Wang, and N. P. Ong, *Phys. Rev. B* **40**, 9389 (1989).
97. W. P. Kirk, P. S. Kobiela, R. N. Tsumura, and R. K. Pandey, *Ferroelectrics* **92**, 151 (1989).
98. N. V. Zavaritskii, A. V. Samoilov, and A. A. Yurgens, *Sov. Phys.-JETP Lett.* **48**, 242 (1988).
99. M. Suzuki, U. Okuda, I. Iwasa, A. J. Ikushima, T. Takabatake, Y. Nakazawa, and M. Ishikawa, *Jpn. J. Appl. Phys.* **27**, L308 (1988).
100. V. B. Yefimov, A. A. Levchenko, L. P. Mezhov-Deglin, R. K. Nikolaev, and N. S. Sidorov, *Sov. J. Superconduct.: Phys., Chem., Eng. (Russ. Ed.)* **2**, 16 (1989).
101. A. Jezowski, J. Klamut, R. Horyn, and K. Rogacki, *Supercond. Sci. Technol.* **1**, 296 (1989).
102. A. Jezowski, *Solid State Commun.* **71**, 419 (1989).
103. A. G. Khachaturyan and J. W. Morris, Jr., *Phys. Rev. Lett.* **61**, 215 (1988).
104. G. Sparn, W. Schiebeling, M. Lang, R. Held, U. Gottwick, F. Steglich, and H. Rietschel, *Physica C* **153–155**, 1010 (1988).
105. R. E. Meredith and C. W. Tobias, *J. Appl. Phys.* **31**, 1270 (1960).
106. A. F. Khoder, M. Couach, M. Locatelli, A. Abou-Ghantous, and J. P. Senateur, *Solid State Commun.* **38**, 1297 (1981).
107. J. L. Cohn, S. D. Peacor, and C. Uher, *Phys. Rev. B* **38**, 2892 (1988).
108. R. K. Williams, R. S. Graves, D. M. Kroeger, G. C. Marsh, J. O. Scarbrough, and J. Brynestad, *J. Appl. Phys.* **66**, 6181 (1989).
109. G. Sparn, M. Baenitz, S. Horn, F. Steglich, W. Assmus, T. Wolf, A. Kapitulnik, and Z. X. Zhao, *Physica C* **162–164**, 508 (1989).
110. P. W. Anderson, *Science* **235**, 1196 (1987).
111. Da-Ming Zhu, A. C. Anderson, T. A. Friedmann, and D. M. Ginsberg, *Phys. Rev. B* **41**, 6605 (1990).
112. T. T. M. Palstra, B. Batlogg, L. F. Schneemeyer, and J. V. Waszczak, *Phys. Rev. Lett.* **64**, 3090 (1990).
113. V. Florentiev, A. Inyushkin, A. Taldenkov, O. Melnikov, and A. Bykov, Proc. Intern. Conf. on Transport Properties of Superconductors, Rio de Janeiro, Brasil, May, 1990, in *Progress in High Temperature Superconductivity*, R. Nicolsky, ed. (World Scientific Publishing, Singapore, 1990), p. 462.
114. A. V. Narlikar, C. V. Narasimha Rao, and S. K. Agarwal, in *Studies of High-Temperature Superconductors*, A. Narlikar, ed. (Nova Science Publishers, New York, 1989), Vol. 1, Chap. 15, p. 341.
115. A. Jezowski, A. J. Zaleski, M. Ciszek, J. Mucha, J. Olejniczak, E. Trojnar, and J. Klamut, *Helv. Phys. Acta* **61**, 438 (1988).
116. J. Heremans, D. T. Morelli, G. W. Smith, and S. C. Strike, III, *Phys. Rev. B* **37**, 1604 (1988).
117. K. Mori, K. Noto, M. Sasakawa, Y. Isikawa, K. Sato, N. Kobayashi, and Y. Muto, *Physica C* **153–155**, 1515 (1988).
118. F. G. Aliev, V. V. Moshchalkov, V. V. Pryadun, L. I. Leonjuk, and V. I. Voronkova, *Sov. J. Superconduct.: Phys., Chem., Eng. (Russ. Ed.)* **3**, 348 (1990).
119. R. W. Willekers, H. C. Meijer, N. H. van Dijk, and H. Postma, Proc. Intern. Conf. on Transport Properties of Superconductors, Rio de Janeiro, Brasil, May, 1990, in *Progress in High Temperature Superconductivity*, R. Nicolsky, ed. (World Scientific Publishing, Singapore, 1990), p. 466.
120. R. W. Willekers, H. C. Meijer, N. H. van Dijk, and H. Postma, Proc. Intern. Conf. on Transport Properties of Superconductors, Rio de Janeiro, Brasil, May, 1990, in *Progress in High Temperature Superconductivity*, R. Nicolsky, ed. (World Scientific Publishing, Singapore, 1990), p. 474.
121. S. Simizu, S. A. Friedberg, E. A. Hayri, and M. Greenblatt, *Jpn. J. Appl. Phys.* **26**, Suppl. 26-3, 2121 (1987).
122. M. A. Izbizky, M. Nùñez Regueiro, P. Esquinazi, and C. Fainstein, *Phys. Rev. B* **38**, 9220 (1988).
123. C. Uher and W.-N. Huang, *Phys. Rev. B* **40**, 2694 (1989).
124. K. Fuchs, *Proc. Cambridge Philos. Soc.* **34**, 100 (1938).
125. E. H. Sondheimer, *Adv. Phys.* **1**, 1 (1952).
126. D. S. Yee, R. J. Gambino, M. F. Chisholm, J. J. Cuomo, P. Madakson, and J. Karasinski, in *Thin Film Processing and Characterization of High-Temperature Superconductors*, J. M. E. Harper, R. J. Colton, and L. C. Feldman, eds. *Am. Inst. Phys. Conf. Proc.* **165**, 132 (1988).
127. S. W. Chau, L. H. Greene, W. L. Feldmann, P. F. Miceli, and B. G. Bagley, in *Thin Film Processing and Characterization of High-Temperature Superconductors*, J. M. E. Harper, R. J. Colton, and L. C. Feldman, eds. *Am. Inst. Phys. Conf. Proc.*, **165**, 28 (1988).
128. C. Michel, M. Hervieu, M. M. Borel, A. Grandin, F. Deslandes, J. Provost, and B. Raveau, *Z. Phys. B* **68**, 421 (1987).
129. S. D. Peacor and C. Uher, *Phys. Rev. B* **39**, 11559 (1989).
130. N. Murayama, E. Sudo, M. Awano, K. Kani, and Y. Torii, *Jpn. J. Appl. Phys.* **27**, L1856 (1988).

131. K. Mori, M. Sasakawa, T. Igarashi, Y. Isikawa, K. Sato, K. Noto, and Y. Muto, *Physica C* **162–164**, 512 (1989).
132. F. G. Aliev, V. V. Moshchalkov, and V. V. Pryadun, *Physica C* **162–164**, 572 (1989).
133. Da-Ming Zhu, A. C. Anderson, E. D. Bukowski, and D. M. Ginsberg, *Phys. Rev. B* **40**, 841 (1989).
134. N. V. Zavaritsky, A. V. Samoilov, and A. A. Yurgens, *Physica C*, **169**, 174 (1990).
135. M. F. Crommie and A. Zettl, *Phys. Rev. B* **41**, 10978 (1990).
136. S. S. P. Parkin, V. Y. Lee, E. M. Engler, A. I. Nazzal, T. C. Huang, G. Gorman, R. Savoy, and R. Beuers, *Phys. Rev. Lett.* **60**, 2539 (1988).
137. S. S. P. Parkin, V. Y. Lee, A. I. Nazzal, R. Savoy, R. Beyers, and S. J. La Placa, *Phys. Rev. Lett.* **61**, 750 (1988).
138. H. Ihara, R. Sugise, M. Hirabayashi, N. Terada, M. Jo, K. Hayashi, M. Tokumoto, Y. Kimura, and T. Shimomura, *Nature (London)* **334**, 510 (1988).
139. S. D. Peacor, J. Shewchun, and C. Uher, to be published.
140. D. G. Hinks, B. Dabrowski, J. D. Jorgensen, A. W. Mitchell, D. R. Richards, Shiyou Pei, and Donglu Shi, *Nature (London)* **333**, 836 (1988).
141. S. D. Peacor, R. A. Richardson, J. Burm, C. Uher, and A. B. Kaiser, *Phys. Rev. B* **42**, 2684 (1990).
142. B. Dabrowski, D. G. Hinks, J. D. Jorgensen, R. K. Kalia, P. Vashishta, D. R. Richards, D. T. Marx, and A. W. Mitchell, *Physica C* **156**, 24 (1988).
143. D. G. Hinks, A. W. Mitchell, Y. Zheng, D. R. Richards, and B. Dabrowski, *Appl. Phys. Lett.* **54**, 1585 (1989).
144. J. Chwalek, C. Uher, J. Whitaker, J. Agostinelli, and M. Lelental, *Appl. Phys. Lett.* **57**, 1696 (1990).